FIRAT UNIVERSITY
GRADUATE SCHOOL OF NATURAL AND APPLIED SCIENCES
TÜRKİYE

SYNTHESİS OF SİLVER, CUPPER AND BİMETALLİC NANOPARTİCLER USİNG QUERCETİN AND GALLİC ACİD: OPTİCAL AND MİCROBİAL PROPERTİES

Alla Ahmad Muhamad AMIN

Master's Thesis

DEPARTMENT OF CHEMİSTRY
Program of
Division of Biochemistry

JULY 2021

FIRAT UNIVERSITY
GRADUATE SCHOOL OF NATURAL AND APPLIED SCIENCES
TÜRKİYE

Department of Chemistry

Master's Thesis

SYNTHESİS OF SİLVER, CUPPER AND BİMETALLİC NANOPARTİCLER USİNG QUERCETİN AND GALLİC ACİD: OPTİCAL AND MİCROBİAL PROPERTİES

Author
Alla Ahmad Muhamad AMIN

Supervisor
Prof. Dr. Habibe ÖZMEN

JULY 2021
ELAZIG

FIRAT UNIVERSITY
GRADUATE SCHOOL OF NATURAL AND APPLIED SCIENCES

TÜRKİYE

Department of Chemistry

Master's Thesis

Title:	Synthesis Of Silver, Cupper and Bimetallic Nanoparticler Using Quercetin and Gallic Acid: Optical and Microbial Properties
Author:	Alla Ahmad Muhamad AMIN
Submission Date:	14 June 2021
Defense Date:	01 July 2021

THESIS APPROVAL

This thesis, which was prepared according to the thesis writing rules of the Graduate School of Natural and Applied Sciences, Fırat University, was evaluated by the committee members who have signed the following signatures and was unanimously approved after the defense exam made open to the academic audience.

Signature

Supervisor:	Prof. Dr. Habibe ÖZMEN Firat University, Faculty of Science	Approved
Chair:	Prof. Dr. Ali ÖLÇÜCÜ Frat University, Faculty of Science	Approved
Member:	Prof. Dr. Işıl AYDIN Dicle University, Faculty of Pharmacy	Approved

This thesis was approved by the Administrative Board of the Graduate School on

..... / ..... / 20 .....

Signature

Associated Prof. Dr. Kürşat Esat ALYAMAÇ
Director of the Graduate School

DECLARATION

I hereby declare that I wrote this Master's Thesis titled " Synthesis Of Silver, Cupper and Bimetallic Nanoparticler Using Quercetin and Gallic Acid: Optical and Microbial Properties" in consistent with the thesis writing guide of the Graduate School of Natural and Applied Sciences, Firat University. I also declare that all information in it is correct, that I acted according to scientific ethics in producing and presenting the findings, cited all the references I used, express all institutions or organizations or persons who supported the thesis financially. I have never used the data and information I provide here in order to get a degree in any way.

01 July 2021

Alla Ahmad Muhamad AMIN

PREFACE

First of all, praise and gratitude to God, and I would like to express my special thanks to my professor Dr. Habibe ÖZMEN, who gave me the golden opportunity to do this wonderful project on the subject (synthesis of silver copper bimetallic nanoparticles using quercetin and Gallic acid: optical and anti-microbial properties). Also, so many thanks for Doç.Dr. Gökhan Kürşad İNCİLİ and Dr. Yakup SAY.

Secondly, I would also like to thank my family and friends who have helped me a lot to complete this master thesis.

Alla Ahmad Muhamad AMIN
ELAZIG, 2021

TABLE OF CONTENTS

Page

ABSTRACT

Synthesis Of Silver, Cupper and Bimetallic Nanoparticler Using Quercetin and Gallic Acid: Optical and Microbial Properties

Alla Ahmad Muhamad AMIN

Master's Thesis

FIRAT UNIVERSITY
Graduate School of Natural and Applied Sciences

Department of Chemistry

July 2021, Page: xii + 64

Gallic Acid is a polyphenol and Quercetin is a flavonoid structure, both of which are quite powerful antioxidants and biologically active compounds. One of the important application areas is the pharmaceutical industry. Studies have shown that these substances have anticarcinogenic, antioxidative, antimutagenic, antiallergic and anti-inflammatory effects. Various metallic nanoparticles (NP) obtained from these phenolic compounds have found wide research area especially in the field of nanomedicine. As nanotechnology develops, the usage area of these nanoparticles, which have a size of 1-100 nm, is expanding day by day in the field of medical chemistry, materials science and advanced technology products and pharmaceuticals

In this thesis study, optimal pH to form nanoparticles of silver, copper and their different combinations (Quercetin Ag/CuNP, Gallic Acid Ag/CuNP, Quercetin+Gallic acid AgNP, Quercetin+Gallic acid CuNP, Quercetin+Gallic acid AgCuNP) using quercetin and gallic acid were determined. The synthesized nanoparticles were characterized using UV-VIS spectrophotometer, X-ray diffractometer (XRD), Fourier transform infrared spectroscopy (FTIR), energy dispersive X-ray spectroscopy (EDS) and scanning electron microscopy (SEM).

The minimum inhibition concentration (MIC) values of the synthesized nanoparticles against human pathogens such as Escherichia coli and Staphylococcus aureus were calculated. It was determined that the MIC values of nanoparticles obtained from Gallic acid and quercetin were quite effective compared to Gallic acid and quercetin.

Keywords: Quercetin, Gallic acid, Silver nanoparticle, Copper nanoparticles, Bimetallic nanoparticles, Optical Property, Antimicrobial, Minimum Inhibition Concentration (MIC).

ÖZET

Kuersetin ve Gallik Asit Kullanılarak Gümüş, Bakır ve Bimetalik Nanoparçacıkların Sentezi; Optik ve Antimikrobiyal Özellikler

Alla Ahmad Muhamad AMIN

Yüksek Lisans Tezi

FIRAT ÜNİVERSİTESİ
Fen Bilimleri Enstitüsü

Kimya Anabilim Dalı

Temmuz 2021, Sayfa: xii + 64

Gallik Asit polifenol, Kuersetin ise flavonoid yapısında olup her ikisi de oldukça güçlü antioksidan ve biyolojik olarak aktif bileşiklerdir. Önemli uygulama alanlarından biri ilaç endüstrisidir. Bu maddelerin antikarsinojenik, antioksidatif, antimutajenik, antialerjik ve antiinflamatuar etkileri olduğu yapılan çalışmalarla belirlenmiştir. Fenolik yapıdaki bu bileşiklerden elde edilen çeşitli metalik nanopartüküller (NP) özellikle nanotıp alanında geniş araştırma alanı bulmuştur. Nanoteknoloji geliştikçe 1-100 nm boyuta sahip bu nanopartiküllerin tıbbi kimya, malzeme bilimi ve ileri teknoloji ürünleri ile eczacılık alanında kullanım alanı gün geçtikçe genişlemektedir.

Bu tez çalışmasında Kuersetin ve Gallik asit kullanılarak gümüş, bakır ve bunların farklı kombinasyonlarında (Kuersetin Ag/CuNP, Gallik Asit Ag/CuNP, Kuersetin+Gallik asit AgNP, Kuersetin+Gallik asit CuNP, Kuersetin+Gallik asit AgCuNP) nanopartiküller oluşturmak için optimal pH belirlendi. Sentezlenen nanopartiküller, UV-VIS spektrofotometre, X-ışını difraktometresi (XRD), Fourier dönüşümü kızılötesi spektroskopisi (FTIR), enerji dağıtıcı X-ışını spektroskopisi (EDS) ve taramalı elektron mikroskobu (SEM) kullanılarak karakterize edildi.

Sentezlenen nanopartiküllerin, Escherichia coli, ve Staphylococcus aureus gibi insan patojenlerine karşı minimum inhibisyon konsantrasyon (MIC) değerleri hesaplandı. Gallik asit ve kuersetinden elde edilen nanopartiküllerin MIC değerlerinin Gallik asit ve Kuersetine göre oldukça etkili olduğu belirlendi.

Anahtar Kelimeler: Kuersetin, Gallik asit, Gümüş Nanopartikül, Bakır nanopartiküller, Bimetalik nanopartikül, Optik Özellik, Antimikrobiyal, Minimum inhibisyon Konsantrasyonu (MIC).

LIST OF FIGURES

Page

LIST OF TABLES

SYMBOLS AND ABBREVIATIONS

Symbols

Abbreviations

AgNPs	Silver nanoparticles
CNT	Carbon nanotubes
CuNPs	Copper nanoparticles
DSC	Differential scanning calorimetry
EDX	Energy dispersive x-ray spectroscopy
FTIR	Fourier Transform Infra-Red spectrophoto meter
FWHM	Full width at half maximum
NMs	Nano materials
NPs	Nanoparticles
NSMs	Nano structured materials
SEM	Scanning electron microscope
TGA	Thermo gravimetric analysis
UV-Vis	UV-Visible Spectroscopy
XRD	X-Ray Diffraction

1. INTRODUCTION

Nanoparticles include specific physical, chemical, and biological properties. Describe the characteristics as the group departments with the branch can access them. Due to its sound antimicrobial effects, in particular, nanoparticles of the mineral have been found for use in pharmaceutical and industrial sectors where specific assets are possible [1].

Score-scale factors that achieve the ratio of surface area to the volume are very high, and single chemical and physical defences make their potential antimicrobial agents [2,3]. Silver nanoparticles (AgNPs) can be used in electronics, bio-sensing, apparel, foods incense, incense, cosmetics, and beauty and NPS is widely used in commercial quantities. Its accepted use increases the human impact on NP and the potential danger associated with its brief and toxic toxicity [4]. Of nanoparticles, in specific, nano-powders with extraordinary properties, such as high surface to volume ratio, low heat power, dispersibility, wettability, sticking nature, size range, and versatility in use, has gained the attention of science. Metals and oxides in metals and nano-powder based on ceramics have been recorded as the most commonly used in environmental and energy systems. Typical examples of nanoscale metal powders are including Silver (Ag), Gold (Au), Platinum (Pt), Palladium (Pd), Rhodium (Rh), Nickel (Ni), Iron (Fe), Cobalt (Co), Cadmium (Cd), Copper (Cu) and Iridium (Ir) are all metals. Belongs to for cloth oxide, Manganese dioxide (MnO_2), Titanium dioxide (TiO_2), Zinc oxide (ZnO), four of the strongest examples are Copper oxide (CuO), Iron oxide (Fe_2O_3), and Cerium dioxide (CeO_2) [5,6].

However, the most important advantage of NPs is that it does not cause bacterial resistance, which is currently the biggest problem in the treatment of bacterial mastitis in AgNPs cows, CuNPs, and Silver particle complex copper (AgCuNPs) in different studies from different scientific fields [7]. Also, the colloids of these NPs are widely available and inexpensive commercially. The previously mentioned studies have mainly focused on in vitro testing, but the results can also be used in practice, for example, in the treatment of mastitis and obstructions [8]. NPs must be prescribed as effective agents against pathogenic species that cause udder infection to achieve this goal [9]. Therefore the authors of these articles decided to set up a series of experiments to assess whether AgNPs and CuNPs can be used in the treatment and prevention of subvocal inflammation, for example, a needle and a needle in addition to the antiseptic preparations before [10]. However, mineralized NPs may not be toxic to external glandular tissue in cattle and should also be safe for humans. Consequently, the studies that have been conducted should include the effect of NPS on human and animal cells [11].

Among metal nanoparticles, Copper nanoparticles (CuNPs) continued to increase globally due to their optical, electrical and melting equity [12]. Confusion is cost-effectively related to Silver (Ag), Gold (Au), also Platinum (Pt) [13]. Interest is clear against the literature this stable

CuNPs fusion is difficult to work, and different methods of CuNPs synthesis have been advanced, including physical, chemical, and biological action [14]. Copper and CuNPs accept in incorporate from different plant extracts. Plant extracts of magnolia leaves, Ciumium aromatic, Euphorbia Giulia, Sterculia Uranus, and Euphorbiaceae contain biomolecules in the latex, reducing Copper ions to CuNPs [15,16]. Ask questions around the nanoparticle based in vegetative stratum, which has been shown to exert biological activities like antibacterial, antioxidant, and antitumor agents [17,18].

Researchers have developed several synthetic routes for the fabrication of nanoparticles that revealed a notable benefit to nature & the environment through safe, non-toxic, and environmentally acceptable methods of "green chemistry," which included organisms such as bacteria, fungi, plants [19]. Many researchers and scientists have shown great power in their unique characteristics and found that they have particular applications in different fields, but numerous materials of nanoparticles have reported toxicity at the nanoscale level. To overcome the toxicity issue, nanotechnology and green chemistry merge to produce nanoparticles that are friendly to nature via plants and microbes, etc [20]. Due to its antimicrobial activity, Silver has been selected in either NPs or ionic form and less toxicity to mammalian cells [21].

In this thesis study, the optimal conditions (pH, substance amount temperature and time) to form nanoparticles in Silver, Copper, and different combinations (Quercetin Ag/CuNP, Gallic Acid Ag Cu/NP, Quercetin + Gallic acid Ag/NP, Quercetin + Gallic acid CuNP, Quercetin + Gallic acid AgCuNP) using Quercetin and Gallic acid were determined. The synthesized nanoparticles were characterized using UV-VIS Spectrophotometer, X-ray Diffractometer (XRD), Fourier Transform Infrared Spectroscopy (FTIR), Energy-Dispersive X-ray Spectroscopy (EDS), and Scanning Electron microscopy (SEM). Moreover, Minimum Inhibition Concentration (MIC) values were calculated against human pathogens such as Staphylococcus aureus and Escherichia coli.

1.1. Quercetin

Quercetin is part of the quercetin family of flavonoid-derived polyphenols. This word has been in use after all 1857. Quercetin is present in plants like apples, red wine, onions, and broccoli, a significant origin of quercetin. Several researchers have demonstrated the careful effects of quercetin across various contamination such as respiratory disease, cardiovascular disease, cancer, and neurodegenerative confound. Quercetin has been advertised to modulate intracellular signalling pathways. Quercetin also controls the behaviour of individual Kinases that alter the phosphorylation case of object molecules, leading to the in flexion of cell activity and wound-healing RNA expression [22]. Quercetin is a naturally occurring flavonoid. It is a natural inhibitor of the transport of polar auxins. The ability to quercetin is emulsifiable in ether, and

methyl-alcohol is also soluble in ethyl-alcohol, propanone, pyridine, acetic acid there in water insoluble [23].

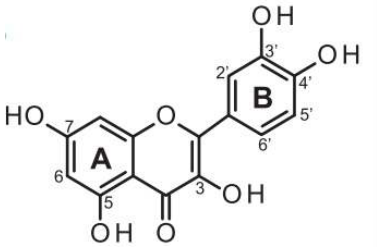

Figure 1.1. Chemical composition of quercetin 2-(3,4-dihydroxyphenyl)-3,5,7-trihydroxy-4H-chromen-4-one

Quercetin is a polyphenol flavonol. It is present in many fruits, berries, leaves, seeds, and grains, red onions, and kale are common foods containing large amounts of quercetin. The quercetin is an important natural free radical chemical agent and easily forms complexes with many metals. Molecular Formula: $C_{15}H_{10}O_7$, molecular weight: 302.2357 gr/mol, common name: quercetin (3, 5, 7, 3', 4'-pentahydroxyl flavone) this consists of two connected aromatic rings (A and B) with a loop of C-prone. It is expected that the most acidic hydroxyl group that's the location of the A ring at seven. Physical state: Yellow crystalline powder, Melting Solubility [24-26].

Quercetin (Figure 1.1) is one of the most common flavonoids in the human diet and is found in fruits, vegetables, edible blight, herbs, or related products (apples, onions , ginkgo leaves, red wine) [27-29]. While pharmacokinetic, as well as knowledge on Quercetin bio-availability is scarce and inconsistent. Quercetin has many positive effects such as antioxidants, anti-tumour, and antibacterial activities. This has thus attracted a great deal of attention [30]. Quercetin has many biological effects, such as an effective inhibitor, Effect on the development of several lines of animal and human cancer cells [31], cardio protection, anti-cancer, anti-ulcer, anti-allergic, anti-inflammatory, anti-inflammatory, Increases the ant proliferative effects of cisplatin in-vitro and in-vivo [32] and antiviral, ant proliferative activities [33]. Also, the antioxidant Quercetin exhibits property and effectiveness against diseases of neurodegenerative origin **[**34,35]. Nuengchamnong and others stated that Quercetin antioxidant activity is higher than the well-known Trolox, Ascorbyl, and Rutin antioxidant molecules **[**36].

This is due to the number and role of the free hydroxyl groups in the Quercetin molecule [37]. Thus, the pharmacological effects of Quercetin, including anti-tumour [38] and effective wound healing; have been extensively investigated [39]. Therefore, to increase the solubility of Quercetin, a stable, safe, and efficient distribution method is required. Alternative forms of Quercetin have been developed, such as liposomes and nano-capsules, reducing the dosage and enhancing the treatment compound effectiveness [40].

1.2. Gallic acid

Gallic acid (really acknowledged like 3,4,5-trihydroxy benzoic acid) is a trihydroxy benzoic acid including the shape $C_6H_2(OH)_3CO_2H$. Walnuts, sumac, witch hazel, tea leaves, oak bark, and some more tree contain phenolic acid. Walnuts, sumac, witch hazel, tea leaves, oak bark, and some more trees contain phenolic acid. This form knowledge about the Folin-Ciocalteu reactions and the exact reason for choosing Gallic acid is used the standard.

The reasons are: partly for historical reasons; furthermore, it is cheap, soluble in water, easily recrystallized from water, easily dried, and stable in dry form. The plant contains in nature Gallic acid and its derivatives, including bark, wood, leaf, fruit, root, and seed, in almost every field. In popular foodstuffs, they are present in various concentrations, such as hazelnut, blueberry, tea, cashew, blackberry, strawberry, plums, grapes, mango, nut, walnut, wine, etc [41].

Gallic acid, a natural plant polyphenol, is a powerful antioxidant [42]. Gallic acid (Trihydroxy benzoic acid) is an inherently phenolic antioxidant with strong antipyretic, anti-mutagenic, and anticancer properties. However, for a shorter half-life and rapid elimination from the body, the molecules will be prescribed frequently to be formed in fruits, berries, nuts, and seeds. Tea, red wine, citrus fruits, and more foods are the suggestions. The structure of gallic acid is given in (Figure 1.2).

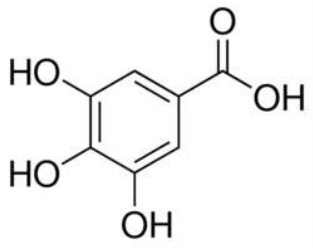

Figure 1.2. Structure of Gallic acid

Natural plants, fruits, or foods have recently been accepted as a valuable ability to expand new and borrowed cancer treatments in recent decades [43,44]. Plant-derived anticancer drugs such as paclitaxel, phenelzine, or vincristine have now been shown to be effective in clinical cancer pathways [45-47]. Gallic acid (Trihydroxy benzoic acid) is a polyhydroxy butyric acid that can begin collecting plants, fruits, and foods [48,49]. Plant elements of antitumor activities are the same for antibacterial, antiviral, and anti-inflammatory activities, as the plant elements of antitumor activities are the same for various plant activities cancers of the prostate and lungs [50-51].

In laboratory studies, we have previously shown this Gallic acid (3,4,5-trihydroxy benzoic acid), a logical flower phenol obtained far from the hydrolysis of tannin, has a good effect on lung cancer cells in human to induce apoptosis [52]. Gallic acid can be orally ingested in on-the-go

foods and herbal medicines and tends to be given more safely to cancer patients linked to harmful chemotherapy drugs. The antitumor effects of the in vivo conduct of gallic acid are no longer recorded. Therefore, interest is needed to explain the in vivo antitumor property of gallic acid in combination with cisplatin against lung cancer cells and its preservative or synergistic action.

1.3. Polyphenols and flavonoids

Polyphenols, a wide range of chemicals found in plants, have piqued interest in recent decagon due to their property and the wish that it will demonstrate beneficial health the results, whether assumption food inputs or supplements [53]. Phenolic composite is the maximum standard chemical classes found in plants. Polyphenols are polyhydric phytochemicals with more structure, with over 8,000 compounds estimated and discovered [54]. Flavonoids, phenolic acids, and stilbenoids are the three principal subcategories of flavonoids.

It is possible to expect bio availability and, at best, low plasma micro molar concentrations. It is doubtful whether polyphenols contribute significantly to the antioxidant capacity of human plasma.

Consumption of flavonoid-rich drugs is considered the translation of foods, especially fruits and vegetables. In terms of human health benefits: Epidemiological benefits associated with reduced Heart disease, cancer, and stomach disease are all on the rise and neuropathy, liver disease, atherosclerosis, obesity, and allergies . A powerful antioxidant is polyphenols. They are strong. Free radicals can be removed. We thought that the first health benefit associated with polyphenol intake from the diet was due to antioxidant.

By definition, the majority of isolated compounds belong to this group the flavonoid subclass. Flavonoids consist of two or more fragrant bells containing one or more hydroxyl-containing compounds phenol groups and bound by carbon bridges [55]. An aromatic ring (ring A) is joined by another organic atom and connected to another organic ring (ring B) using a carbon bridge. When a chain three in total carbons is attached, A hydroxyl group is a kind of hydroxyl group - as a molecular ring, The structure created becomes cyclic (C-ring). The majority of flavonoids have this type of phenylbenzopyrene structure: they are divided into a few (ketones, hydroxyls) and have the C-ring has a double bond or not. These subcategories are Flavon, Isoflavones, Flavanone, Flavonol, Chalcones, Dihydrocaps, and Anthocyanidins.

The subcategories of flavanols are divided into monomers (catechins) and polymers (proanthocyanidins, theaflavins, and the origins) [56]. Subcategories depend on the C-B-ring ring's stance and its functionality.

Phenolic acids are generally two significant divisions classes. It consists of benzoic acid containing seven carbon atoms or cinnamic acid-containing nine carbon atoms [57]. These are all hydroxyl compounds. Gallic acid, Chlorogenic acid, caffeic acid, ferulic acid, and coumaric acid

are also antioxidants. Are all examples of acids and genetic acids are prime representative examples of isolated compounds. Multivalent stilbenes form a minor subclass of stilbenoids, of which resveratrol is the principal representative.

These polyphenols are found in plants and are esterified with glucose or other carbohydrates (glycosides) or as free aglycones. This contributes to their sophistication and a large number of distinct and recognized individual materials Polyphenols obtained from fruits as a source of dietary polyphenols (strawberries, apples, citrus fruits, cherries), vegetables (onion, celery, beer grains, soybeans), herbs, roots, and spices (ginkgo, turmeric), red wine and green tea [58].

Recently, many citrus studies have been conducted. It also contains Green tea contains flavonoids and polyphenols. These compounds include antibacterial, antitoxin, antiviral, and antifungal functions are shown in conclusion [59]. In some studies, flavonoids and other polyphenol compounds have potent in vitro antioxidant activity in the system, but some others, they may serve as antioxidants. Whether any of the pro-oxidants, antioxidants or many other biological effects of flavonoids contribute to or add to the health advantages of a flavonoid-rich diet, plant-based foods and products are unknown [60].

Phenolic compounds help protect the digestive system from the effects of active species found in food or produced in the intestines and stomach. The health benefits of aggregate flavonoids are unknown, and flavonoids in fortified foods and supplements are not yet widely consumed. A large class of compounds found in plants are polyphenols the presence of various phenolic units or structural blocks per molecule distinguishes them. The phenol unit is made up of a 6-membered aromatic hydrocarbon ring directly attached to the hydroxyl group (-OH). Phenol (C_6H_5OH) is the most basic of the group and has long been used as a preservative (Figure 1.3).

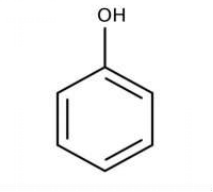

Figure 1.3. Structure phenol

For Polyphenols, various biological properties have been proposed, including antioxidant, antimicrobial, anticancer, anti-inflammatory, and anti-diabetic effects [61,62].

In chemical structure, polyphenol compounds are diverse, and this is one basis for achieving classification. The degree of oxidation, hydroxylation, methylation and glycosylation is the most common variation in the chemical backbone. Phenolic acid, flavonoids, and no flavonoids are the major classes of polyphenols, and the latter subclass includes stilbenoids,

lignans, tannins, and diallyl heptanoids (Figure 1.4). Non-flavonoid polyphenols contain less common subclasses.

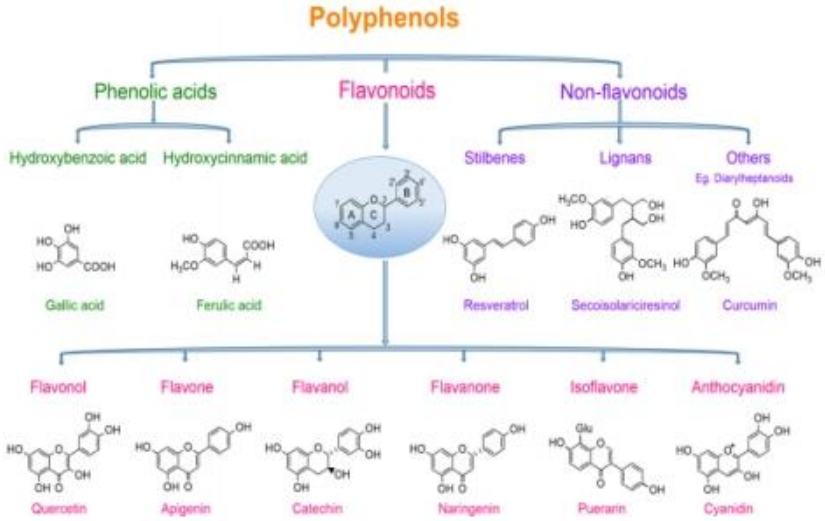

Figure 1.4. Structure polyphenols classification.

1.4. Methods for Nanoparticle synthesis

1.4.1. Chemical methods of synthesis

Chemical decrease with organic and inorganic decrease agents is the maximum widely accepted method for synthesizing silver nanoparticles. Sodium citrate, Ascorbic acid, Sodium borohydride ($NaBH_4$), Elemental hydrogen, Polyol, Tollens reagent, N, N-dimethyl formamide (DMF), poly block co polymer (ethylene glycol) and other reducing agents are commonly used to dissolve silver ion (Ag^+) in water, whether aqueous or non-aqueous. The agents that reduce described above decrease silver ions (Ag^+), contributing to a structure silver metallic (Ag^o) and subsequent oligomer cluster formation. These clusters inevitably result in the formation of silver metal colloidal particles [63].

The use of protective agents to stabilize the dispersible nanoparticles is essential. It prevents their aggregation during the preparation of metal nanoparticles and during the defence of nanoparticles that can be absorbed or bound to nanoparticles surface [64]. The presence of functional surfactants for particle surface interactions (e.g. thiols, amines, acids, and alcohols) stabilizes the development of particles also protects particles derived. Sedimentation, agglomeration, and erosion all result in a loss of surface properties create.

The Tollens technique, a straightforward one-step procedure, has recently been used to synthesize controlled-sized silver nanoparticles. Tollens is a modified version of Tollens. Process, silver ions are decreased by sugars ammonia is present to produce Films of silver nanoparticles (50-200 nm), silver hydrosol silver nanoparticles (20-50 nm) in a variety of different shapes are

all examples of silver nanoparticles will happen [65]. The job of the protectant is to protect the nanoparticles from agglomeration [66]. Polymers are the most widely used protective agents. Ethylene glycol (poly) is a chemical used to make PEG (vinyl pyrolidone), poly (methyl methacrylate) (PMMA), and poly (methacrylic acid) (PMAA), two types of polymers (PVP).

These are inexpensive and straightforward nanoparticle synthesis processes; usually, at temperatures below 3500^{o}C can be create large quantities of materials with different particle sizes and shapes. The advantage of the chemical synthesis approach is construction and quality in construction. Synthesize new sophisticated products into finished products. While there are many techniques, such as the precipitation method, in which nanoparticles are produced in the form of precipitates, the immobilization method is used to produce particles in ash or powder [67].

1.5. Physical methods of synthesis

Nanoparticles can be used in a variety of ways and produced using a variety of physical processes. These methods are of two types: mechanical form and vapour deposition form. These technologies are used at high temperatures. Usually, the maximum working temperature is over 3500^{o}C. Metal nanoparticles are fabricated by the physical method either by evaporation or condensation or by the laser ablation process. The reaction is carried out in evaporation condensation at ambient pressure, using a tube furnace. Inside the sail, the target material is kept, and the gas concentration in the furnace is evaporated into a carrier gas [68]. Ag, Au, Pb, and fullerene nanoparticles were successfully synthesized using an evaporation process. However, this approach has certain drawbacks, like a giant tube oven that powers a large oven that absorbs a large amount of electricity into space, growing the air temperature about the source. It takes a long time to bring about thermal equilibrium [69] fabrication laser ablation of silver nanoparticles. The ablation process depends on the particles manufactured by the laser on the wavelength of the laser, as the beam pulses the laser period. Laser fluency, length of ablation period, and active liquid medium may or may not contain surfactants [70]. The physical processes that work best are laser evaporation, condensation, and ablation. Evaporation was previously used to synthesize and condense processes for several metal nanoparticles, including silver; copper, lead sulphide, cadmium sulphide, and fullerene are all examples of metal sulphides.

Chemical methods have the advantage of avoiding contamination of thin films with solvents and ensuring uniform nanoparticle distribution. On the other hand, physical methods have the disadvantage of avoiding solvent contamination in thin films [71,72]. Silver nanoparticles have been demonstrated to be manufactured with a household heating source; a small ceramic heater is constructed. The evaporated vapour will cool at an appropriate amount because the temperature gradient near the surface of the boiler is steeper than that of a tube furnace. Small nanoparticles can form in high concentrations as a result. For long-term inhalation

experiments, this type of physical approach may be used as a generator of nanoparticles as a titration system for toxicology research and equipment testing with nanoparticles [73]. Ablation of bulk materials by laser metal materials in the solution can produce silver nanoparticles [74,75].

The ablation effectiveness and properties of silver nanoparticles are affected by laser energy wavelength affecting the metallic object, a laser's duration pulse (within the femtosecond, picosecond, and nanosecond ranges), the laser fluency, and the procedure for the ablation period active liquid medium with or without surfactants [76,77].

The laser ablation technique has several advantages over other colloid treatment techniques, including the lack of chemical reagents, which are a type of reagent used to make chemicals in the suggestions. A pure and unpolluted metal, therefore, colloids can be made ready with its application methodology for future use [78].

1.5.1. Biological methods of synthesis

While chemical and physical methods are very good at generating specific nanoparticles, some production costs, dangerous by-product release, long manufacturing time, and difficulty in purification, global warming and climate change have contributed to the synthesis of the macro molecule, in a fraction of a minute the synthesis claim of buildings to the need for environmentally sustainable technology in materials science [79].

Because the direction of biological or green synthesis is exceptionally random, economical, eco-friendly and non-toxic, using biological species like microorganisms, plant extracts, and biomass may be the best alternative approach to synthesize. By using physical and chemical methods, nanoparticles can be created [80]. Biological factors like bacteria, fungi, leaves, algae, also plants are taken into consideration. As part of the current and practical biosynthesis approach, materials will catalyse complex interactions. Due to its enzymatic reactions, photochemical properties, and medicinal nature, the current potential of a biological system has gained commercial significance [81]. As a result of their synthesis of nanoparticles, the biological system produced a remarkable and pioneering improvement. The method of the process by which the bio-reduction of mineral salts is carried out remains a mystery [82].

In recent years, researchers have become increasingly interested in methods of green chemistry that use natural lowering, covering, silver nanoparticles with the desired shape and size, and stabilizing agents [83,84].

Using bio molecular combinations discovered in extracts of many organisms (e.g. Amino acids, polysaccharides, and vitamins are all examples of enzymes/proteins), metal ion bio-reduction is environmentally friendly but chemically complex. Various studies have demonstrated the effective composition of silver nanoparticles using species (biological processes and microorganisms) [85,86].

1.6. Characterization Methods

1.6.1. UV-VIS spectra analysis

Absorption Spectroscopy is a term that refers to the study of light used to figure out a solution's optical properties. The volume of light absorbed is determined after the light is consumed into the sample solution. The wavelengths are mixed, but the absorbance remains constant regardless of wavelength. The optical properties of studying nanoparticles are more complex. For example, the calculated absorption range may not reflect the appropriate absorption because the pair of light absorbed and scattered from the molecule is the extinction of the radiation. These wavelengths arise due to the broad resonance of the molecule.

1.6.2. FT-IR analysis

FTIR is a chemical analytical technique that tests the wavelength of infrared intensity v/s or the size of an optical wave. It has been used to examine potential biomolecules and also to link interactions between them. The vibration properties of the sample's chemical functional groups are determined by infrared spectroscopy. When infrared radiation interacts with material, the chemical bonds will reveal the shape of expansion, contraction, and bending. These chemical functional groups appear to absorb electromagnetic radiation from forming the rest of the molecule in a unique wavelength range. We used FTIR spectroscopy for the determination of the functional groups. FTIR is shown Figure 1.6.

1.6.3. SEM and EDX analysis

SEM stands for Scanning Electron Microscopy (SEM) and is a set of electron microscopy that produces an image of a pattern by scanning an area with a focused electron beam. The electron is communicated by the atoms in the sample and produces various signals that provide information about the surface topography and the formation of the example. SEMs (scanning electron microscopes) are microscopes that use electrons to create three-dimensional (three-dimensional) images. As the more narrow electron beam, SEM microscopic images accept a broad base of the field, resulting in a distinctive 3D shape that is appropriate for securing the surface architecture of the sample.

1.6.4. XRD analysis

X-ray diffraction (XRD) analysis is a method used in materials science to determine the crystallographic structure. (XRD) is a method of combining a sample, crystal structure, texture, or orientation in the analysis process. It is used to identify the crystalline steps in the material and reveal details about the chemical composition.

1.7. Nanoparticles anti microbiological

There are many chemical and physical techniques in the production of nanoparticles that are well known. Still, there are drawbacks to them if they can increase their production, hazardous by-amount, great synthesis times, and complication in approval [87]. Global warming, along with climate change, will reduce global toxic and dangerous waste if you can increase it through green synthesis with advanced advances in science and industry [88]. As the name implies, the synthesis of nanoparticles helps to synthesize very complex reactions in a matter of minutes, drawing your attention to the synthesis of the need for benign environmental materials technologies.

The use of animal-like biological microorganisms, organisms found in plants, bio toxins may be the optimum alternative to physical also chemical methods for the fusion of nanoparticles. As a result, they are highly spontaneous, economical, and environmentally friendly due to their biological or green synthesis. As part of a modern, practical biosynthesis strategy, natural resources like electricity, Bacteria, fungi, yeasts, algae, and plants are all kinds of microorganisms (**Figure 1.5**). It can also act as catalysts. Due to enzymatic reactions, photochemical properties, and plant nature, the current landscape of the commercial health biological system has been found. Due to their mechanism, the natural system has made a unique and pioneering advance in the synthesis of nanoparticles, which reduces the bio degradation of metal salts that have not yet been reopened [89].

The synthesis of nanoparticles from biological systems for medical, pharmaceutical, cosmetic and environmental applications has attracted great interest. Bio-made because nanoparticles may be dispersed or penetrated through Pollutants and explain a redox reaction to clear surface materials and be used for purification. Nature has s few prepared equipment for the synthesis of nanomaterials also micro particles that helps to develop a relatively modern and undiscovered research area depend on the synthesis of biomaterials.

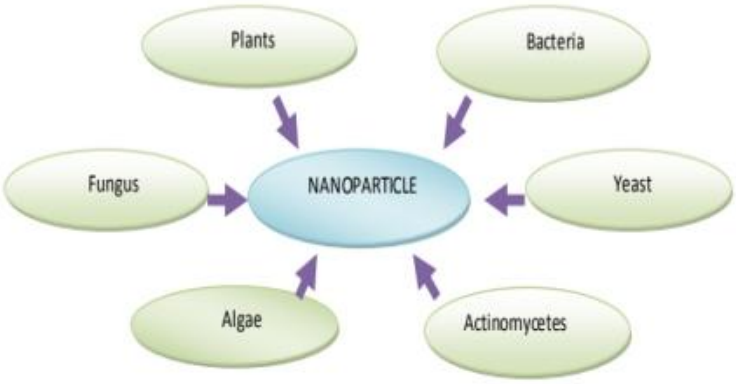

Figure 1.5. Different pathways for nanoparticle synthesis

Bacteria

Many microorganisms can synthesize mineral nanoparticles such as silver, gold, magnesium, cadmium sulfide and silicon oxide nanoparticles. The protection of a bacterial cell to silver ions in the nanoparticle synthesis medium [90]. It includes previously been reported that Bacillus subtilis 168 can produce Au^{3+} Plants Yeast Bacteria Fungus Algae Actinomycetes nanoparticle 9 ions to produce 5-25 nm octagonal gold particles in bacterial cells by nurture cells with gold chloride [91] at ambient temperature and Reduce pressure. The bacterial strain of silver resistance Pseudomonas stutzeri AG259 may accumulate silver nanoparticles in cells with a particle size of 35 to 46 nm with silver sulfide [92]. Lactobacillus, a prevalent bacterial strain found in buttermilk, synthesizes a well-defined morphology of both Au and Ag NP under normal conditions. Synthesis of Ag metal nanoparticles using Klebsiella pneumonia, Escherichia coli, and Enterobacter cloacae culture supernatants was described by [93]. maximum metal ions get a toxic result on bacteria, so the defence mechanism created by bacteria to counteract such toxicity is to reduce ions or form water-soluble complexes [94].

In general, living organisms' enzymes play an essential role in biological regeneration, but other studies are produced conflicting findings in cases where biological degradation processes were not enzymatic. Bacillus megatherium D01, Lactobacillus sp. A09 was able to reduce silver ions. Silver ions are relieved when they interact with groups on microorganism cell walls.

The presence of the nitrate reductase enzyme, which disciple nitrates into nitrite, is the most well-known mechanism for forming biological silver particles. Alpha nicotinamide adenine dinucleotide reductase (NADPH) - approved in vitro nitrate reductase synthesis, bacteria, alpha nicotinamide adenine dinucleotide phosphate (NADPH) - a nitrate reductase depletion step. As a result, when the nitrate is reduced, the electrons are converted. This is found in Bacillus licheniformis, which relies on NADPH and NADPH enzymes as nitrate reductase to convert Ag^{+} to active Ag^{o}.

Fungi are it possible to generate their value relative to energy because, when included, they secrete proteins that, if they change, are converted directly into nanoparticles [95]. Strength has been described as the best nano-plant for air bacteria because if a high bond with metal ions is maintained in a closed area, it facilitates them with solid bed release. You can grow on the surface of the mineral deposit. Metals as catalysts are distributed efficiently. The advantage of making extracellular nanoparticles from fungi is that large quantities of pure, protein-free enzymes can be used in a simple process.

Reported proteins stabilize a very steady improvement in the particles via fungi in the development of Ag hydrosols using Fusarium oxysporum [96]. Using Aspergillus fumigation, extracellular biosynthesis of Ag molecules was observed in the range of 5-25 nm [97]. The biochemistry of Phaenerochaete chrysosporium, also known as the white mould fungus, has been used to study the biomimetics of Ag nanoparticles [98]. Creation of spherical and stable Ag particles in the range of 10-60 nm using Fusarium architecture [99].

Actinomycetes:

Actinomycetes are microorganisms that later have essential properties such as fungi and bacteria. Actinomycetes now focus on the synthesis of metal nanoparticles due to their use in the production of secondary metabolites such as antibiotics [100]. Thermomonospora sp, a tradition of Au nanoparticles using excessive actinomycetes, the alkali, and Rhodococcus sp., they discovered that nanoparticles have a more significant impact on the cytoplasmic membrane than on the cell wall.

This may be because enzymes in the cell wall and cytoplasmic membrane reduce metal ions, but not in the cytosol [101].

Algae:

Algae in the plant kingdom are collections of texts that have been studied for their use in nanotechnology. Reported the synthesis of Chlorella Vulgaris algae with Au nanoparticles [102]. Reported the controlled synthesis of Au nanoparticles using the green algae Plectonema boryanum with the team using the aqueous solutions Au (S_2O_3) 23 and $AuCl_4$ [103]. The rapid development of gold nanoparticles through extracellular biosynthesis has been observed in the seaweed Sargassum wightii [104]. Morley reported the production of CdS nanocrystals for phytochelatin coating using the algal phytoplankton Phaeodactulum tricornatum. Reported the synthesis of 5 nm PtCl62 aqueous Pt using Shewanella algae at neutral pH and room temperature [105].

Plants:

Plants of different microorganisms like bacteria, algae, fungi, also yeast can be used in the biosynthesis of nanoparticles. However, a modern trend has recently emerged, such as using plants to produce nanoparticles due to the automatic and cost-effective protocol and cost-effective

nature [106]. It is applicable for large-scale production and one-step biosynthesis methods. The presence of chemicals is the primary proposed mechanism for the synthesis of plant nanoparticles [107]. The most important chemicals are flavonoids, terpenoids, carboxylic acids, quinones, aldehydes, ketones, and amides responsible for the automatic reduction of ions, flavonoids, terpenoids, carboxylic acids, quinones, aldehydes, ketones, and amides [108]. The presence of chemicals is thought to be the primary mechanism involved in the formation of plant-mediated nanoparticles [109,110].

The main chemicals necessary for the automatic reduction of ions are flavonoids, terpenoids, carboxylic acids, quinones, aldehydes, ketones, and amides [111]. Plants such as Cinnamomum camphora, Pelargonium grade lens, Azadirachta indica , Emblica Officinalis, Aloe vera, Alfalfa bud, Helia [112,113].

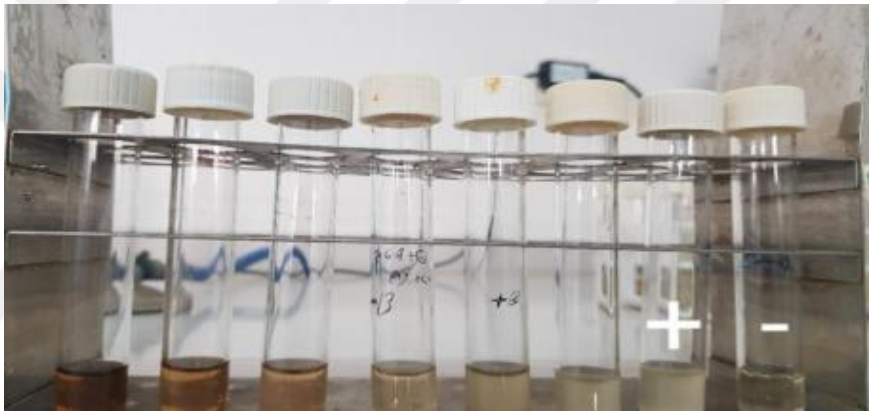

Figure 1.6. Determining the minimum inhibitory concentration (MIC) of the matters by using the broth dilution method.

After the incubation period, it was observed that clearance (negative) and turbidity (positive). Positive means that bacteria grow at this tube, but the mean point at these two tubes is the minimum inhibitory concentration (MIC) (Figure 1.6). At this point (2.11 mg), kill 6 logs of the bacteria Escherichia coli.

1.8. Review of literature

NPS, used in bio-assay, clothing, food production, paint, sunscreen, cosmetics, and uses, is produced in various commercial products such as nanoparticles (AgNP). Daily use for needings increases human exposure to NP and both short and long-term toxicity and overall risk. Interest in metal nanoparticles as antimicrobial agents has been around for more than ten years [114].

Nanoparticles are in very little quantity due to the ability to make many particles and the large surface-to-volume ratio. Ag nanoparticles are a widely used method for medical

applications [115]. Copper is non-toxic to mammals, but toxicity to many microbes offers a new perspective on antibacterial therapy. Many practices have been advanced to produce Ag and Cu nanoparticles using both physical and material. The most common technique of preparing Ag nanoparticles is to reduce a silver salt solution in water or an organic solvent to produce a colloidal preparation [116]. The most common method for synthesizing Cu nanoparticles is by creating micro emulsions. However, it requires a large number of surfactants and organic solvents, which increases the production cost. Physical methods using laser, radiolysis, or aerosol erosion methods are necessary, but expensive tools also consume large amounts of energy [117].

These methods use valuable substances that are toxic and pollute the environment. Chemical reduction methods are the cheapest and best opportunity for the provider to adapt to the situation. Ag nanoparticles have been synthesized using water as a solvent and emitted as a coating material and have been shown to have advantages over other methods along with environmental chemicals [118,119]. Ag, Au, Pd, Se, Cu, and Pt are examples of metal nanoparticles. Biological catalysts were further used to constitute Proteins/enzymes, polysaccharides, alkaloids, flavonoids, terpenoids, phenolic compounds, and vitamins are all con founders in the reduction, creation, and classification of plant mineral nanoparticles [120-122]. Shankar and co-worker have created synthetic nanoparticles through plant-mediated synthesis. In this experiment, Azadirachta indica (Neem) leaf broth was used to produce core-shell nanoparticles Ag-Au, Ag, and bimetallic use of chemicals such as flavonoids and terpenoids in the leaves to reduce the same silver and gold ions mixture. This is possible because of reducing sugars and terpenoids that act as reducing / inhibiting aids in this study. The reaction rate was monitored using a UV-Vis spectrophotometer. From their findings, the reaction rate was faster in mixing two metals (1:1in Ag^{+}: $AuCl^{-4}$). Spherical Au/Ag composite nanoparticles by an average size of 50-100 nm were approved by TEM [123-125].

The EDAX spectrum also indicates silver and gold in one of the core particles in the experiment. In the formation of metal hybrids, Ag NPs were formed after the equilibrium of Au NPs as reported. In use, Ag NPs are assembled on the largest Au NPs surface, indicating the measurement and shape of Au/Ag shell core nanoparticles [126,127]. Another study in this experiment considered the formation of other metal bimetallic nanoparticles and metal hybrids using plant extracts rich in chemicals to replace harsh and toxic organic solvents. Silver nanoparticles (AgNP) were synthesized at room temperature using reducing properties of mulberry leaf extract and silver nitrate. Silver nanoparticles were characterized using attractive UV shielding spectroscopy, Scanning electron microscopy (SEM) and X-ray jumping (XRD). Also, silver nanoparticles have been shown to have effective antibacterial activity against Staphylococcus aureus and Shigella [128,129]. The use of antibacterial agents can be used to combat infections. Under these conditions, routine use of antibiotics leads to antibiotic resistance

caused by bacterial microorganisms. This study focuses on the production of nanoparticles (NPs) that increase the movement of vancomycin in vitro antibiotics for multidrug resistance (MDR).

Emissions are only available for the biosynthesis of silver nanoparticles (AgNP), where the vapour is isolated from aquatic plants recruited from low molecular weight polyols. In this first study, the juice and leaves of Ph. L leaf and seed extract was used to synthesize relatively "green" AgNP and isolated [130]. AgNP was generated from Ag (I) ions by extract colour change, UV-Vis absorption, and plasmon surface intensification (SPR). The size, distribution, and primary and crystalline state of AgNP generated were determined by electron microscopy and spectroscopy. The results indicate the formation of a globular AgNP of several paracetamols with a size of 52.6 nm (broth leaf) and 24.2 nm (grain broth) for good which is isolated in the organism used copper nanoparticles during the chemical reduction process Atomic force microscope (AFM) Slows down the morphology of the study surface. The formation of nanoparticles from copper has been confirmed by UV-Vis spectrophotometer (X-ray diffraction) (XRD) and infrared spectroscopy (FTIR). The diameter of copper nanoparticles using chemical reduction methods is between 14nm and 55nm. The structure of the face-centred cubic crystal (FCC) of copper nanoparticles was demonstrated through fabrication analysis [131].

2. MATERIAL AND METHODS

2.1. Reagents and Equipment

- Silver nitrate ($AgNO_3$).
- Copper (II) nitrate (Cu $(NO_3)_2.3H_2O$).
- Quercetin.
- Gallic Acid.
- Potassium Bromide (KBr).
- Distilled water.
- Acetone
- Ethyl alcohol
- Sodium carbonate
- Qualitative filter paper 125 mm, watch glasses, measuring cylinders, different sizes of tube, pipet, volumetric flasks clear glass, mortar pestle glass, beakers, conical flasks, test tube racks Funnels, graduated cylinder, Beakers, hot plate, tongs, wortex, micro-pipette, Benzene burner, petri dishes, wire brush, Magnetic Stirrer. Internal digital (Shimadzu Corporation, Japan) analytical balance (with a readability of 0.01 mg), used during the experiment (Figure 2.1.).

2.2. Instrument required

The following equipment was used: The infrared spectrum is registered in the ambit of 5000-3000 cm^{-1} on a Perkin-Elmer spectrum one, Perkin Elmer Fourier Transform Infra-Red (FTIR), UV-Vis spectrophotometer double beam PC 8 Auto Cell, Scanning Electron Microscope (SEM) of the Model Oxford INCAX Act, X-ray Diffraction (XRD) MiniFlex model.

Figure 2.1. Materials

2.3. Quercetin nanoparticles

2.3.1. Quercetin and Ag nanoparticles

Nanoparticles were synthesized using of quercetin and $AgNO_3$. The silver nitrate ($AgNO_3$) solution was prepared at a concentration of 0.01 M in 100 mL of distilled water (0.1699 gram $AgNO_3$ with 100 mL, covered with Aluminum prepare for not reacting with light after preparation). Four beakers were added 10 mL 0.01 M quercetin (0.3022 gram quercetin was solved with 100 mL ethyl alcohold, and 10 mL of $AgNO_3$ (0.01 M) was added drop by drop and mixed homogeneously for four hours for the reaction to happen and producing more quantity of nanoparticles. PH of the solutions were adjusted using 0.01 M Na_2CO_3 (Sodium carbonate) and 0.01 M CH_3COOH (Acetic acid) for each of pH =3, pH=7, pH=9 and pH=11. The best nanoparticles were obtained at pH=9 for this reaction. The colloid solutions were collected and washed several times then stored at room temperature for further experiments. The obtained AgNPs were further purified by centrifugation at 4000 rpm followed by redispersion of the pellet in distilled water then putting into watch glass and entering an oven for drying (Figure 2.2).

Figure 2.2. Preparation of quercetin and silver nanoparticles.

2.3.2. Quercetin and Copper nanoparticles

Nanoparticles were synthesized using of quercetin and Cu $(NO_3)_2.3H_2O$. The Copper nitrate three hydrate (Cu $(NO_3)_2.3H_2O$) solution was prepared at a concentration of 0.01 M in 100 ml of distilled water (0.2416 gram Cu $(NO_3)_2.3H_2O$ was solved with 100 mL water). Four beakers were added 10 mL 0.01 M quercetin (0.3022 gram of quercetin was solved in 100 mL ethyl alcohol), and 10 mL of Cu $(NO_3)_2.3H_2O$ (0.01 M) was added drop by drop and mixed homogeneously for four hours for the reaction to happen and producing more quantity of nanoparticles. PH of the solutions were adjusted using 0.01 M Na_2CO_3 (Sodium carbonate) and 0.01 M CH_3COOH (Acetic acid) each of pH =3, pH=7, pH=9 and pH=11. The best nanoparticles were obtained at pH=9 for this reaction. The colloid solutions were collected and washed several times then stored at room temperature for further experiments. The obtained CuNPs were further purified by centrifugation at 4000 rpm followed by redispersion of the pellet in distilled water then putting into watch glass and entering an oven for drying (Figure 2.3).

Figure 2.3. Preparation of quercetin and copper nanoparticles .

2.4. Gallic acid nanoparticles

2.4.1. Gallic acid and silver nanoparticles:

Nanoparticles were synthesized using of Gallic acid and $AgNO_3$. The silver nitrate ($AgNO_3$) solution was prepared at a concentration of 0.01 M in 100 mL of distilled water (0.1699 gram $AgNO_3$ with 100 mL, covered with Aluminum prepare for not reacting with light after preparation). Four beakers were added 10 mL 0.01 M Gallic acid (0.1700 gram Gallic acid was solved with 100 mL ethyl alcohol), and 10 mL of $AgNO_3$ (0.01 M) was added drop by drop and mixed homogeneously for four hours for the reaction to happen and producing more quantity of nanoparticles. PH of the solutions were adjusted using 0.01 M Na_2CO_3 (Sodium carbonate) and 0.01 M CH_3COOH (Acetic acid) each of pH =3, pH=7, pH=9 and pH=11. The best nanoparticles were obtained at pH=9 for this reaction. The colloid solutions were collected and washed several times then stored at room temperature for further experiments. The obtained AgNPs were further purified by centrifugation at 4000 rpm followed by redispersion of the pellet in distilled water then putting into watch glass and entering an oven for drying (Figure 2.4).

Figure 2.4. Preparation of Gallic acid and silver nanoparticles.

2.4.2. Gallic acid and copper nanoparticles

Nanoparticles were synthesized using of Gallic acid and Cu $(NO_3)_2.3H_2O$. The Copper nitrate (Cu $(NO_3)_2.3H_2O$) solution was prepared at a concentration of 0.01 M in 100 ml of distilled water (0.2416 gram Cu $(NO_3)_2.3H_2O$ was solved with 100 mL water). Four beakers were added 10 mL 0.01 M Gallic acid (0.1700 gram of Gallic acid was solved in 100 mL ethyl alcohol), and 10 mL of Cu $(NO_3)_2.3H_2O$ (0.01 M) was added drop by drop and mixed homogeneously for four hours for the reaction to happen and producing more quantity of nanoparticles. PH of the solutions were adjusted using 0.01 M Na_2CO_3 (Sodium carbonate) and 0.01 M CH_3COOH (Acetic acid) each of pH =3, pH=7, pH=9 and pH=11. The best nanoparticles were obtained at pH=9 for this reaction. The colloid solutions were collected and washed several

times then stored at room temperature for further experiments. The obtained CuNPs were further purified by centrifugation at 4000 rpm followed by redispersion of the pellet in distilled water then putting into watch glass and entering an oven for drying (Figure 2.5).

Figure 2.5. Preparation of Gallic acid and Copper nanoparticles.

2.5. Gallic acid and Quercetin nanoparticles

2.5.1. Gallic acid, Quercetin and silver nanoparticles

Nanoparticles were synthesized using of Gallic acid +Quercetin and $AgNO_3$. The silver nitrate ($AgNO_3$) solution was prepared at a concentration of 0.01 M in 100 mL of distilled water (0.1699 gram $AgNO_3$ with 100 mL, covered with Aluminum prepare for not reacting with light after preparation). Four beakers were added 10 mL 0.01 M Gallic acid+ 10 mL 0.01 M Quercetin and 20 mL of $AgNO_3$ (0.01 M) was added drop by drop and mixed homogeneously for four hours for the reaction to happen and producing more quantity of nanoparticles. PH of the solutions were adjusted using 0.01 M Na_2CO_3 (Sodium carbonate) and 0.01 M CH_3COOH (Acetic acid) each of pH =3, pH=7, pH=9 and pH=11. The best nanoparticles were obtained at pH=9 for this reaction. The colloid solutions were collected and washed several times then stored at room temperature for further experiments. The obtained AgNPs were further purified by centrifugation at 4000 rpm followed by redispersion of the pellet in distilled water then putting into watch glass and entering an oven for drying (Figure 2.6).

Figure 2.6. Preparation of Quercetin, Gallic acid and Silver nanoparticles .

2.5.2. Gallic acid, Quercetin and copper nanoparticles

Nanoparticles were synthesized using of Gallic acid +Quercetin and Cu $(NO_3)_2.3H_2O$. The Copper nitrate (Cu $(NO_3)_2.3H_2O$) solution was prepared at a concentration of 0.01 M in 100 ml of distilled water (0.2416 gram Cu $(NO_3)_2.3H_2O$ was solved with 100 mL water). Four beakers were added 10 mL 0.01 M Gallic acid + 10 mL 0,01 M Quercetin and 20 mL of Cu $(NO_3)_2.3H_2O$ (0.01 M) was added drop by drop and mixed homogeneously for four hours for the reaction to happen and producing more quantity of nanoparticles. PH of the solutions were adjusted using 0.01 M Na_2CO_3 (Sodium carbonate) and 0.01 M CH_3COOH (Acetic acid) each of pH =3, pH=7, pH=9 and pH=11. The best nanoparticles were obtained at pH=9 for this reaction. The colloid solutions were collected and washed several times then stored at room temperature for further experiments. The obtained Cu NPs were further purified by centrifugation at 4000 rpm followed by redispersion of the pellet in distilled water then putting into watch glass and entering an oven for drying (Figure 2.7).

Figure 2.7. Preparation of Quercetin, Gallic acid and copper nanoparticles.

2.5.3. Gallic acid, Quercetin, silver and copper nanoparticles

Nanoparticles were synthesized using of Gallic acid Quercetin and Cu $(NO_3)_2.3H_2O$, $AgNO_3$. Four beakers were added 10 mL 0.01 M Gallic acid + 10 mL 0,01 M Quercetin and 10 mL 0.01M Cu $(NO_3)_2.3H_2O$, 10 mL 0.01 M $AgNO_3$ was added drop by drop and mixed homogeneously for four hours for the reaction to happen and producing more quantity of nanoparticles. PH of the solutions were adjusted using 0.01 M Na_2CO_3 (Sodium carbonate) and 0.01 M CH_3COOH (Acetic acid) each of pH =3, pH=7, pH=9 and pH=11. The best nanoparticles were obtained at pH=9 for this reaction. The colloid solutions were collected and washed several times then stored at room temperature for further experiments. The obtained AgCuNPs were further purified by centrifugation at 4000 rpm followed by redispersion of the pellet in distilled water then putting into watch glass and entering an oven for drying (Figure 2.8).

Figure 2.8. Preparation of Quercetin, Gallic acid, Silver and Copper nanoparticles.

2.6. Characterization of Nanoparticles

A high-performance UV-Vis spectrophotometer was used, which carried out between 300-700 nm wavelength ranges. Absorption measurements were made for all Nano samples in a colloidal form, and placed in a quartz cuvette in which the radiation travels for a distance of one cm through the solution and works with an accuracy of one nanometer so that we used water and ethanol were used as blank. The characteristic technique described above is carried out using an aqueous dispersion of nanoparticles.

FT-IR analysis was performed on clean and dry nanoparticles to identify potential active groups that could support the presence of capping and settlement by plant extracts. FTIR Spectrometer One Spectrum Potassium bromide (KBr) pellet was used in a diffusion reflection for solid nanoparticles produced, and the salt plate NaCl to colloidal nanoparticles synthesized.

The surface shape of the images of the nanoparticles was recorded by scanning the Electron Microscope (SEM), which measures 5-13 mm at working distance, 5-10 kV high voltage, and Emission current are 75-80. The energy-dispersed X-ray spectrometer (EDX) operates at a high voltage of 127 KeV and 20 A currents. The morphology of nanoparticles was studied using the XRD. X-ray diffraction (XRD) measurements were performed on drop-coated films to define the crystalline state of the Ag, Cu, and Ag-Cu nanoparticles. At room temperature, the scanning rate ranges from 100 to 800 in 2 hours.

The optical study, XRD, SEM, EDX analyses were carried out at MUNZUR UNIVERSITY Labs, Turkey Tunceli. For UV-Vis, an FTIR spectrophotometer was analyzed at Firat University.

2.7. Antimicrobial Activity

Antimicrobial activities of the synthesized NPs colloidal were assessed using the standard dilution micro method. After the incubation period were observed clearance and turbidity. Its mean that when is show the cloudy, it means positive is know that bacteria growth at this tube, but negative the means is not bacteria growth at this tube, point at this two tubes is the minimum inhibitory concentration (MIC). At this point is kill 6 log of the bacteria Escherichia coli at 37^{o} C for 24 hours, also, at this point kill 6 log bacteria Staphylococcus aureus it means (1.000.000).

The first get the nanoparticles (0.015 gram) were put them in the severely diluted tube. A freshly prepared bacterial culture to grow used two types of bacteria, Escherichia coli, and Staphylococcus aureus. After the incubation period it was observed that clearance (negative) and turbidity (positive). Minimum inhibitory concentration (MIC) values were determined by batch culture process. Increasing amount of NPs was added in 1 mL nutrient broth. After incubation at 37° C on a rotary shaker, growth inhibition was measured against control (broth without NPs) at 600 nm by a UV–visible spectrophotometer.

3. RESULTS AND DISCUSSION

3.1. Quercetin Nanoparticles

3.1.1. Quercetin and silver nanoparticles

UV-vis spectroscopy

UV-Vis spectroscopy using the (UVWIN 5 software) spectrophotometer in the wavelength range between 300 and 700 nm was performed for optical investigation. The UV-Vis absorption spectrum of quercetin was shown in (Figure 3.1) with λ max at 373.050 nm.

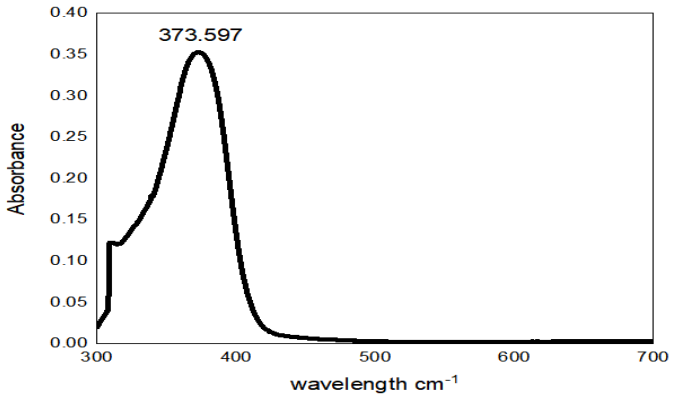

Figure 3.1. UV-VIS spectrum of Quercetin

One of the most commonly used UV-visible spectroscopies is structural characterization methods for silver from nanoparticles. A band of maximum surface absorption 487.96 nm suggesting the existence of objects with a spherical shape or nearly spherical Ag nanoparticles was shown by the absorption spectrum (Figure 3.2) of the dark yellow-brown silver colloids.

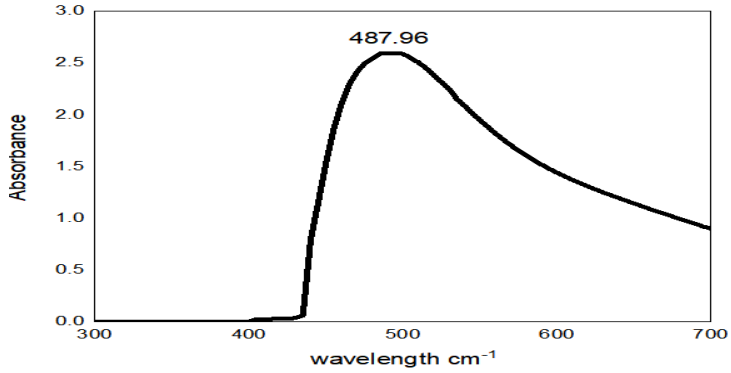

Figure 3.2. UV-VIS spectrum of AgNPs synthesized with Quercetin

FTIR Analysis

FTIR research is one of the essential tools for recognizing encapsulated knowledge molecules with chemicals quickly and accurately. 3410 and 3297 cm^{-1} were used to detect quercetin with the characteristic density of stretching of OH groups, while 1382 cm^{-1} was used to see OH bending of the phenolic function, and 1607, 1560, and 1517 cm^{-1} were used to detect stretch bands. CO-stretching in the aryl ether ring, phenol CO-stretching, ketone stretching, and bending as was shown in 935, 821, 679, 600, 1263, 1200, and 1165 cm^{-1} ın (Figure 3.3).

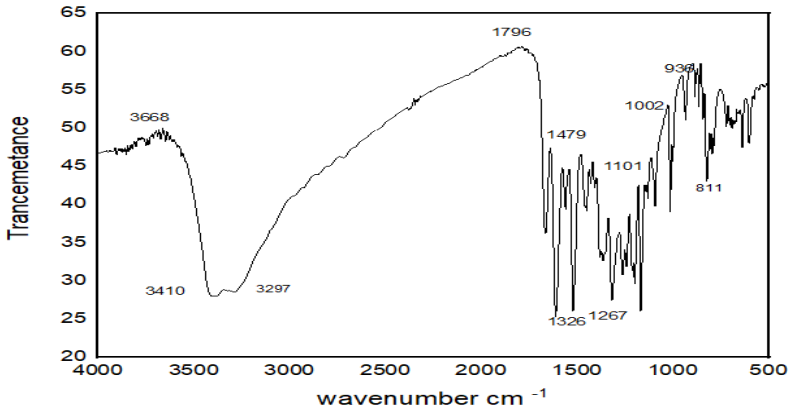

Figure 3.3. FTIR spectrum of Quercetin.

Further information on the combination of silver nanoparticles was investigated Analyzed with FTIR**.** It was discovered that the FTIR spectrum of AgNPs circulating quercetin has characteristic peaks at 3449.2, 2918.5, 1568.4, 1410.5, 1041.1, 802.65, 651.51, 500.38 and 466 cm^{-1}. The character is a height of 1568.4 and 1041.1 cm^{-1} mapped as a C=C aromatic expansion and a C-N curvature of aliphatic amine and flavonoids, confirming the absence of quercetin. The large range of 3449.2 cm^{-1} is attributed to the expansion of amine N-H, while the peak near 1568.4 cm^{-1} was designated as aromatic C=C in the carboxyl group as quercetin peaks, responsible for the formation of carbon, alcohol, and amine groups (Figure 3.4).

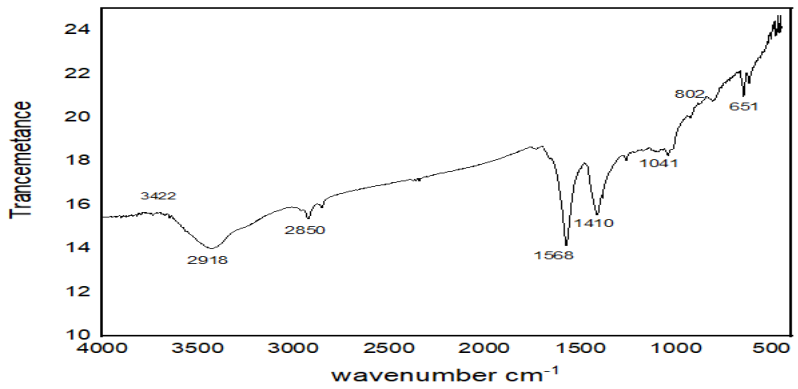

Figure 3.4. FTIR spectrum of AgNPs synthesized with Quercetin.

SEM Analysis

More a better understanding of the morphology and size information of the silver nanoparticles was provided by SEM. The photos show the cubic shapes of the nanoparticles. In the scanned electron micrograph image of the silver nanoparticle pellet solution, an investigation into the elementary mapping of silver nanoparticles shows a high distribution of metal silver (Figures 3.5).

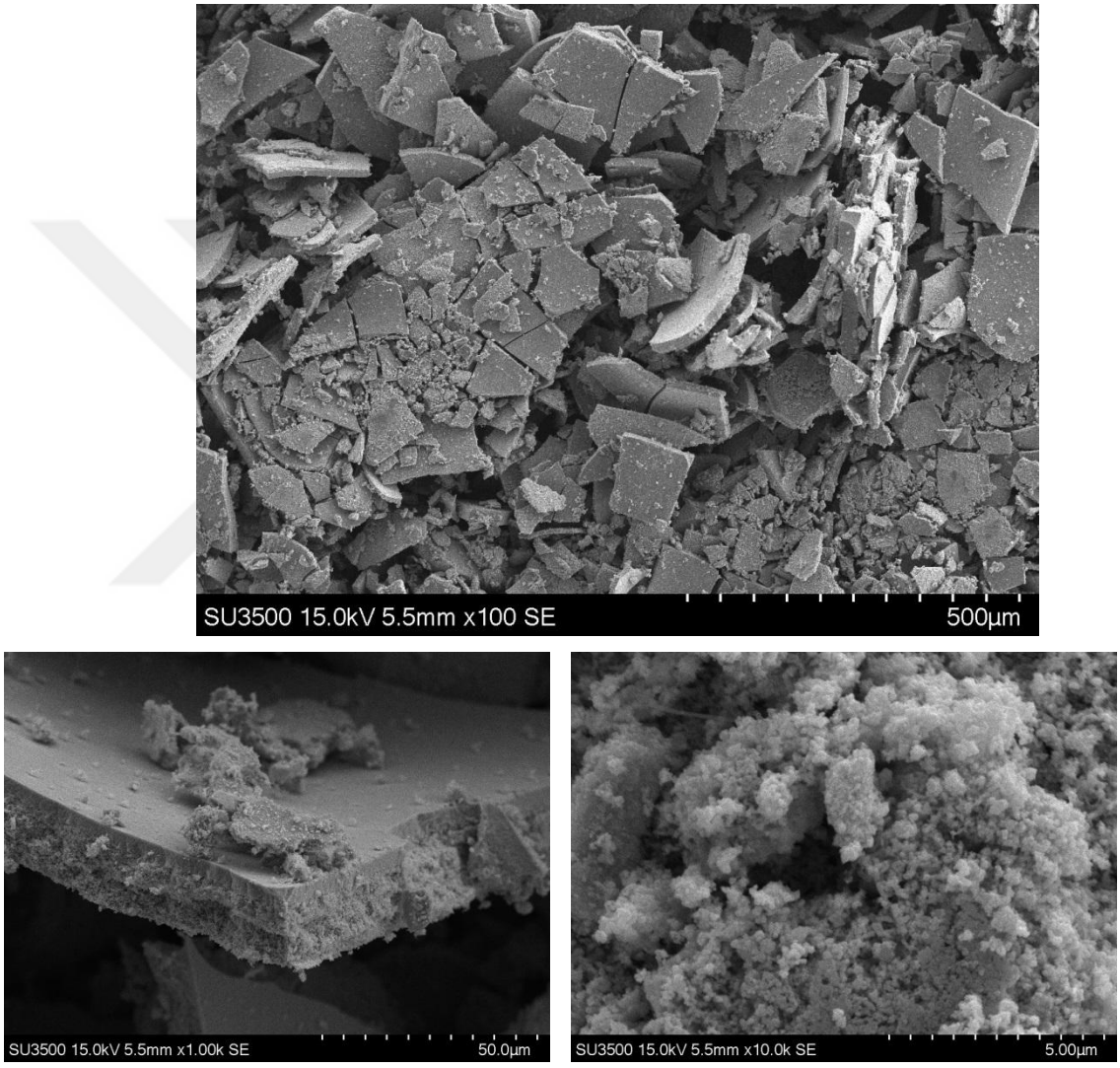

Figure 3.5. SEM image of silver nanoparticles synthesized by Quercetin at various enlargement levels (500 µm, 50.0 µm, 5.00 µm).

EDX Analysis

Energy Dispersed X-Ray Analysis (EDX), referred to as EDS as EDAX, is used in X-ray technology for the elemental composition of the material for classification. The EDX analysis generates spectra that reflect the vertex corresponding to the elements that make up the analyzing sample's actual composition.

In a strong silver signal and a lousy carbon, a peak is seen in the EDX profile which can start with biomolecules at the AgNP surface. Few nasty C signals have also been observed.

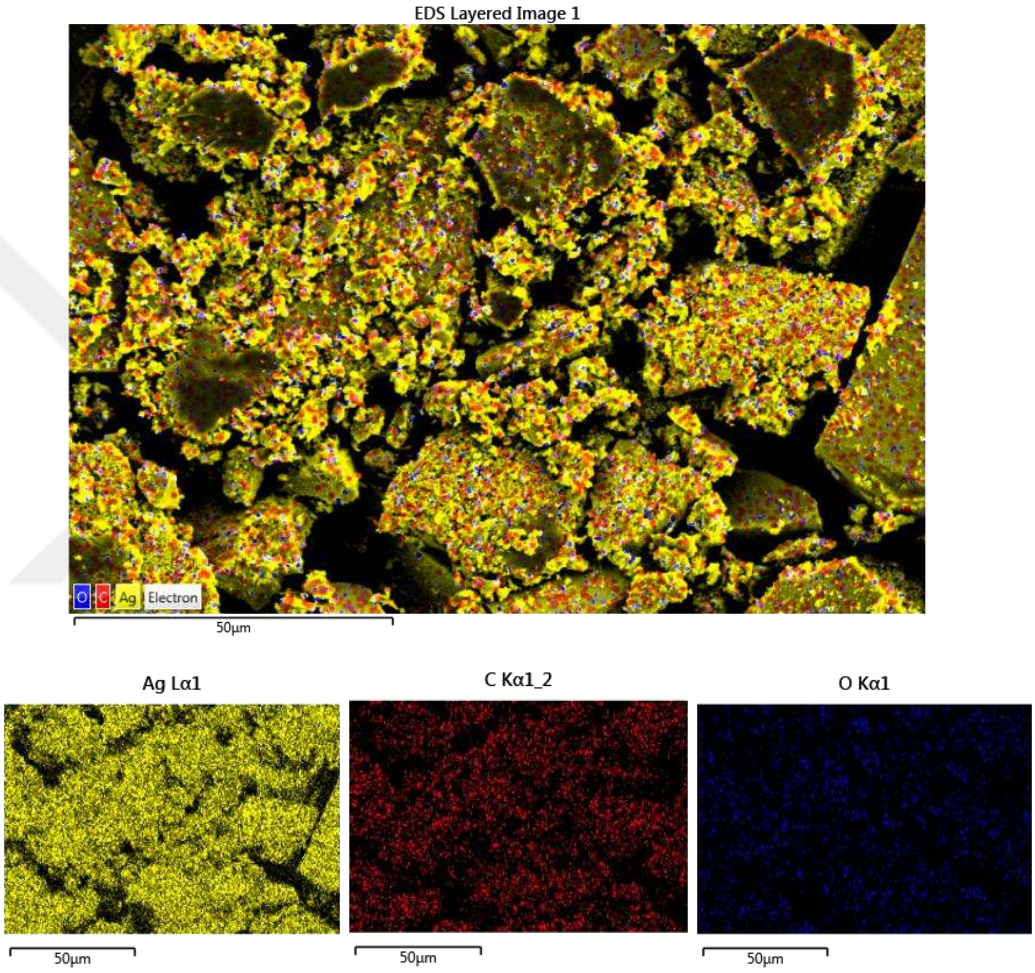

Figure 3.6. EDX spectrum of silver nanoparticles synthesized by Quercetin and elemental mapping, layered image.

A substantial silver signal along with weak oxygen and a carbon peak is seen in the EDX profile (Figure 3.6), which may begin with biomolecules that have been attached to the AgNP surface (Figure 3.7).

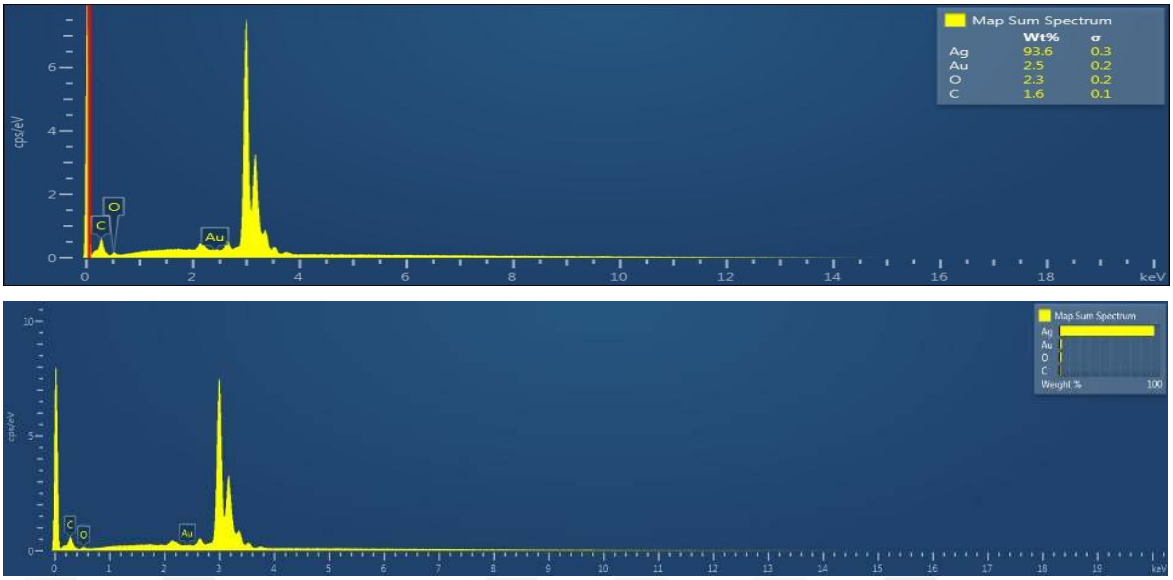

Figure 3.7. Elemental composition analysis and field electron micrograph of AgNPs

XRD Analysis

The silver nanoparticles' XRD measurements showed. The reflection peaks correspond to the reflections of 1536.926, 371.3638, 424.759, 490.181 and 126.032 at 2 Theta values of 38.05, 44.165, 64.418, 77.34 and 81.232 (Figure 3.8).

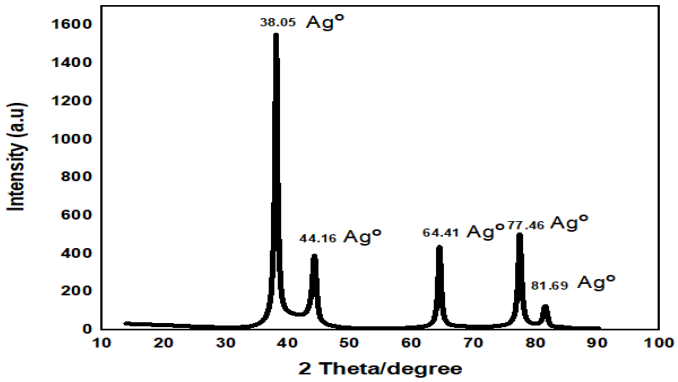

Figure 3.8. XRD spectrum of AgNPs synthesized with Quercetin.

Antimicrobial

Types of antimicrobial activities of the synthesized silver colloidal were assessed using the standard dilution micro method. After the incubation period, we observed clearance and turbidity. When we show the cloudy, it means positive we know that bacteria grow at this tube, but negative the mean point at these two tubes is the minimum inhibitory concentration (MIC). At this point (2.11 mg), kill 6 logs of the bacteria Escherichia coli at 37^{o} C for 24 hours. Also, at this point (4. 69 mg) kill 6 log bacteria Staphylococcus aureus it means (1.000.000).

Table 3.1. Minimum inhibitory concentrations (MIC) of Quercetin, Ag+ and AgNPs (Mean± Standard Deviation).

No	Matter	Escherichia coli	Staphylococcus aureus
1	Quercetin+ Ag (mg)	2.11±1.22	4.69±2.68
2	Quercetin (mg)	188±81	375±162
3	Ag (mg)	26±9	21±9

The compared solid and liquid concentration of Ag .this number (2.11±1.22 mg) lower than this number (188±81mg) for Escherichia coli and (4.69±2.68mg) higher than this number (375±162) for Staphylococcus aureus (mg), only Ag needs for (26±9 mg) to kill 6 logs of the bacteria Escherichia coli (mg) and (21±9 mg) to kill six records of the Staphylococcus aureus (mg) (Table 3.1).

3.1.2. Quercetin and copper nanoparticles

UV-VIS spectroscopy

One of the most commonly used UV-visible spectroscopies is structural characterization methods for copper from nanoparticles. A band of maximum surface absorption 472.82 nm suggesting the existence of objects with a spherical shape or nearly spherical Ag nanoparticles was shown by the absorption spectrum of the dark yellow-brown silver colloids. UV-VIS spectrum of CuNPs synthesized with Quercetin was observed a maximum absorption at 472.822 nm (Figure 3.9).

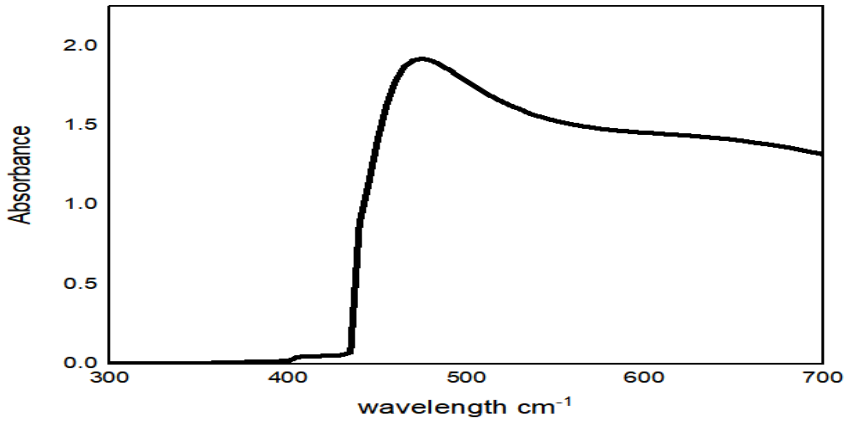

Figure 3.9. UV-VIS spectrum of CuNPs synthesized with Quercetin

FTIR Analysis

Inter-molecular and Intra- molecular hydrogen bonds are known to be responsible for expanding the -OH band in the FTIR spectra. In the region 3500 -3000 cm^{-1}, a broad uptake of a hydroxyl group (O-H) appears at 3311.5 cm^{-1}. The bands in the area 2000-1500 cm^{-1} are due to the binding of C=C. This band appears at 1468 cm^{-1} (Figure 3.10).

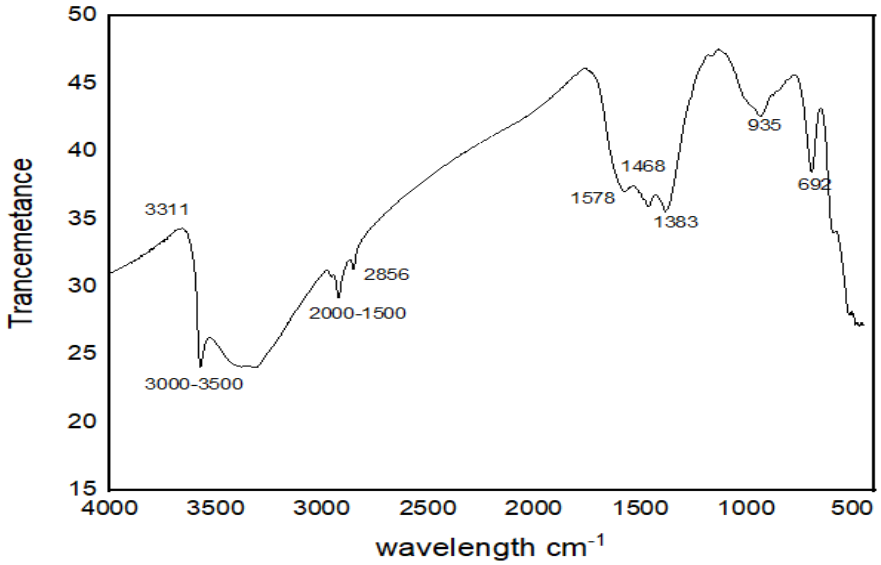

Figure 3.10. FTIR spectrum of CuNPs synthesized with Quercetin.

SEM Analysis

SEM Analysis In the scanned electron micrograph image of the copper nanoparticle pellet solution, an analysis of the elemental mapping of copper nanoparticles shows a low distribution of metallic copper (Figure 3.11).

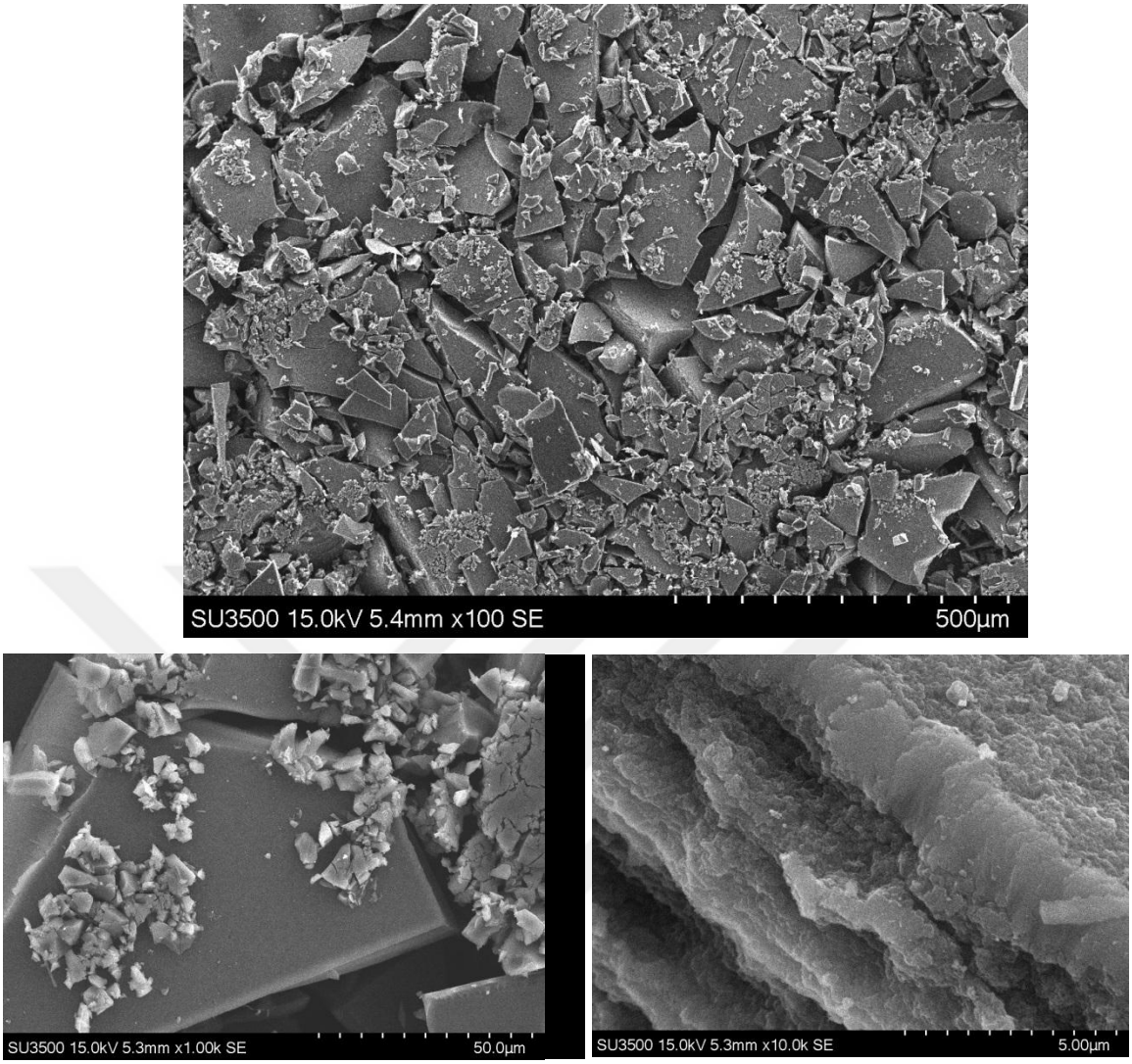

Figure 3.11. SEM image of CuNPs synthesized by Quercetin at various enlargement levels (500 µm, 50.00 µm, 5.00 µm).

EDX Analysis

It shows a strong carbon signal together with a weak copper and an oxygen peak, which can start during drying due to the scorching of nanoparticles. Several soft Cl, Ca, and S signals were also observed. A low amount of copper with atomic composition of 19.41 per cent (Figure 3.12) was shown.

The result of the EDX study showed that in the synthesis, there was a small amount of Cu with atomic composition of 18.8. per cent (Figure 3.13).

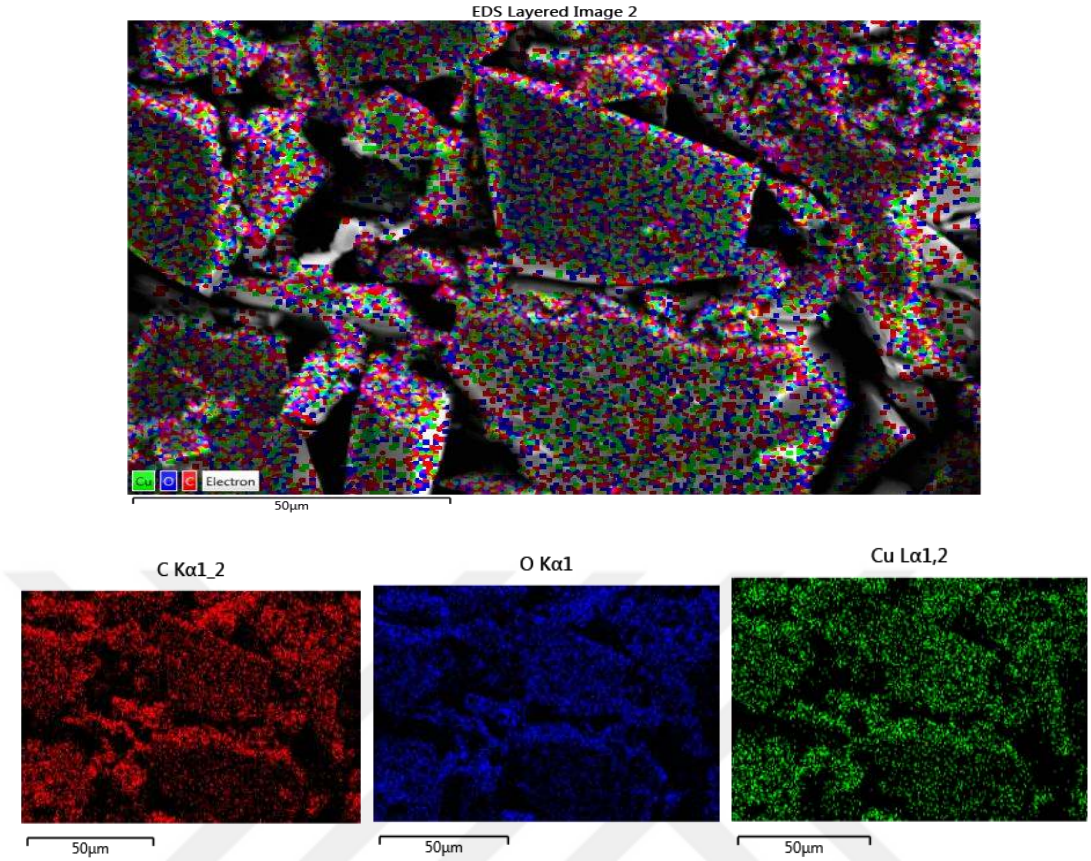

Figure 3.12. EDX spectrum of copper nanoparticles synthesized by Quercetin and elemental mapping, layered image.

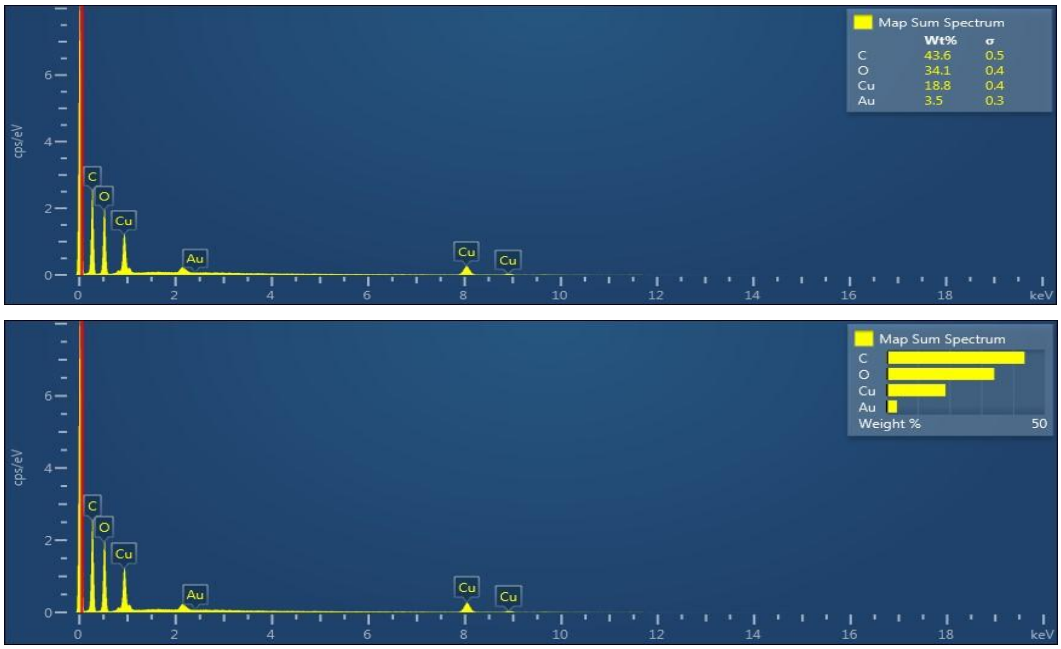

Figure 3.13. Quercetin and copper nanoparticles spectrum EDX elemental mapping: copper nanoparticles field electron micrograph.

XRD Analysis

The copper nanoparticles' XRD measurements showed. The reflection peaks correspond to the reflections of 27.393 at 2 Theta values of 1347 **(Figure 3.14).**

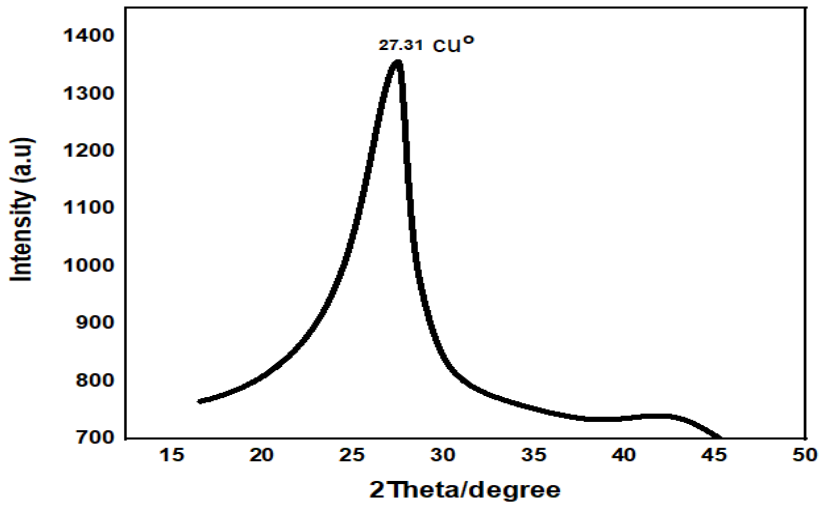

Figure 3.14. XRD spectrum of CuNPs synthesized with Quercetin

Antimicrobial

At this point (7.50±0.00 mg), kill 6 logs of the bacteria Escherichia coli at 37° C for 24 hours. Also, at this point (6.25±2.17 mg) kill 6 log bacteria Staphylococcus aureus it means (1.000.000) (Table 3.2.).

Table 3.2. Minimum inhibitory concentrations of Quercetin+ Cu nanoparticles (MIC) Mean±Standard Deviation).

No	Matter	*Escherichia coli*	*Staphylococcus aureus*
1	Quercetin+ Cu (mg)	7.50±0.00	6.25±2.17
2	Cu (mg)	2832±981	1416±491
3	Quercetin (mg)	188±81	375±162

The compared solid and liquid concentration of Cu. This number (7.50±0.00 mg) lower than this (2832±981mg) number for Escherichia coli and (6.25±2.17mg) lower than this (1416±491mg) for Staphylococcus aureus. Only Cu needs for (2832±981mg) to kill 6 logs of the bacteria Escherichia coli (mg) and (1416±491 mg) to kill six records of the Staphylococcus aureus (mg).

3.2. Gallic acid nanoparticles

3.2.1. Gallic acid and Silver nanoparticles

UV- VIS spectroscopy

UV-Vis spectroscopy using the (UVWIN 5 software) spectrophotometer in the wavelength range between 300 and 700 nm was performed for optical investigation. The UV-Vis absorption spectrum of Gallic acid was shown in (Figure 3.15) with λ max at 466.73 nm.

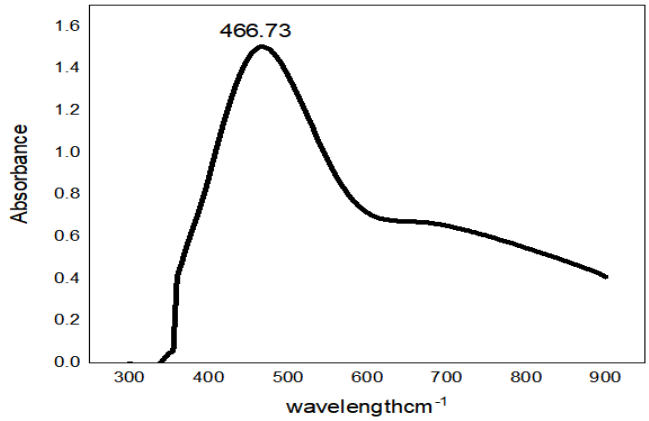

Figure 3.15. Gallic acid UV-Vis absorption spectrum, with a maximum at 464.181 nm.

One of the most commonly used UV-visible spectroscopies is structural characterization methods for silver from nanoparticles. A band of maximum surface absorption 739.33 nm suggesting the existence of objects with a spherical shape or nearly spherical Ag nanoparticles was shown by the absorption spectrum of the dark yellow-brown silver colloids. UV-VIS spectrum of AgNPs synthesized with Gallic acid was observed a maximum absorption at 429.708 nm (Figure 3.16).

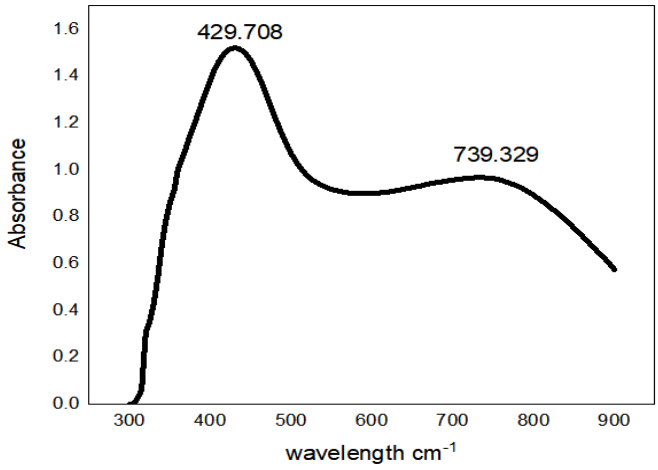

Figure 3.16. UV-VIS spectrum of AgNPs synthesized with Gallic acid

FTIR Analysis

This peak 3372 cm^{-1} (COOH), for stretching hydroxyl (O-H) at 3288 cm^{-1}, for stretching C=O at 1699 cm^{-1}. The peaks of 1696 cm^{-1} and 1249 cm^{-1} suggest that Carboxylic groups are present. The absorption bands at 1600-1620 cm^{-1} and the extreme absorption at 864-868 cm^{-1} confirm the aromatic character of the compound. The bands between 1200 and 1270 cm^{-1} reflect the vibration of phenol and carboxyl C-O deformation (Figure 3.17).

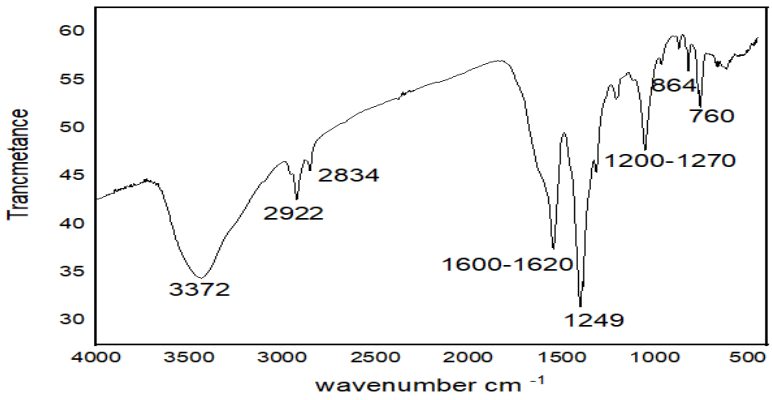

Figure 3.17. FTIR spectra of Gallic acid.

The FTIR spectrum of Gallic acid 3445, 2925, 2340, 1548, 1397, 1313, 1118, 1054, 876, and 617 cm^{-1}. The large uptake of the hydroxyl group (O-H) occurs at 3445.5 cm^{-1} in the 3500-3000 cm^{-1} region. Due to symmetrical stretching and curved vibrations of saturated hydrocarbons, there were weak bands at 2925 and 1313 cm^{-1}, respectively. The absorption bands at 2340 and 1202 cm^{-1} were due to the C-N band and the amide stretch, respectively, which could be involved in AgNPs biosynthesis in the form of egg white (by reducing the metal salt $AgNO_3$). Also, the weak bands C-O bands of alcohols and phenols at 1118 and 1054 cm^{-1} represented. At 876 cm^{-1}, the observed tensile vibration is due to C=C of the aromatic group region and a high peak at The C-X groups of alkyl halides were presented at 617 cm^{-1} (Figure 3.18).

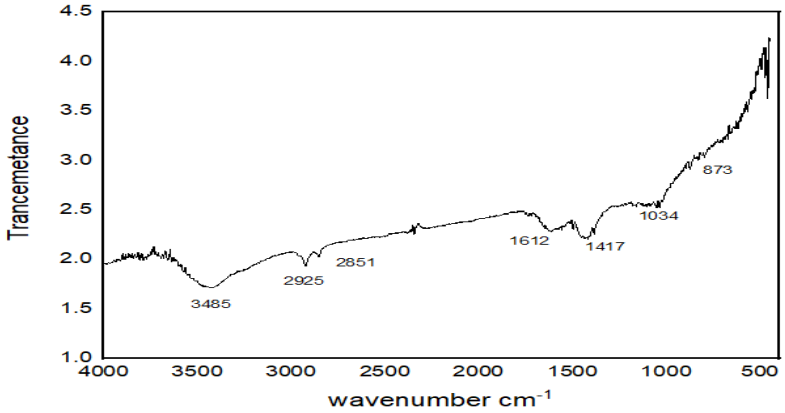

Figure 3.18. FTIR spectra of AgNPs synthesized with Gallic acid

SEM Analysis

More a better understanding of the morphology and size information of the silver nanoparticles was provided by SEM. The photos show the cubic shapes of the nanoparticles. In the scanned electron micrograph image of the silver nanoparticle pellet solution, an investigation into the elementary mapping of silver nanoparticles shows a high distribution of metal silver. SEM Analysis in the scanned electron micrograph image of the silver nanoparticle pellet solution, an analysis of the elemental mapping of silver nanoparticles shows a low distribution of metallic silver (Figure 3.19).

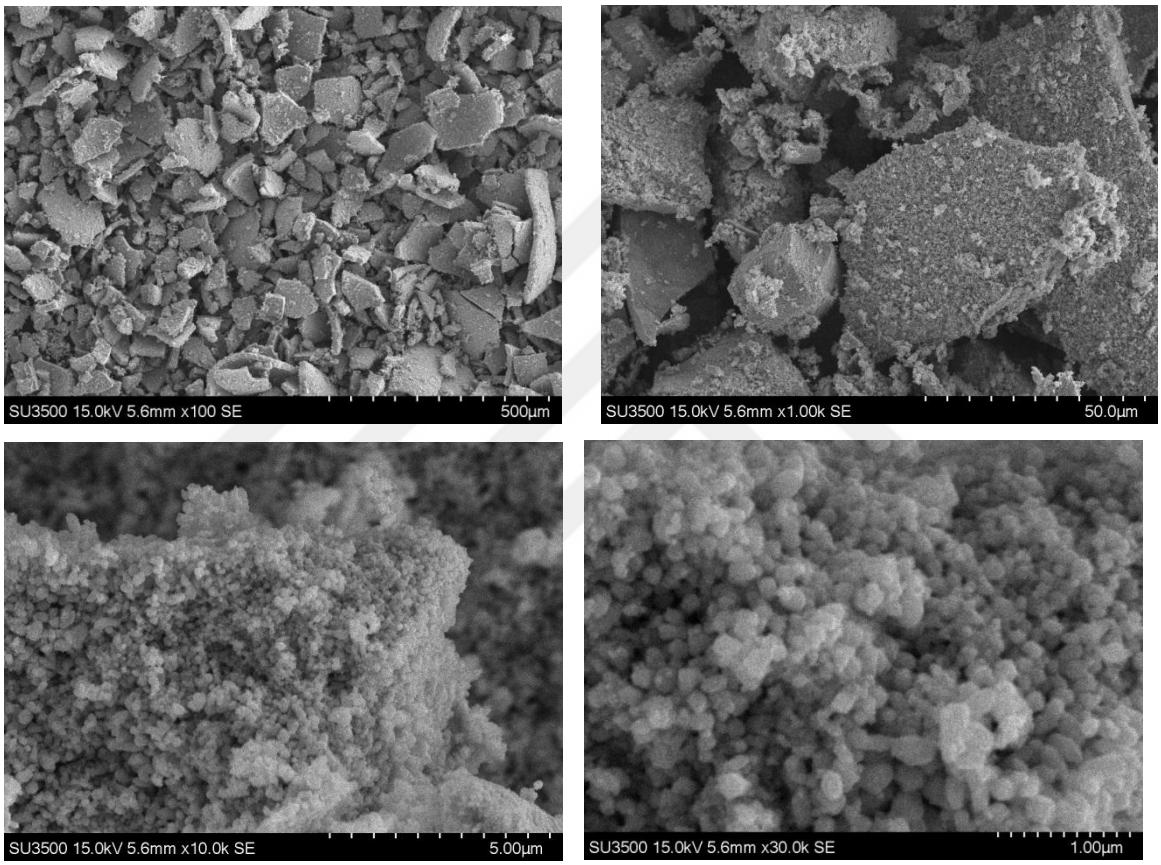

Figure 3.19. SEM image of silver nanoparticles synthesized by Gallic acid at various enlargement levels (500 µm, 50.0 µm, 5.00 µm, 1.00 µm).

EDX Analysis

It shows a strong carbon signal together with a strong silver and weak gold peak, which can start during drying due to the scorching of nanoparticles. Several soft Au, and O signals were also observed. A high amount of silver with atomic composition of 95.6 per cent (Figure 3.20) was shown.

The result of the EDX study showed that in the synthesis, there was a small amount of Au with atomic composition of 2.5 per cent (Figure 3.21).

A substantial silver signal along with weak oxygen and a carbon peak is seen in the EDX profile, which may begin with biomolecules that have been attached to the AgNP surface. Few inferior C, O and Au signals have been observed as well (Figure 3.21).

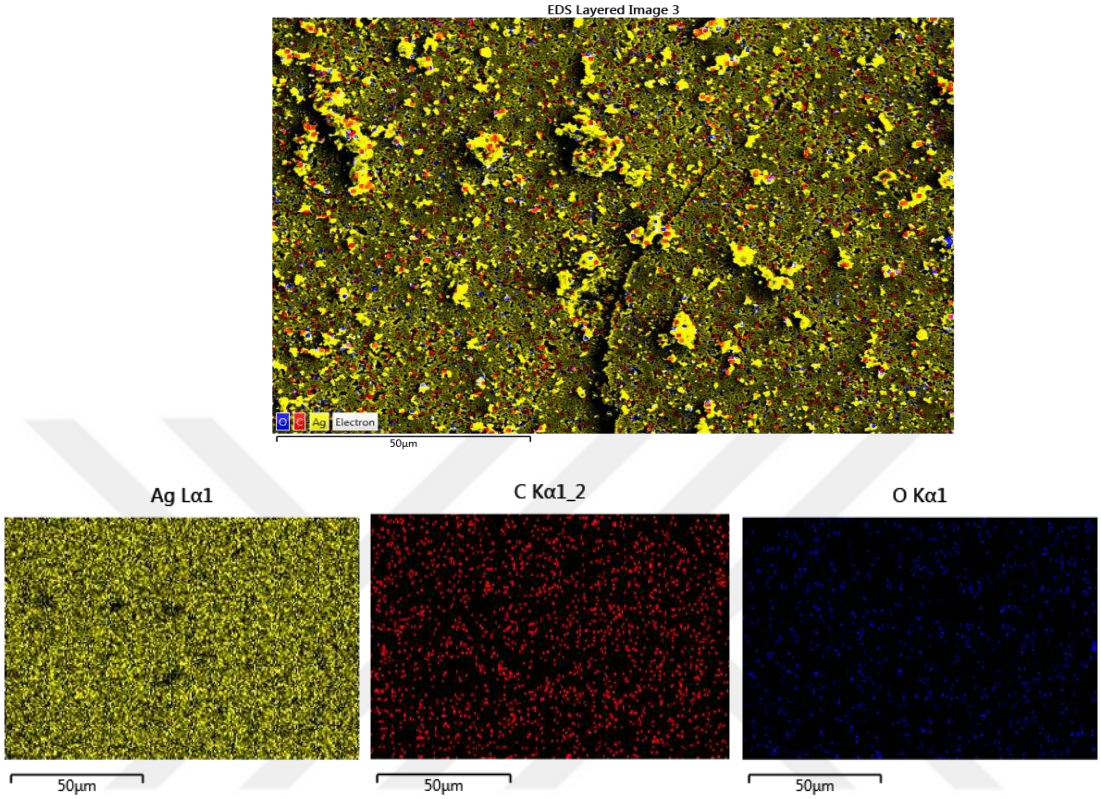

Figure 3.20. EDX spectrum of silver nanoparticles synthesized by Gallic acid and elemental mapping, layered image.

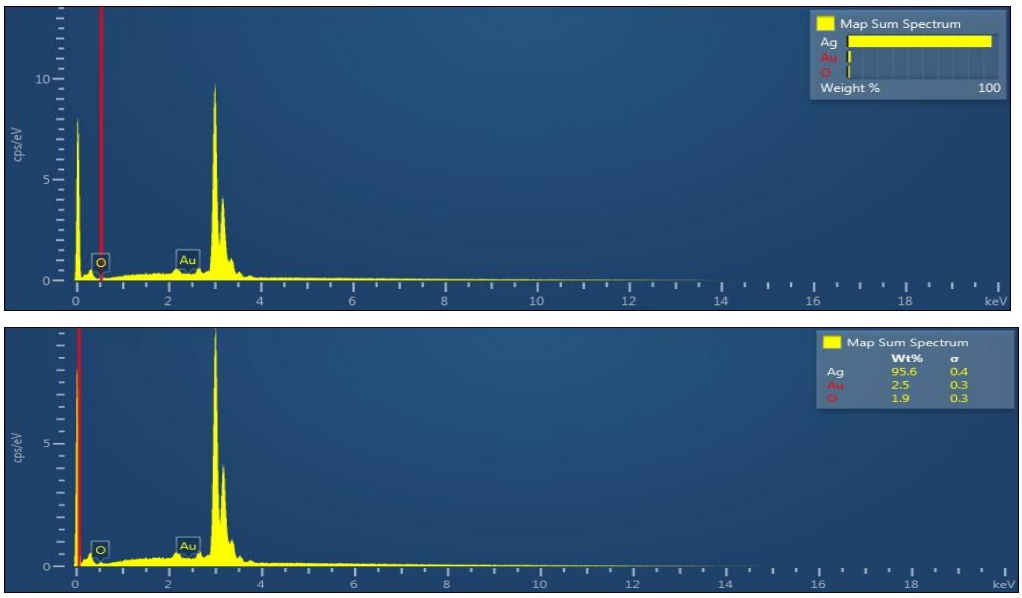

Figure 3.21. Elemental composition analysis and field electron micrograph of AgNPs

XRD Analysis

The silver nanoparticles' XRD measurements showed. The reflection peaks correspond to the reflections of 152.87, 72.733, 46.131, 46.949 and 17.509 at 2 Theta values of 38.05, 44.35, 64.487, 77.51, and 81.559 pictures show the plane shapes of the nanoparticles (Figure 3.22).

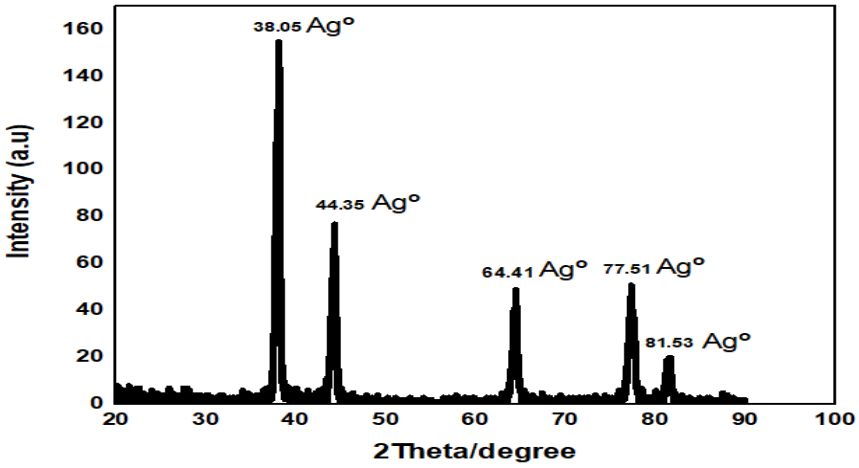

Figure 3.22. XRD spectrum of AgNPs synthesized with Gallic acid.

Antimicrobial

At this point (3.75±0.0 mg), kill 6 logs of the bacteria Escherichia coli at 37° C for 24 hours. Also, at this point (37.50±0.00 mg), kill 6 log bacteria Staphylococcus aureus (Table 3.3.).

Table 3.3. Minimum inhibitory concentrations of solid nanoparticles (MIC) Mean± Standard Deviation).

No	Matter	Escherichia coli	Staphylococcus aureus
1	Gallic acid+ Ag (mg)	3.75±0.00	37.50±0.00
2	Gallic Acid (mg)	133±46	106±46
3	Ag (mg)	26±9	21±9

The compared solid and liquid concentration of Ag, this number (3.75±0.00 mg) lower than this number (133±46 mg) for Escherichia coli and (37.50±0.00 mg) lower than this number (106±46 mg) for Staphylococcus aureus (mg). Only Ag needs for (26±9 mg) to kill 6 logs of the bacteria Escherichia coli (mg) and (21±9 mg) to kill six records of the Staphylococcus aureus (mg).

3.2.2. Gallic acid and copper nanoparticles

UV-VIS spectroscopy

The UV-Vis absorption spectrum of copper nanoparticles at 442.316 nm in(Figure 3.23).

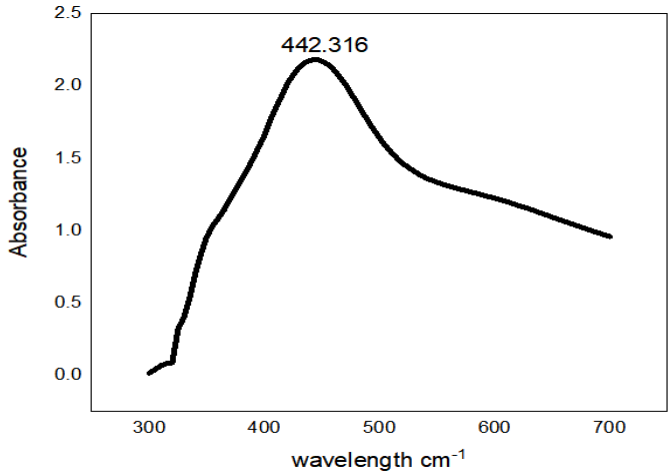

Figure 3.23. UV-VIS spectrum of CuNPs synthesized with Gallic acid

FTIR Analysis

Figure 3.24. shows that copper nanoparticles are mediated by the FTIR spectrum of Gallic acid 3485, 2925, 2851, 1612, 1417, 1034, 1051, and 873 cm^{-1}. These findings have revealed the robustness of the CuNPs synthesis in this work since nanoparticles can be collected under a wide range of conditions. This peak 3485 cm^{-1} (COOH), several peaks have shown no major changes in the area of 2925 cm^{-1} (C-H stretching) and 1051 and 1034 cm^{-1} (C-O stretching), this peak 2851cm^{-1}(Ar C-Stretching), this peak 1612 cm^{-1} (C=O), this peak 1417 cm^{-1}(C=C bending mode), the spectrum 873 cm^{-1} (=C-H Aromatic ring).

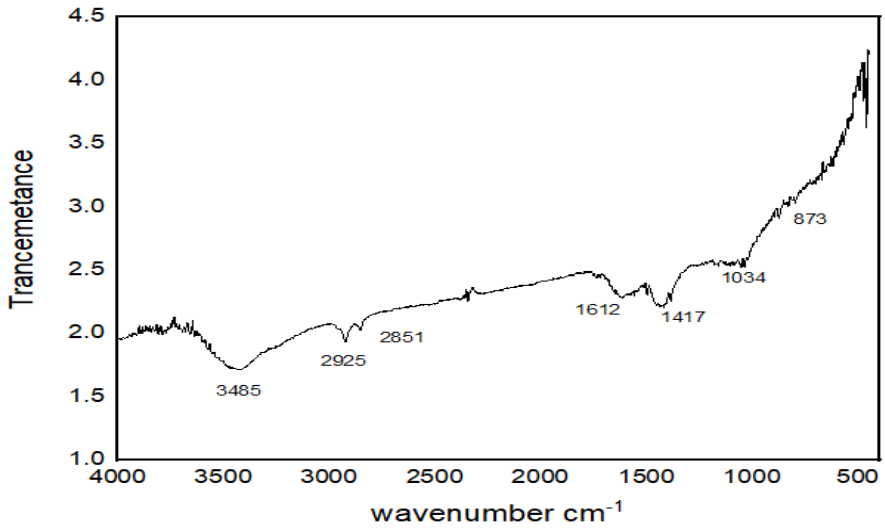

Figure 3.24. FTIR spectra of Gallic acid and copper nanoparticle.

SEM Analysis

SEM Analysis In the scanned electron micrograph image of the copper nanoparticle pellet solution, an analysis of the elemental mapping of copper nanoparticles shows a low distribution of metallic copper (Figure 3.25).

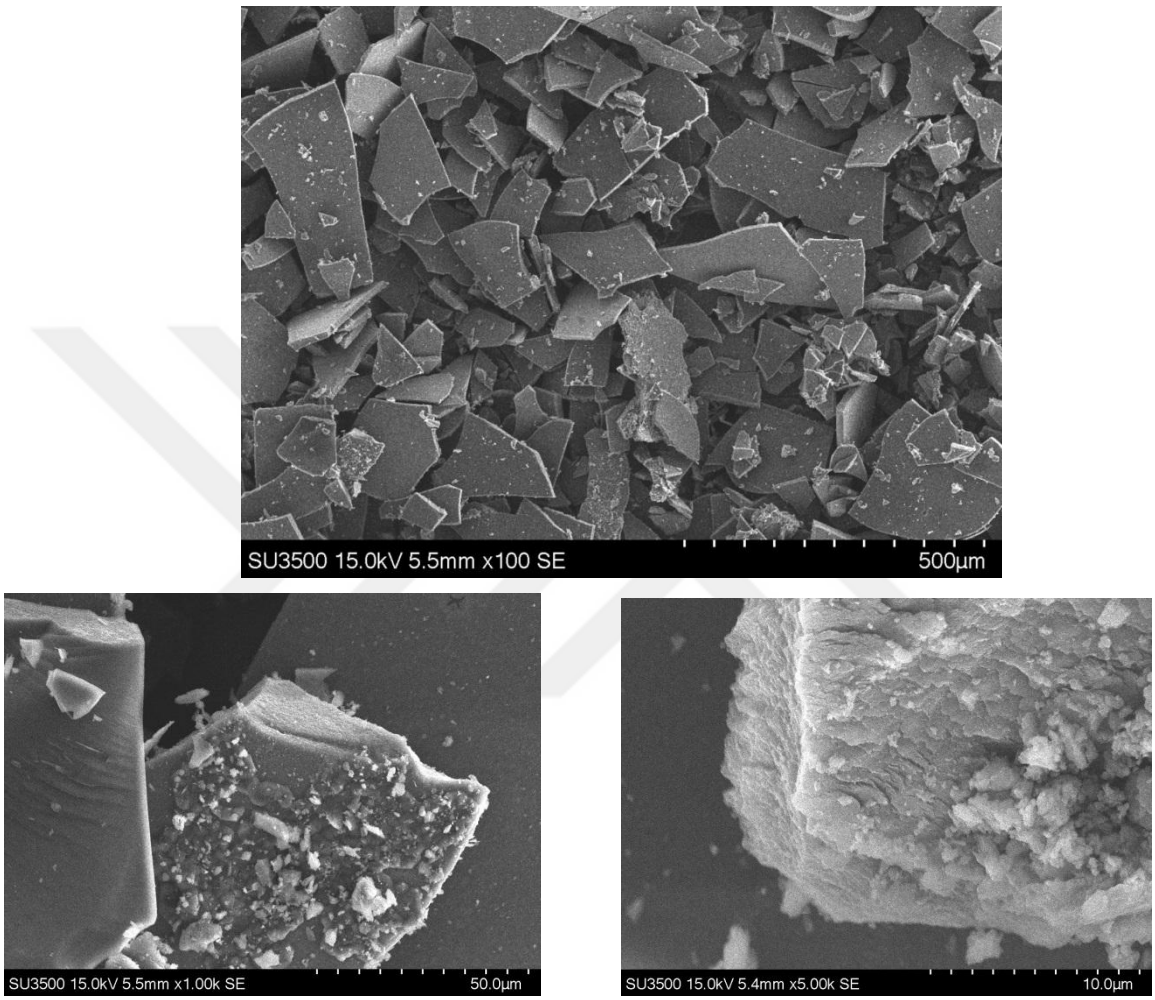

Figure 3.25. SEM image of copper nanoparticles synthesized by Gallic acid at various enlargement levels (500 µm, 50.0 µm, 10.00 µm).

EDX Analysis

In a strong copper signal and a weak carbon and silver, a peak is seen in the EDX profile which can start with biomolecules at the CuNPs surface (Figure 3.26).

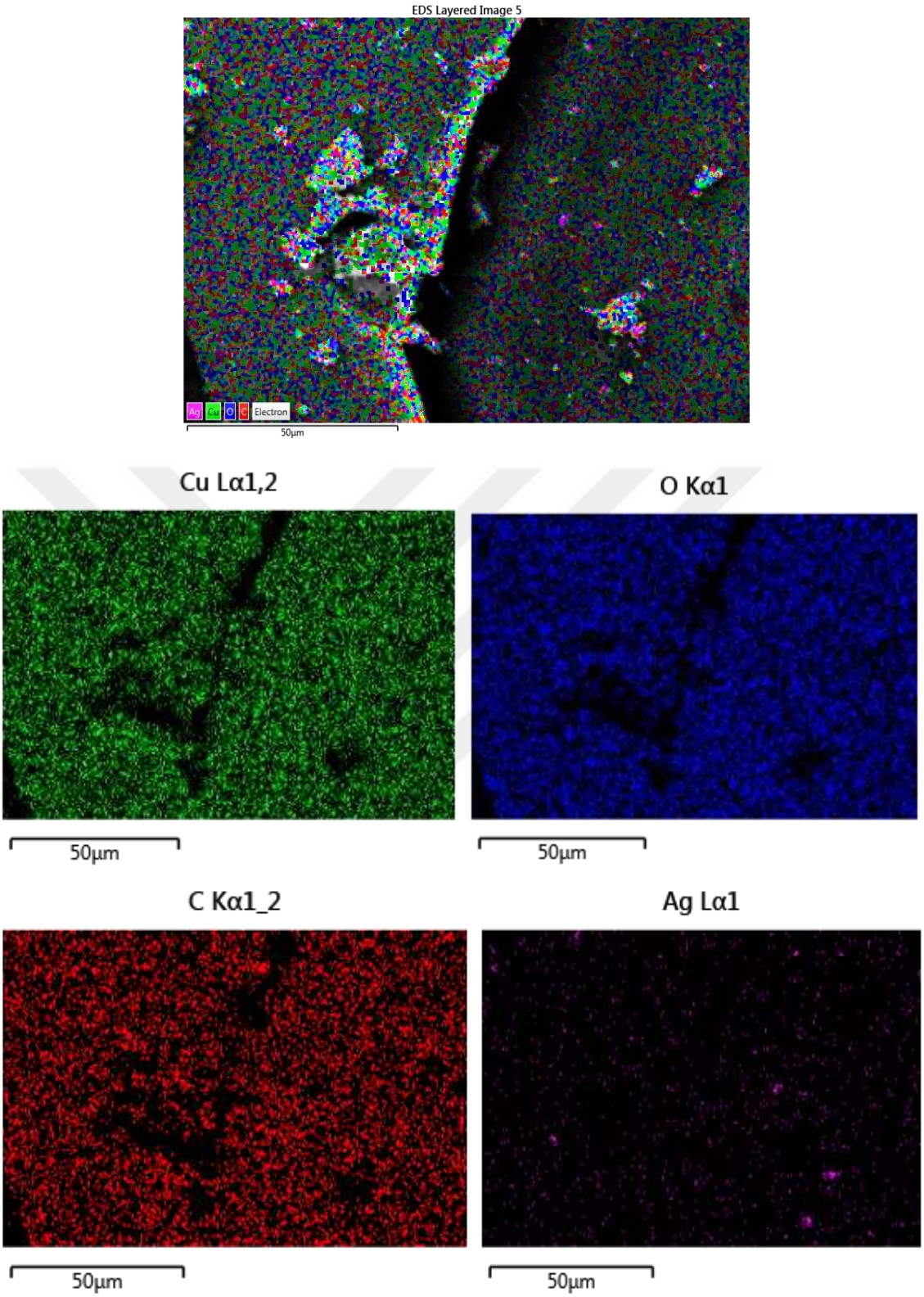

Figure 3.26. EDX spectrum of copper nanoparticles synthesized by Gallic acid and elemental mapping, layered image

It shows a strong carbon signal together with a strong copper and weak gold and silver peak, which can start during drying due to the scorching of nanoparticles. A high amount of copper with atomic composition of 37.4 per cent (**Figure 3.27**) was shown. A substantial copper signal along with weak oxygen and a carbon peak is seen in the EDX profile, which may begin with biomolecules that have been attached to the CuNP surface. Few inferior C, O and Au signals have been observed as well The EDX analysis revealed a significant amount of Cu, with atomic composition of 37.4 per cent of the synthesis (**Figure 3.27**).

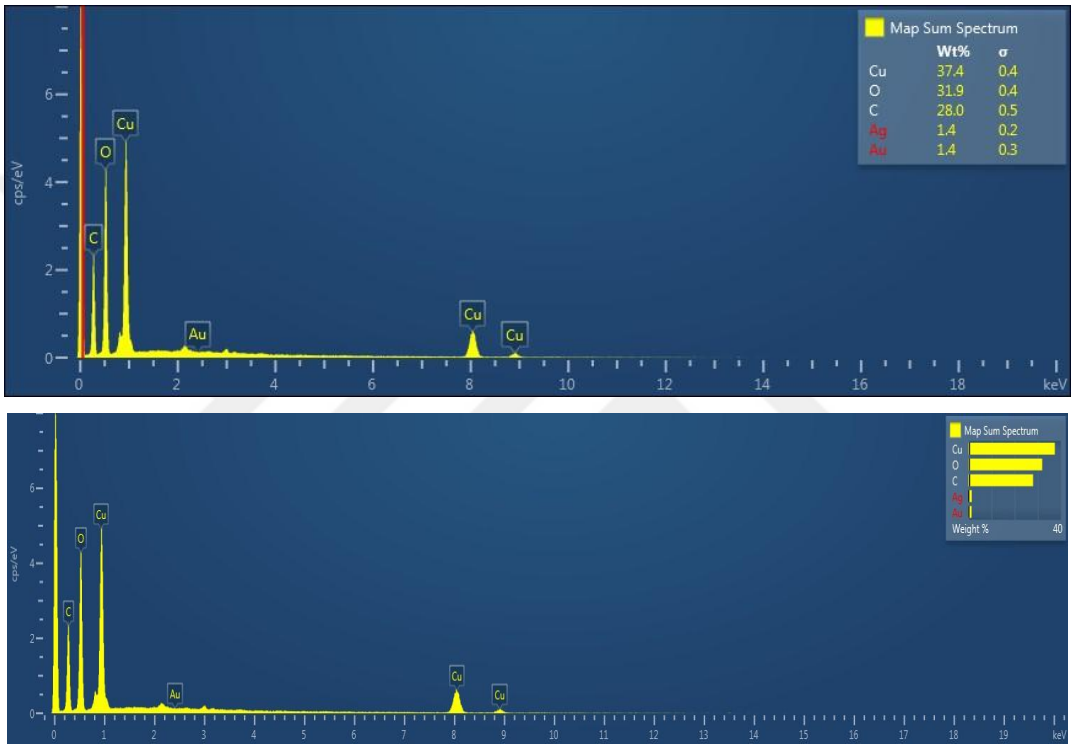

Figure 3.27. Elemental composition analysis and field electron micrograph of CuNPs

XRD Analysis

The copper nanoparticles' XRD measurements showed. The reflection peaks correspond to the reflections of 780.135, 735.002, 1465.53 and 758.97 at 2 Theta values of 20.009, 22.409, 31.47, and 54.687 (Figure 3.28).

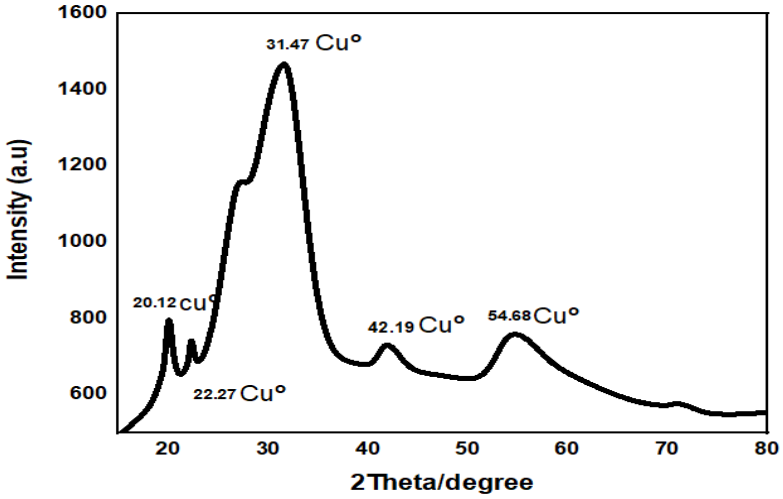

Figure 3.28. XRD spectrum of CuNPs synthesized with Gallic acid.

Antimicrobial

At this point (10.00±2.17 mg), kill 6 logs of the bacteria Escherichia coli at 37° C for 24 hours. Also, at this point (10.00±2.17 mg) kill 6 log bacteria Staphylococcus aureus it means (1.000.000) (Table 3.4.).

Table 3.4. Minimum inhibitory concentrations of solid nanoparticles (MIC) Mean± Standard Deviation).

No	Matter	Escherichia coli	Staphylococcus aureus
1	Gallic Acid+ Cu (mg)	10.00±2.17	10.00±2.17
2	Gallic Acid (mg)	133±46	106±46
3	Cu (mg)	2832±981	1416±491

The compared solid and liquid concentration of Cu. This number (10.00±2.17 mg) lower than this (133±46 mg) number for Escherichia coli and (10,00±2,17mg) lower than this (106±46 mg) for Staphylococcus aureus. Only Cu needs for (2832±981mg) to kill 6 logs of the bacteria Escherichia coli (mg) and (1416±491 mg) to kill 6 logs of the Staphylococcus aureus (mg).

3.3. Gallic acid, Quercetin nanoparticles

3.3.1. Gallic acid, Quercetin Silver nanoparticles

UV- VIS **spectroscopy**

The UV-Vis absorption spectrum of silver nanoparticles at 462.42 nm (Figure 3.29).

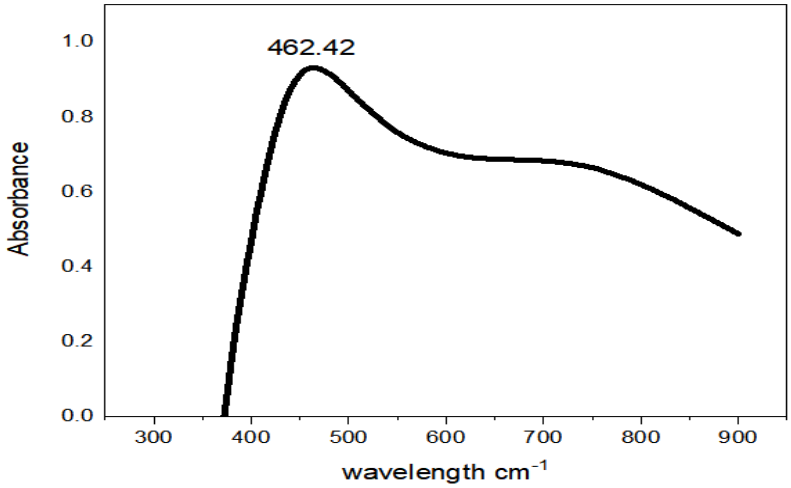

Figure 3.29. UV-VIS spectrum of AgNPs synthesized with Quercetin+Gallic acid

FTIR Analysis

The silver nanoparticles are mediated by the Gallic acid and quercetin FTIR spectrum 3761, 3425, 2922, 2848, 2340, 1612, 1534, 1383 and 668 cm^{-1}. The absorption peaks of silver nanoparticles were observed in the IR spectra at 3425 cm^{-1} (OH group alcohols and phenols); 1612 cm^{-1} (C - O group carboxylic acids); 1383 cm^{-1} (C = O group carboxylic acids); and 1038 cm^{-1} (C = O group carboxylic acids) (C-OH). The IR spectra of silver nanoparticles peak at 3661 cm^{-1} O-H stretching alcohol and phenols, according to a recent study. This peak is located at 2922 and 2848 cm-1 O-H stretching (carboxylic acid), and this peak is located at 2340 cm^{-1} C triple N stretching in (Figure 3.30).

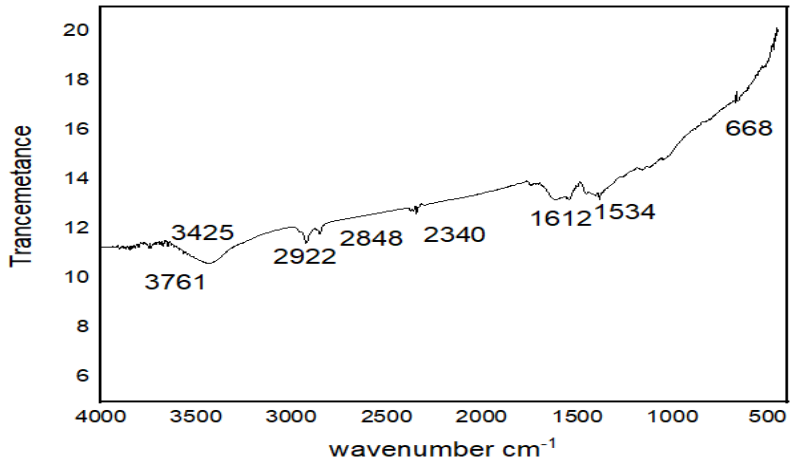

Figure 3.30. FTIR spectra of Quercetin, Gallic acid with silver nanoparticle.

SEM Analysis

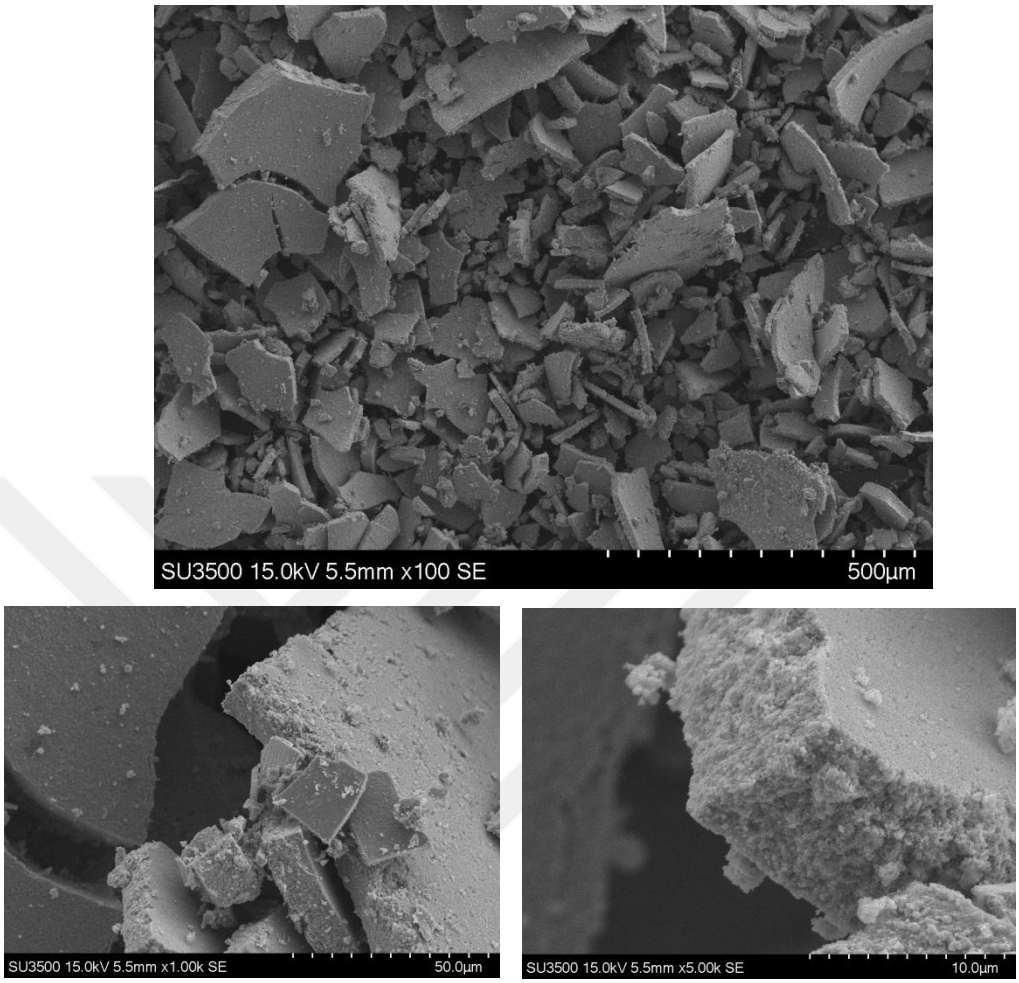

Figure 3.31. SEM image of silver nanoparticles synthesized by Quercetin + Gallic acid at various enlargement levels (500 µm, 50.0 µm, 10.00 µm).

SEM research shown in (Figure 3.31) the morphological features of synthesized copper nanoparticles have been studied (above). SEM studies showed that most of the particles are spherical.

EDX Analysis

In a strong oxygen signal and a weak carbon and silver, a peak is seen in the EDX profile which can start with biomolecules at the AgNPs surface (Figure 3.32).

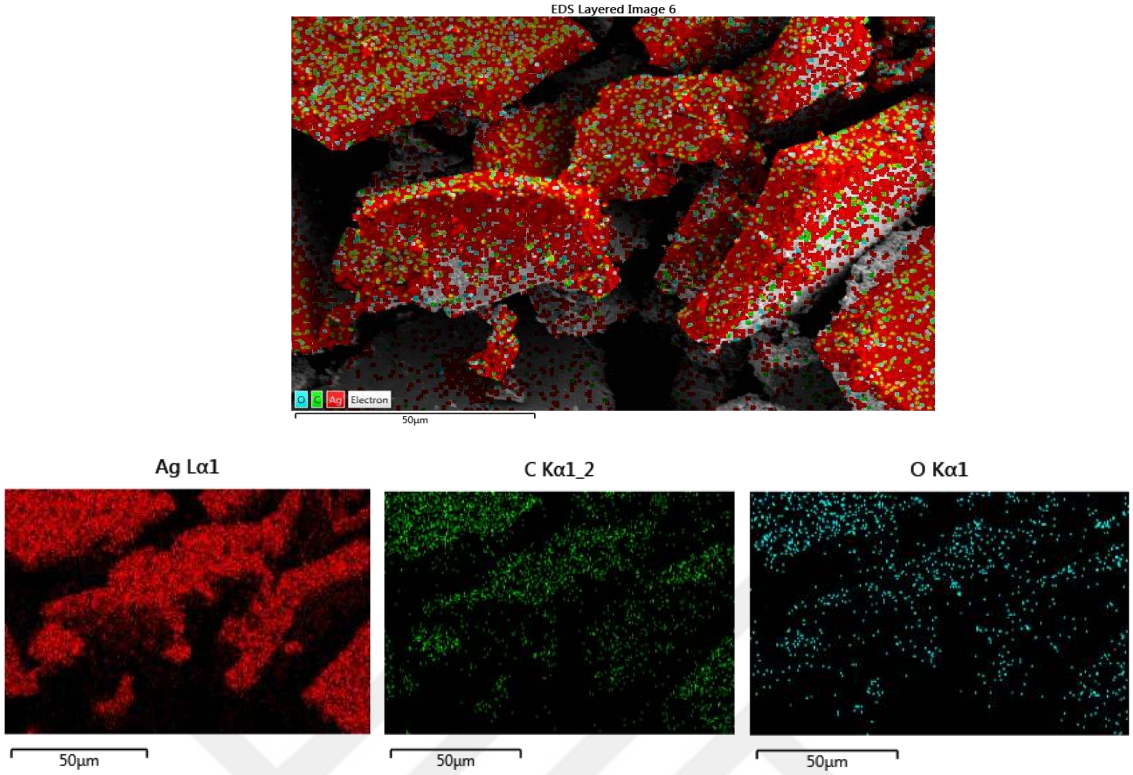

Figure 3.32. EDX spectrum of silver nanoparticles synthesized by Quercetin+ Gallic acid and elemental mapping, layered image.

The result of the EDX analysis indicates the presence of a high amount of Ag with an atomic composition of 92,2 % of the synthesis (Figure 3.33).

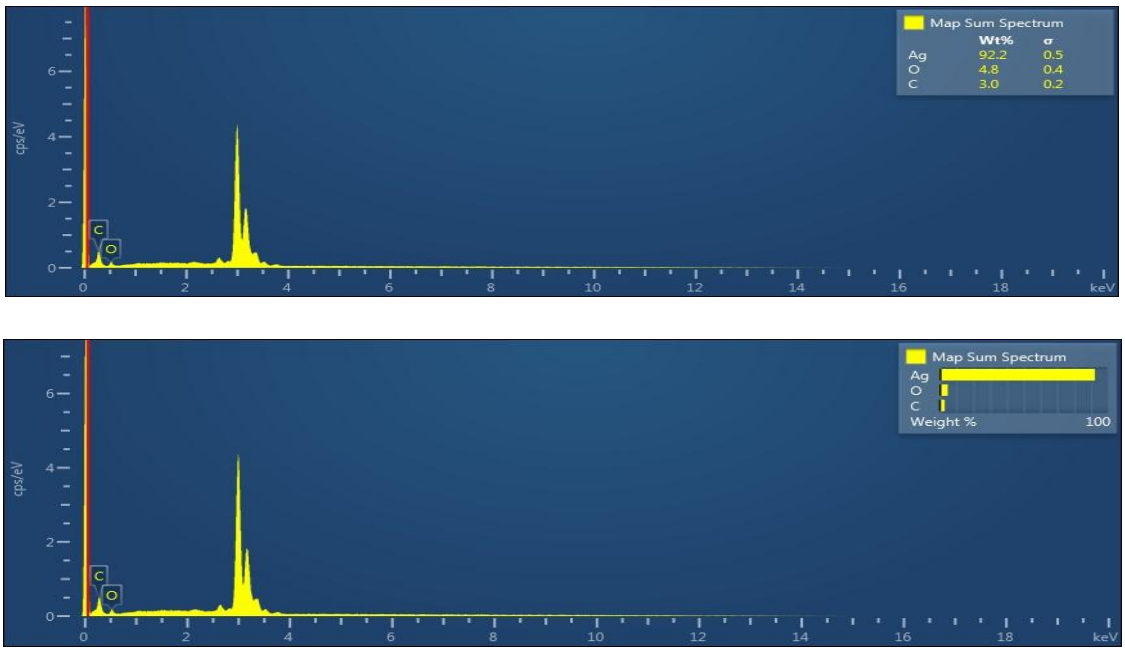

Figure 3.33. Elemental composition analysis and field electron micrograph of AgNPs

XRD Analysis

The silver nanoparticles XRD measurements. The reflection peaks correspond to the reflections of 631. 748, 1052, 857, 941 .539, 1, 806.8477, 618.279, and 607.979 at 2 Theta values of 38.05, 44.25, 64.42 and 77.22 pictures show the cubic shapes of the nanoparticles (Figure 3.34).

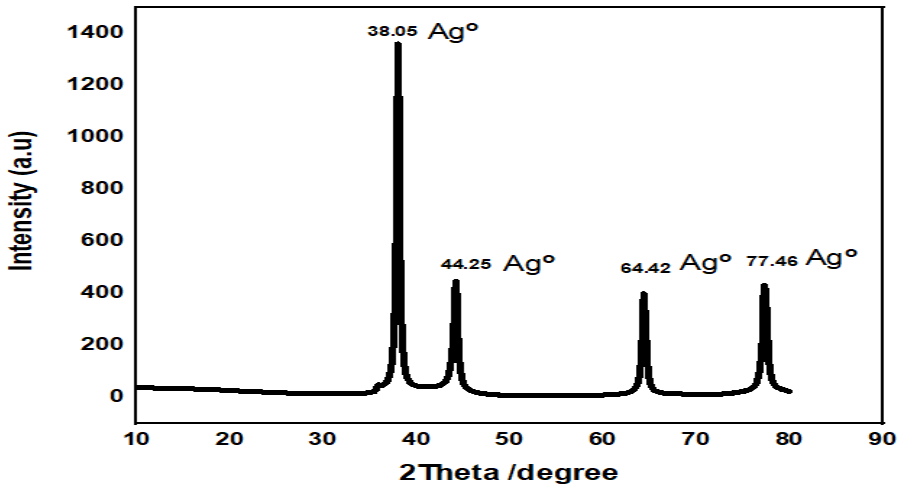

Figure 3.34. XRD spectrum of AgNPs synthesized with Quercetin+Gallik acid

Antimicrobial

At this point (7.50±0.0 mg) kill 6 log of the bacteria Escherichia coli at 37^{o} C for 24 hours. Also, at this point (5.00±2.65 mg) kill 6 log Bactria Staphylococcus aureus.

The compared solid and liquid concentration of Ag. This number (7.50±0.0 mg) lower than this (184±64 mg) number for Escherichia coli and *(*5.00±2.65mg*)* lower than this (221±0 mg) for Staphylococcus aureus .only cu needs for (26±9 mg) to kill 6 log of the bacteria Escherichia coli(mg) and (21±9 mg) to kill 6 log of the Staphylococcus aureus (mg) (Table 3.5.).

Table 3.5. Minimum inhibitory concentrations (MIC) of Quercetin+Gallic acid AgNPs (Mean±Standard Deviation).

No	Matter	Escherichia coli	Staphylococcus aureus
1	Quercetin+Gallic acid+Ag	7.50±0.00	5.00±2.65
2	Gallic Acid+Quercetin (mg)	184±64	221±0
3	Ag (mg)	26±9	21±9

3.3.2. Gallic acid, Quercetin and copper nanoparticles

UV-VIS spectroscopy

The UV-Vis absorption spectrum of copper nanoparticles at 426.994 nm (**Figure 3.35**).

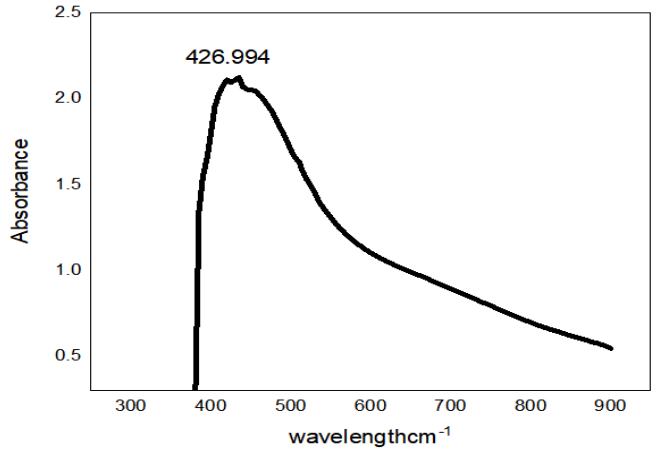

Figure 3.35. UV-VIS spectrum of CuNPs synthesized with Quercetin+Gallic acid

FTIR Analysis

The copper nanoparticles are mediated by the Gallic acid and quercetin FTIR spectrum 3731, 3415, 2922, 2848, 1538, 1400, 1309, 1262, 1108, 819, and 758 cm^{-1}. The peaks at the wavelength range from 3700 to 3100 cm^{-1} displayed O–H stretching modes in CuNPs. Also, C–H stretching vibrations at the heights of 3000–2800 cm^{-1} were attributed. Moreover, the peaks 1643, 1538, 1400, 1309, 1103, 1226, 1108, 819 cm^{-1} demonstrated carboxylic group (C=O), C-OH vibrations, Carboxylic acid (C-O), (C-O) stretches, =C-H bending (Aromatic ring) (Figure 3.36).

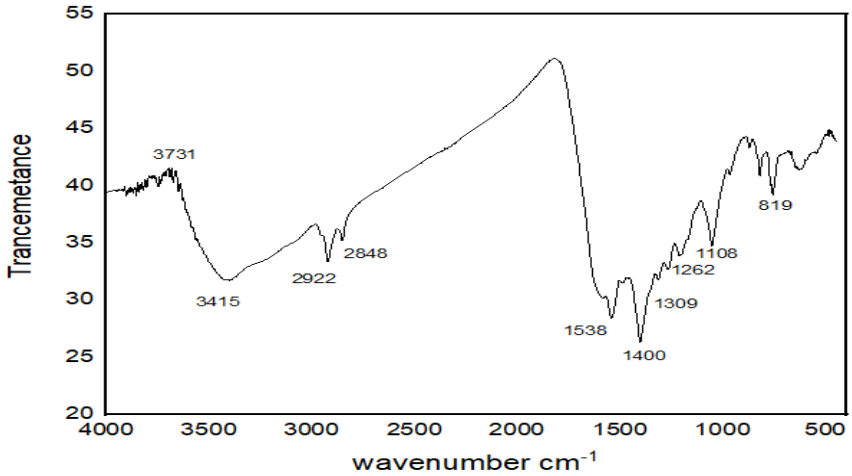

Figure 3.36. FTIR spectra of Quercetin, Gallic acid and copper nanoparticle.

SEM Analysis

The morphological features of synthesized copper nanoparticles have been studied (above). SEM studies showed that most of the particles are spherical in (Figure 3.37).

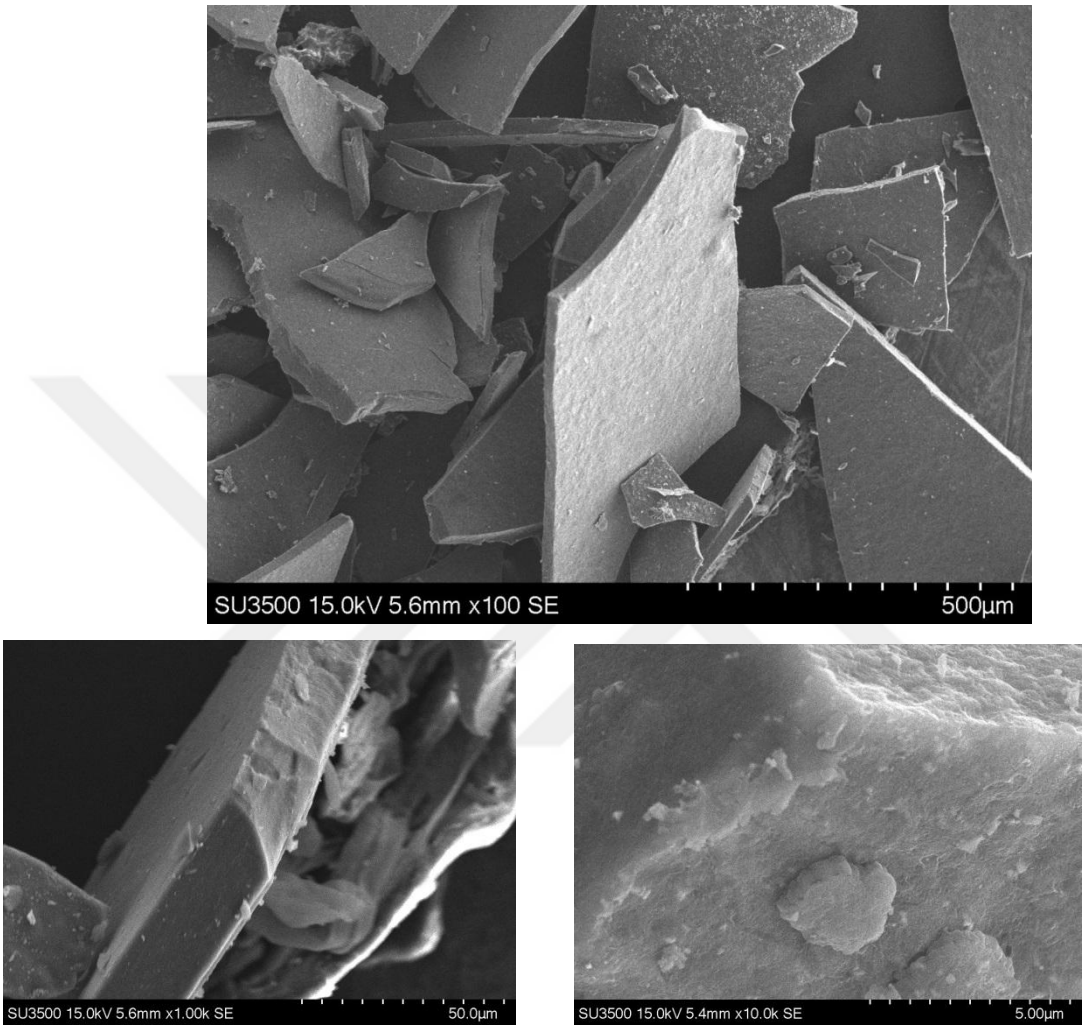

Figure 3.37. SEM image of copper nanoparticles synthesized by Quercetin + Gallic acid at various enlargement levels (500 µm, 50.0 µm, 5.00 µm).

EDX Analysis

In a strong oxygen signal and a weak carbon and copper, a peak is seen in the EDX profile which can start with biomolecules at the CuNPs surface (Figure 3.38).

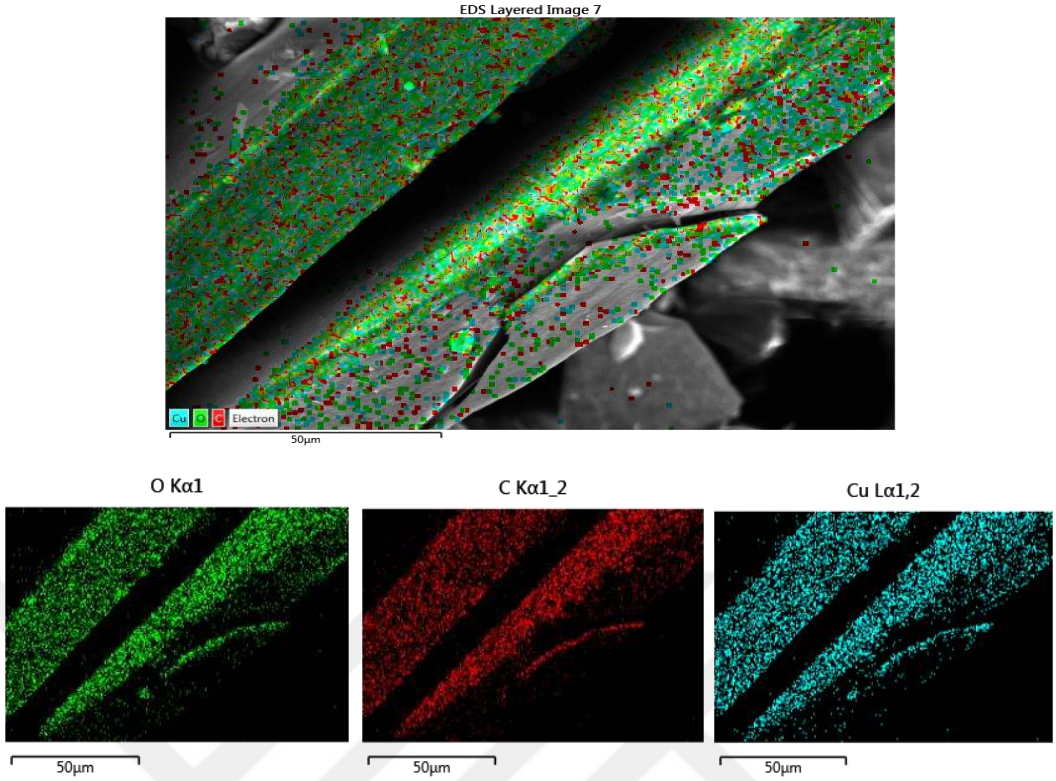

Figure 3.38. EDX spectrum of copper nanoparticles synthesized by Quercetin+Gallic acid and elemental mapping, layered image.

The result of the EDX analysis indicates the presence of a high amount of Cu with an atomic composition of 21.8 %. But the number of carbon atoms 37,0 % even higher than copper, also, the atomic composition of oxygen 34,9 %, Au 3,0 %, Na 1,5, % (Figure 3.39).

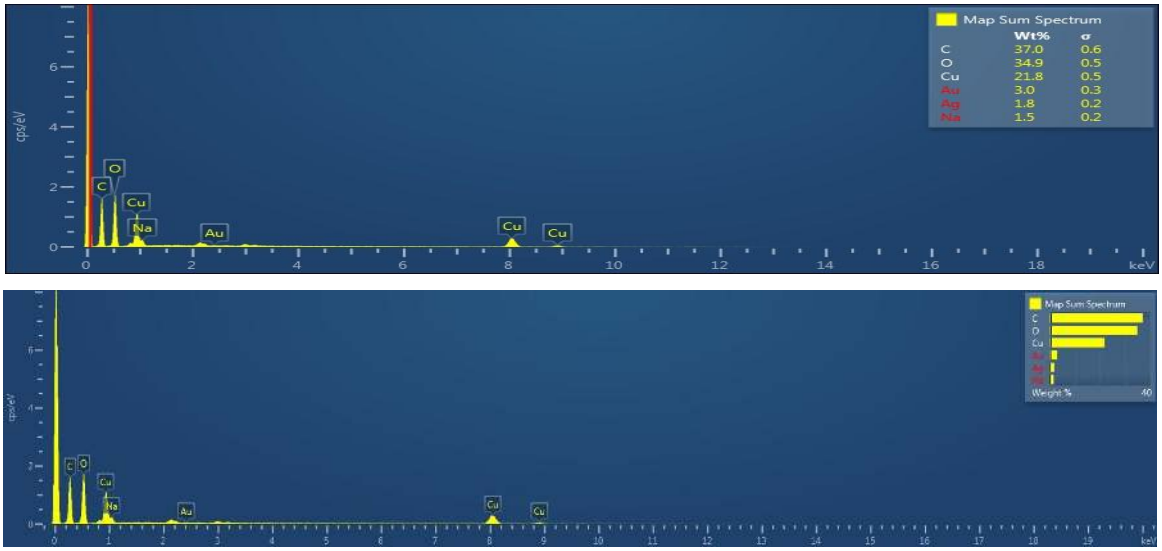

Figure 3.39. Elemental composition analysis and field electron micrograph of CuNPs

XRD Analysis

The copper nanoparticles' XRD measurements showed. The reflection peaks correspond to the reflections of 631.748, 1052.857, 941.539, 1655.800, 806.8477, 618.279, and 607.979 at 2 Theta values of 20.335, 27.329, 30.817, 37.94, 44.052, 64.418, and 77.22 (Figure 3.40).

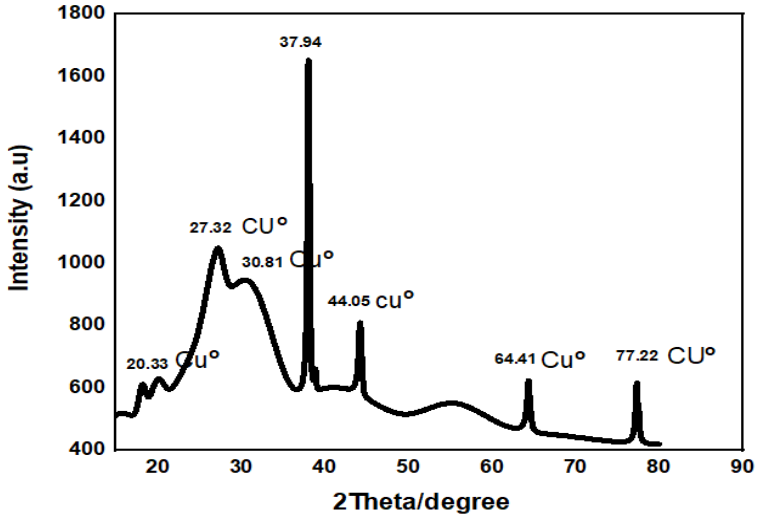

Figure 3.40. XRD spectrum of CuNPs synthesized with Quercetin+Gallik acid

Antimicrobial

At this point (7.50±0.00 mg) kill 6 log of the bacteria Escherichia coli at 37° C for 24 hours. Also, at this point (8.75±2.17 mg) kill 6 log bacteria Staphylococcus aureus (Table 3.6.).

Table 3.6. Minimum inhibitory concentrations of solid nanoparticles (MIC) Mean± Standard Deviation).

No	Matter	Escherichia coli	Staphylococcus aureus
1	Quercetin+ Gallic acid+ Cu (mg)	7.50±0.00	8.75±2.17
2	Gallic acid+ Quercetin(mg)	184±64	221±0
3	Cu (mg)	2832±981	1416±491

The compared solid and liquid concentration of Cu .This number (7.50±0.0 mg) lower than this (184±64 mg) number for Escherichia coli *and (*875±217 mg*)* lower than this (221±0.0 mg) for Staphylococcus aureus. Only Cu needs for (2832±981 mg) to kill 6 log of the bacteria Escherichia coli (mg) and (1416±491 mg) to kill 6 log of the Staphylococcus aureus (mg).

3.3.3. Gallic acid, Quercetin, silver and copper nanoparticles

UV-VIS spectroscopy

The UV-Vis absorption spectrum of silver and copper nanoparticles at 468.65 nm in (Figure 3.41).

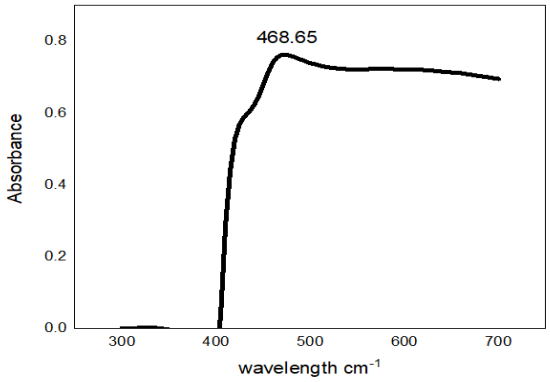

Figure 3.41. UV-VIS spectrum of AgCuNPs synthesized with Quercetin+Gallic acid

FTIR Analysis

Infrared spectroscopy of Fourier transform (FTIR) was used identification of the potentially liable biomolecules to minimize and stabilize AgNPs and CuNPs. The FT-IR spectra of AgNPs and CuNPs, synthesized nanoparticles made with extracts of water and ethanol it is hawthorn. Nanoparticles of metal were synthesized using $AgNO_3$ and Cu $(NO_3)_2.5H_2O$. The key spectrum is showing bands at 3432, 2925, 2854, 1628, 1121, 1138 and 812 cm^{-1}.This 3432 cm^{-1} middle 3300-3500 cm^{-1} N -H stretch max this 2925 cm^{-1} OH (carboxylic acid) stretch peak. This peak 2854 cm^{-1} C-H. This peak 1628 cm^{-1} C=O stretching. The wave number 1121cm^{-1} C=O stretching. The group of peaks in the range of 1600-1400 cm^{-1} corresponds to C= C bonds stretching this spectrum 1138 cm^{-1} C=C and 812 cm^{-1} spectrum =C-H bending (Aromatic ring) (Figure 3.42).

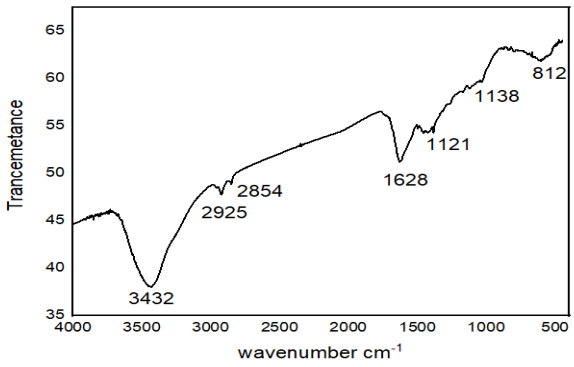

Figure 3.42. FTIR spectrum of AgCuNPs synthesized with Quercetin+Gallic acid.

SEM Analysis

SEM research was shown in the morphological features of synthesized silver and copper nanoparticles have been studied. SEM studies showed that most of the particles are spherical (Figure 3.43).

.

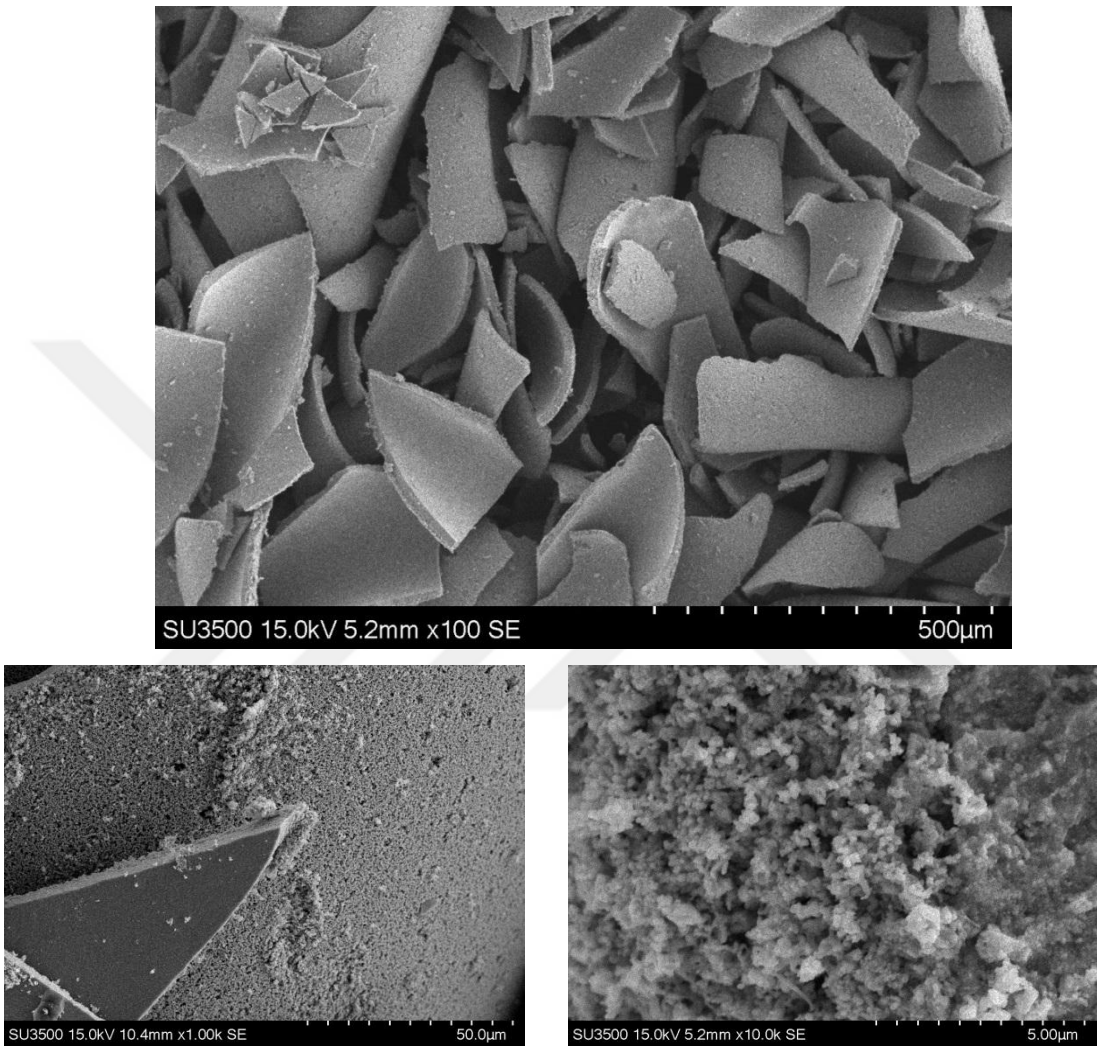

Figure 3.43. SEM image of silver nanoparticles synthesized by Quercetin at various enlargement levels (500 µm, 50.0 µm, 5.00 µm).

EDX Analysis

In a strong silver signal and a weak carbon, a peak is seen in the EDX profile which can start with biomolecules at the CuNPs surface (Figure 3.44).

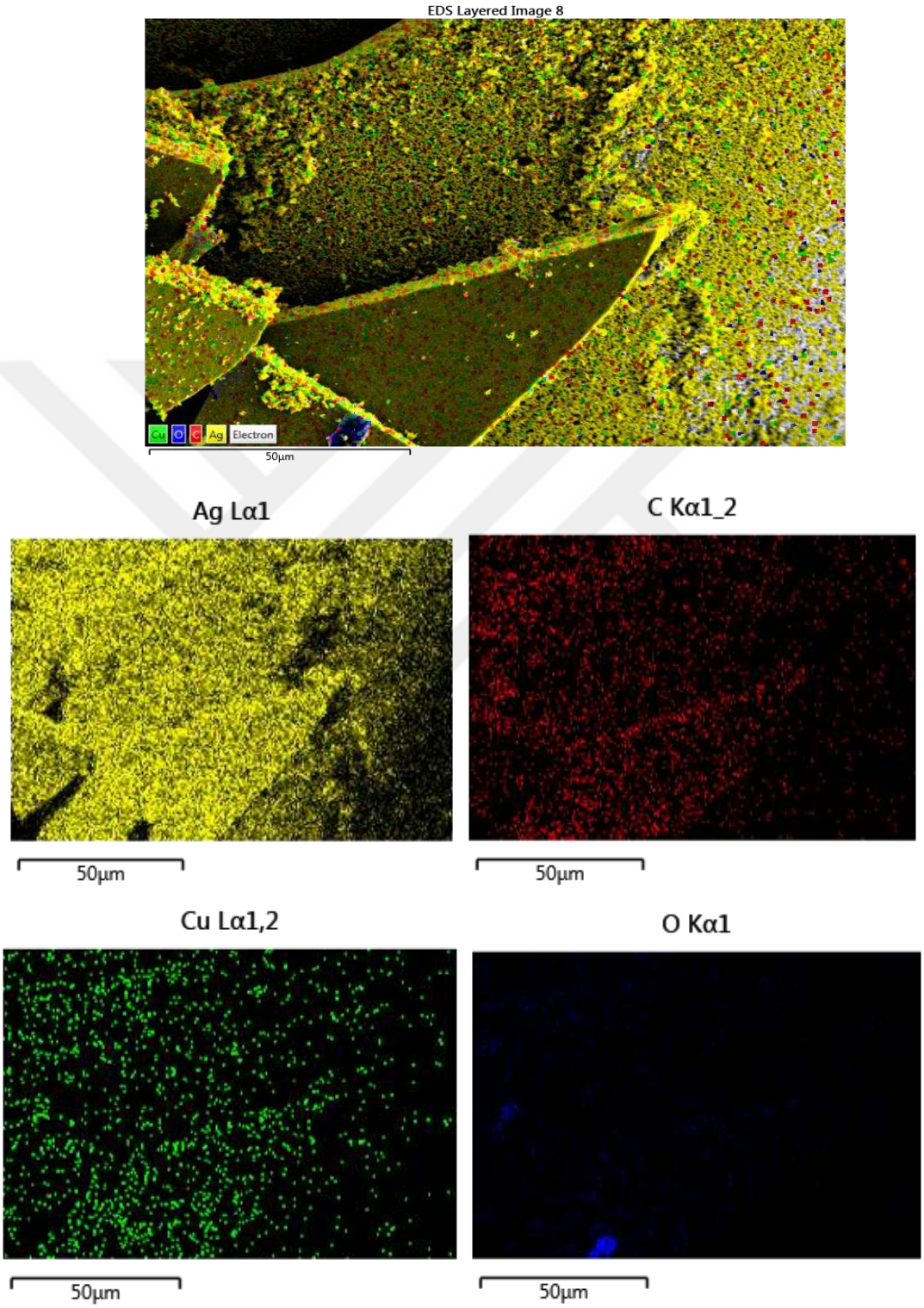

Figure 3.44. EDX spectrum of AgCuNPs nanoparticles synthesized by Quercetin+Gallic acid and elemental mapping, layered image.

The result of the EDX analysis indicates the presence of a high amount of Ag with an atomic composition of 48.82 %, Cu atoms 4.88 % even higher than copper, also, the atomic composition of oxygen 4.77 %, C 2.95 %, Mg 1.00 % (Figure 3.45.).

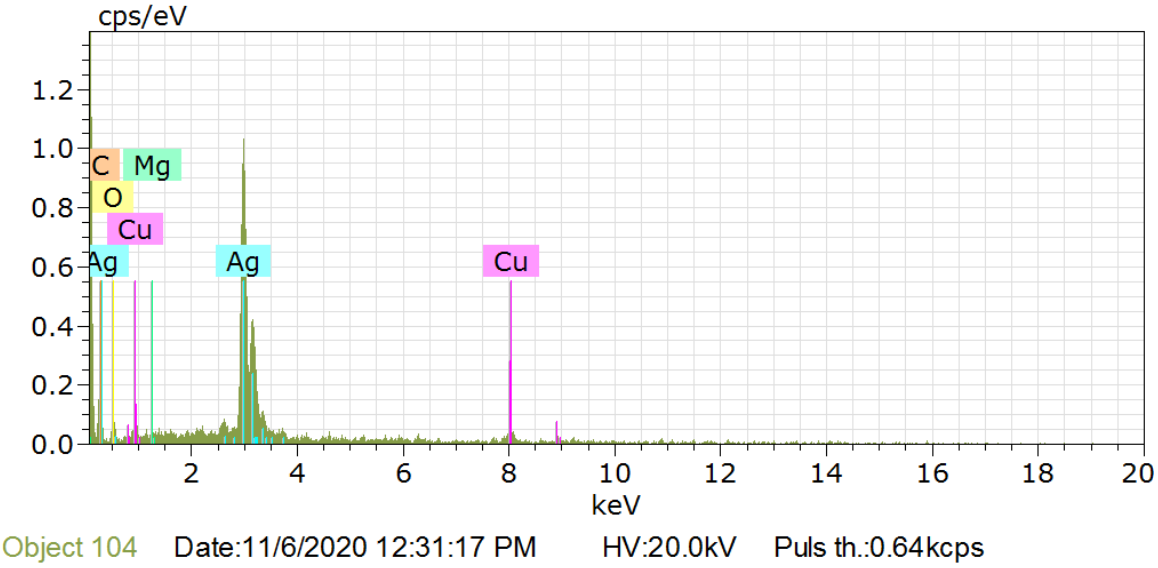

El	AN	Series	unn. C [wt.%]	norm. C [wt.%]	Atom. C [at.%]	Error (1 Sigma) [wt.%]
Ag	47	L-series	48.82	78.21	40.61	2.00
Cu	29	K-series	4.88	7.82	6.89	0.65
O	8	K-series	4.77	7.64	26.75	2.86
C	6	K-series	2.95	4.73	22.06	1.31
Mg	12	K-series	1.00	1.60	3.69	0.23
		Total:	62.43	100.00	100.00	

Figure 3.45. XRD spectrum of AgCuNPs synthesized with Quercetin nanoparticles.

XRD Analysis

The silver and copper nanoparticles' XRD measurements showed (Figure 3.46). The reflection peaks correspond to the reflections of 2016.97, 673.43, 531.19 and 563.67 at 2 Theta values of 38.22 (Ag), 44.38 (Cu), 64.52 (Cu) and 77.46 (Cu).

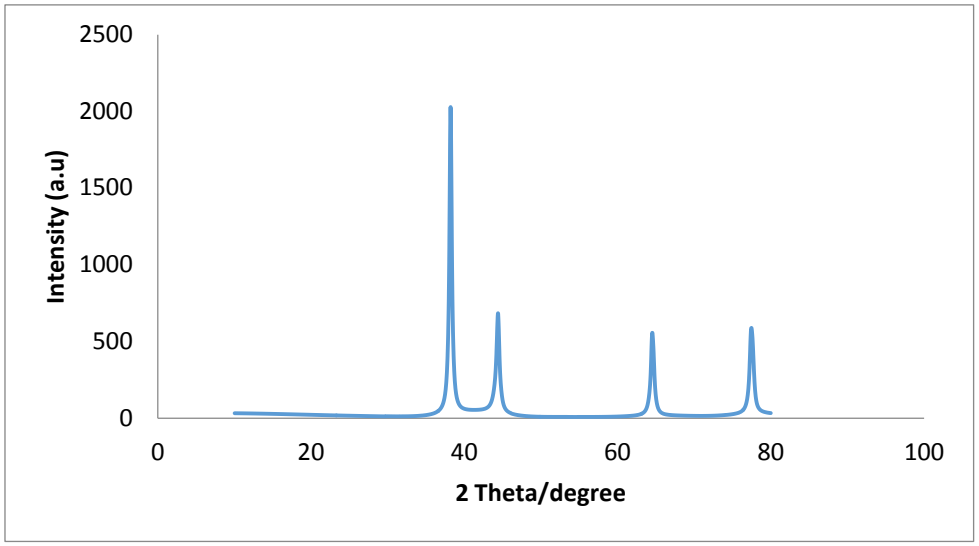

Figure 3.46. XRD spectrum of AgCuNPs synthesized with Quercetin+Gallik acid

Antimicrobial

At this point (3.13±1.08 mg), kill 6 logs of the bacteria Escherichia coli at 37^{o} C for 24 hours. Also, at this point (5.63±3.25 mg), kill 6 log bacteria Staphylococcus aureus. The compared solid and liquid concentration of Ag and Cu, this number (3.13±1.08 mg) lower than this (184±64 mg) number for Escherichia coli and (5.63±3.25 mg) lower than this (221±0 mg) for Staphylococcus aureus only Ag and Cu needs for (301±0 mg) to kill 6 logs of the bacteria Escherichia coli(mg) and (150±0 mg) to kill 6 logs of the Staphylococcus aureus (mg) (Table 3.7.).

Table 3.7. Minimum inhibitory concentrations (MIC) of AgCuNPs synthesized with Quercetin+Gallic Acid (Mean± Standard Deviation).

No	Matter	Escherichia coli (mg)	Staphylococcus aureus (mg)
1	Gallic acid+Quercetin+Ag+Cu(mg).	3.13±1.08	5.63±3.25
2	Gallic Acid+Quercetin	184±64	221±0
3	Ag+Cu	301±0	150±0

CONCLUSION

Quick and easy synthesis of Ag monometallic particles, monometallic nanoparticles, and Ag-Cu bimetallic particles by the method through the Quercetin and Gallic acid by reducing AgNO3 and Cu $(NO_3)_2.3H_2O$ solutions. It was successfully achieved by returning. It is worth mentioning that the nanoparticles formed by Ag and Cu, which are found together with Quercetin and Gallic acid were examined in this study and showed a rapid and successful big improvement.

The crystal structure, morphology with UV/VIS, FTIR, XRD, and SEM spectroscopy were used to characterize the optical properties of the silver-copper nanoparticles. The formation of Ag, Cu, and Ag-Cu NPs was monitored by surface Plasmon resonance (λ max at 300-700 nm) and UV-vis spectra in all nanoparticles and without the use of heat. We first observed the formation of nanoparticles as early as one hour in the water solution and the reactions were completed within two hours for NPs. The XRD models confirmed the formation of Ag, Cu, and Ag-Cu bimetallic nanoparticles, due to their presenting peaks of their own. SEM analysis shows that the morphology of the Ag NPs has a cubic shape; The Ag-CuNPs are also the same, while the CuNPs showed spherical shapes. The EDX spectrum emphasizes high silver signals in AgNPs and Ag-CuNPs synthesized by Quercetin and Gallic acid, the peak of copper was recorded for CuNPs synthesized by Gallic acid recorded strong peaks compared to Quercetin, the EDX spectrum was very weak in CuNPs synthesized by Qurcetin.

The antimicrobial activity showed that the colloidal AgNPs, CuNPs and AgCoNPs synthesized by Quercetin and Gallic acid inhibited the growth of the test bacteria S.aureus, and E.coli. Quercetin is stronger than Gallic acid because its lower concentration kills the same number of bacteria 6 logs (1,000,000). The difference between Escherichia coli (3.75 ± 0.00) (mg) and Staphylococcus aureus (37.50 ± 0.00) (mg) means Escherichia coli more sensitive than Staphylococcus aureus also Staphylococcus aureus more resistant than Escherichia coli, in combination with quercetin and Ag nanoparticles (2.11 mg) higher than liquid Ag (0.26 ± 0.09 mg), because 2.11 mg nanoparticles are critical in Ag nanoparticles, and only 188 mg are used quercetin.

The synthesized nanoparticles can be used for the manufacture of antibacterial drugs due to the bacterial activity of the Nano, as a result lays the manufacture of materials active against bacteria.

REFERENCES

[1] Kaviarasu, C., & Ravichandran, M. (2020). Nanomaterials through Powder Metallurgy: Production, Processing, and Potential Applications toward Energy and Environment. *Handbook of Nanomaterials and Nanocomposites for Energy and Environmental Applications*, 1-40.

[2] Merzbacher, C. (2020). National Nanotechnology Initiative: A Model for Advancing Revolutionary Technologies. In *Women in Nanotechnology* (pp. 121-133). Springer, Cham.

[3] Ramteke, L., Gawali, P., Jadhav, B. L., & Chopade, B. A. (2020). Comparative study on antibacterial activity of metal ions, monometallic and alloy noble metal nanoparticles against nosocomial pathogens. *BioNanoScience*, *10*(4), 1018-1036.

[4] Zhang, Y., Zhang, Q., Ouyang, X., Lei, D. Y., Zhang, A. P., & Tam, H. Y. (2018). Ultrafast light-controlled growth of silver nanoparticles for direct plasmonic color printing. *ACS nano*, *12*(10), 9913-9921.

[5] Hunault, M. O., Loisel, C., Bauchau, F., Lemasson, Q., Pacheco, C., Pichon, L., ... & Pallot-Frossard, I. (2017). Nondestructive redox quantification reveals glassmaking of rare French Gothic stained glasses. *Analytical chemistry*, *89*(11), 6277-6284.

[6] Varshney R, Bhadauria S, Gaur MS. Biogenic synthesis of silver nanocubes and nanorods using sundried Stevia rebaudiana leaves. Adv. Mat. Lett. 2010; 1(3): 232-237.http://dx.doi.org/10.5185/ amlett.2010.9155.

[7] Ibraheem, S. A., Kadhem, H. A., Hadeethi, S. A., Jabir, M. S., Grigore, R., Popa, M., ... & Florin, M. D. (2019). Effects of silver nanoparticles on nosocomial Pseudomonas aeruginosa strains–an alternative approach for antimicrobial therapy. *Romanlan Biotechnological Letters*, *24*, 286-293.

[8] Jagielski, T., Bakuła, Z., Pleń, M., Kamiński, M., Nowakowska, J., Bielecki, J., & Grudniak, A. M. (2018). The activity of silver nanoparticles against microalgae of the Prototheca genus. *Nanomedicine*, *13*(9), 1025-1036.

[9] Becerra, J., Ortiz, P., Zaderenko, A. P., & Karapanagiotis, I. (2020). Assessment of nanoparticles/nanocomposites to inhibit micro-algal fouling on limestone façades. *Building Research & Information*, *48*(2), 180-190.

[10] Mohamed, A. M., Sorokin, V. V., Skladnev, D. A., Shevlyagina, N. V., Zhukhovitsky, V. G., & Pshenichnikova, A. B. (2020). Biosynthesis of Silver Nanoparticles by Methylophilus quaylei, Characterization and Its Impact on Established Biofilms. *BioNanoScience*, *10*(4), 885-898.

[11] Jahan, I., & IŞILDAK, İ. (2020). Microwave irradiation system for a rapid synthesis of non-toxic metallic copper nanoparticles from green tea. *Trakya University Journal of Natural Sciences*.

[12] Milanezi, F. G., Meireles, L. M., de Christo Scherer, M. M., de Oliveira, J. P., da Silva, A. R., de Araujo, M. L., ... & Scherer, R. (2019). Antioxidant, antimicrobial and cytotoxic activities of gold nanoparticles capped with quercetin. *Saudi pharmaceutical journal*, *27*(7), 968-974.

[13] Jagielski, T., Bakuła, Z., Pleń, M., Kamiński, M., Nowakowska, J., Bielecki, J., ... & Grudniak, A. M. (2018). The activity of silver nanoparticles against microalgae of the Prototheca genus. *Nanomedicine*, *13*(9), 1025-1036.

[14] Li G, He D, Qian Y, Guan B, Gao S, Cui Y, Yokoyama K, Wang L. Fungus-mediated green synthesis of silver nanoparticles using Aspergillus terreus. Int. J. Mol. Sci. 2011; 13: 466-476; http://dx.doi. org/10.3390/ijms13010466.

[15] Mohamed, A. M., Sorokin, V. V., Skladnev, D. A., Shevlyagina, N. V., Zhukhovitsky, V. G., & Pshenichnikova, A. B. (2020). Biosynthesis of Silver Nanoparticles by Methylophilus quaylei, Characterization and Its Impact on Established Biofilms. BioNanoScience, 1-14.

[16] Jahan, I., & Işildak, İ. Microwave Irradiation System For A Rapid Synthesis Of Non-Toxic Metallic Copper Nanoparticles From Green Tea. Trakya University Journal of Natural Sciences.

[17] Milanezi, F. G., Meireles, L. M., de Christo Scherer, M. M., de Oliveira, J. P., da Silva, A. R., de Araujo, M. L., ... & Scherer, R. (2019). Antioxidant, antimicrobial and cytotoxic activities of gold nanoparticles capped with quercetin. *Saudi pharmaceutical journal*, *27*(7), 968-974.

[18] Ramos, M. K., & Zarbin, A. J. (2020). Graphene/copper oxide nanoparticles thin films as precursor for graphene/copper hexacyanoferrate nanocomposites. Applied Surface Science, 146000.

[19] Jadoun, S., Arif, R., Jangid, N. K., & Meena, R. K. (2020). Green synthesis of nano-particles using plant extracts: a review. Environmental Chemistry Letters, 1-20.

[20] Bhushan, B. (2020). Frontiers in Nanotribology: Magnetic Storage, Bio/Nanotechnology, Cosmetics, and Bioinspiration. Journal of Colloid and Interface Science.
[21] Al-Hakkani, M. F. (2020). Biogenic copper nano-particles and their applications: A review. SN Applied Sciences, 2(3), 1-20.
[22] Hu, M. (2007). Commentary: Bio-availability of flavonoids and polyphenols: call to arms.
[23] Omran, B. A. (2020). Fundamentals of Nanotechnology and Nanobiotechnology. In Nanobiotechnology: A Multidisciplinary Field of Science (pp. 1-36). Springer, Cham.
[24] Tasca, F., & Antiochia, R. (2020). Biocide Activity of Green Quercetin-Mediated Synthesized Silver Nano-particles. Nano-materials, 10(5), 909.
[25] Praphawatvet, T., Peters, J. I., & Williams III, R. O. (2020). Inhaled nano-particles—An updated review. International Journal of Pharmaceutics, 119671.
[26] Al-Hakkani, M. F. (2020). Biogenic copper nano-particles and their applications: A review. SN Applied Sciences, 2(3), 1-20.
[27] Wang, D., Jin, H., Ling, X., Peng, H., Yu, J., & Cui, Z. (2020). Regulation of velocity zoning behaviour and hydraulic jump of impinging jet flow on a spinning disk reactor.
[28] Jampilek, J. O. S. E. F., & Kralova, K. (2019). Natural biopolymeric nano-formulations for brain drug delivery. Nanocarriers for Brain Targetting: Principles and Applications; Keservani, RK, Sharma, AK, Kesharwani, RK, Eds, 131-203.
[29] Attatsi, I. K., & Nsiah, F. (2020). Application of silver nanoparticles toward Co (II) and Pb (II) ions contaminant removal in groundwater. Applied Water Science, 10(6).
[30] Mansha, M., Khan, I., Ullah, N., & Qurashi, A. (2017). Synthesis, characterization and visible-light-driven photoelectrochemical hydrogen evolution reaction of carbazole-containing conjugated polymers. International Journal of Hydrogen Energy, 42(16), 10952-10961.
[31] Ma, W., Lopez, G., Ameduri, B., & Takahara, A. (2020). Fluoropolymer nanoparticles prepared using trifluoropropene telomer based fluorosurfactants. Langmuir, 36(7), 1754-1760.
[32] Bai, X., Wang, Y., Song, Z., Feng, Y., Chen, Y., Zhang, D., & Feng, L. (2020). The Basic Properties of Gold Nanoparticles and their Applications in Tumor Diagnosis and Treatment. International Journal of Molecular Sciences, 21(7), 2480.
[33] Chemical Engineering Journal, 390, 124392.Yuan, Y., Xiong, Y., Li, J., Yin, W., Peng, Q., Lu, H., ... & He, X. (2020). Large-scale synthesis of hollow carbon fibers with ultra-large diameter by thermally controlled pyrolysis. Journal of the American Ceramic Society.
[34] Ijaz, I., Gilani, E., Nazir, A., & Bukhari, A. (2020). Detail review on chemical, physical and green synthesis, classification, characterizations and applications of nanoparticles. Green Chemistry Letters and Reviews, 13(3), 59-8.
[35] Emeji, I. C., Ama, O. M., Aigbe, U. O., Khoele, K., Osifo, P. O., & Ray, S. S. (2020). Properties and Synthesis of Metal Oxide Nanoparticles in Electrochemistry. In Nanostructured Metal-Oxide Electrode Materials for Water Purification (pp. 85-96). Springer, Cham.
[36] Mchedlov-Petrossyan, N. O. (2020). Fullerenes in Aqueous Media: A Review. Theoretical and Experimental Chemistry, 1-31.
[37] Kapoor, S., Goyal, M., & Jindal, P. (2020). Effect of functionalized multi-walled carbon nanotubes on thermal and mechanical properties of acrylonitrile butadiene styrene nanocomposite. Journal of Polymer Research, 27(2), 40.
[38] Ijaz, I., Gilani, E., Nazir, A., & Bukhari, A. (2020). Detail review on chemical, physical and green synthesis, classification, characterizations and applications of nanoparticles. Green Chemistry Letters and Reviews, 13(3), 59-81.
[39] Duarte, M., Benítez, A., Gómez, K., Zuluaga, B., Meza, J., Cardona-Maya, Y., ... & Isaza, C. (2020). Nanomechanical characterization of a metal matrix composite reinforced with carbon nanotubes. AIMS Materials Science, 7(1), 33.
[40] Commentary: Bio-availability of flavonoids and polyphenols: call to arms: M. Hu; Mol. Pharm. 4, 803 (2007) .
[41] Sanapala, P., & Pola, S. (2020). Toxicological Evaluation of Nanoparticles Using Prokaryotic Model Organisms. In Model Organisms to Study Biological Activities and Toxicity of Nanoparticles (pp. 277-296). Springer, Singapore.
[42] Antioxidant activity of tea polyphenols in vivo: evidence from animal studies: B. Frei & J. V. Higdon; J. Nutr. 133, 3275S (2003).
[43] Green tea polyphenols: biology and therapeutic implications in cancer: S. Shankar, et al.; Front. Biosci. 12, 4881 (2007).
[44] Flavonoids: antioxidants or signalling molecules?: R. J. Williams, et al.; Free Radic. Biol. Med. 36, 838 (2004).

[45] Beneficial action of Citrus flavonoids on multiple cancerrelated biological pathways: O. Benavente-Garcia, et al.; Curr. Cancer Drug Targets 7, 795 (2007).
[46] Reading the tea leaves: anticarcinogenic properties of (-)-epigallocatechin-3-gallate: J. R. Carlson, et al.; Mayo Clin. Proc. 82, 725 (2007).
[47] Overview of antibacterial, antitoxin, antiviral, and antifungal activities of tea flavonoids and teas: M. Friedman; Mol. Nutr. Food Res. 51, 116 (2007).
[48] Dietary polyphenols: good, bad, or indifferent for your health?: B. Halliwell; Cardiovasc. Res. 73, 341 (2007).
[49] Milanezi, F. G., Meireles, L. M., de Christo Scherer, M. M., de Oliveira, J. P., da Silva, A. R., de Araujo, M. L., ... & Scherer, R. (2019). Antioxidant, antimicrobial and cytotoxic activities of gold nanoparticles capped with quercetin. Saudi pharmaceutical journal, 27(7), 968-974.
[50] Merzbacher, C. (2020). National Nanotechnology Initiative: A Model for Advancing Revolutionary Technologies. In Women in Nanotechnology. Springer, Cham.
[51] Rawashdeh, R. Y., Sawafta, R., & Malkawi, H. I. (2020). Dental Materials Incorporated with Nanometals and Their Effect on the Bacterial Growth of Staphylococcus aureus. International Journal of Nanomedicine, 15, 4325.
[52] Rawashdeh, R. Y., Sawafta, R., & Malkawi, H. I. (2020). Dental Materials Incorporated with Nanometals and Their Effect on the Bacterial Growth of Staphylococcus aureus. International Journal of Nanomedicine, 15, 4325.
[53] Some, S., Sarkar, B., Biswas, K., Jana, T. K., Bhattacharjya, D., Dam, P., ... & Saha, S. (2020). Bio-molecule functionalized rapid one-pot green synthesis of silver nanoparticles and their efficacy toward the multidrug resistant (MDR) gut bacteria of silkworms (Bombyx mori). RSC Advances, 10(38), 22742-22757.
[54] Goodsell, D. S. (2004). Bionanomedicine in action. Bionanotechnology: Lessons from Nature; John Wiley & Sons Inc.: Hoboken, NJ, USA.
[55] Swilam, N., & Nematallah, K. A. (2020). Polyphenols profile of pomegranate leaves and their role in green synthesis of silver nanoparticles. Scientific Reports, 10(1), 1-11.
[56] Dyal, C., Nguyen, N., Hadden, J., Gou, L., Tan, L., Murphy, C. J., ... & Nivens, D. (2006). Green synthesis of gold and silver nanoparticles from plant extracts. *Chem Mater*, *231*, 301-315.
[57] Lee, K., Huang, Z. N., Mirkin, C. A., & Odom, T. W. (2020). Endosomal Organization of CpG Constructs Correlates with Enhanced Immune Activation. Nano Letters.
[58] Bayda, S., Adeel, M., Tuccinardi, T., Cordani, M., & Rizzolio, F. (2020). The history of nanoscience and nanotechnology: From chemical–physical applications to nanomedicine. Molecules, 25(1), 112.
[59] Sridharan, K., Srinivasu, B., & Pudi, V. (2020). Basics of CNTFET and Ternary Logic. In Low-Complexity Arithmetic Circuit Design in Carbon Nanotube Field Effect Transistor Technology (pp. 9-20). Springer, Cham.
[60] Huang, L., Lin, H., Zheng, C. Y., Kluender, E. J., Golnabi, R., Shen, B., & Mirkin, C. A. (2020). Multimetallic High-Index Faceted Heterostructured Nanoparticles. Journal of the American Chemical Society, 142(10), 4570-4575.
[61] Yao, X., Wang, J., Wu, G., Xu, J., & Yang, S. W. (2016). How to Fabricate a Surface-Grafted Polythiophene on H-Si (100) 2× 1 Surface via Self-Assembling and in Situ Surface Polymerization: A Theoretical Guide. The Journal of Physical Chemistry C, 120(44), 25612-25619.
[62] Dyck, O., Lingerfelt, D., Kim, S., Jesse, S., & Kalinin, S. V. (2020). Direct matter disassembly via electron beam control: electron-beam-mediated catalytic etching of graphene by nanoparticles. Nanotechnology, 31(24), 245303.
[63] Umemura, K., Ishibashi, Y., & Oura, S. (2016). Physisorption of DNA molecules on chemically modified single-walled carbon nanotubes with and without sonication. European Biophysics Journal, 45(6), 483-489.
[64] Shen, J., Li, K., Cheng, L., Liu, Z., Lee, S. T., & Liu, J. (2014). Specific detection and simultaneously localized photothermal treatment of cancer cells using layer-by-layer assembled multifunctional nanoparticles. ACS applied materials & interfaces, 6(9), 6443-6452.
[65] Ayala-Orozco, C., Urban, C., Knight, M. W., Urban, A. S., Neumann, O., Bishnoi, S. W., ... & Shea, M. (2014). Au nanomatryoshkas as efficient near-infrared photothermal transducers for cancer treatment: benchmarking against nanoshells. ACS nano, 8(6), 6372-6381.
[66] Thangadurai, T. D., Manjubaashini, N., Thomas, S., & Maria, H. J. (2020). Physics and Chemistry of Nano-structures. In Nanostructured Materials (pp. 47-53). Springer, Cham.

[67] Saeed, K., & Khan, I. (2020). Preparation and characterization of functionalized multiwalled carbon nanotubes filled polyethylene oxide nanocomposites. Journal of Rubber Research, 1-6.
[68] Sanapala, P., & Pola, S. (2020). Toxicological Evaluation of Nanoparticles Using Prokaryotic Model Organisms. In Model Organisms to Study Biological Activities and Toxicity of Nanoparticles (pp. 277-296). Springer, Singapore.
[69] Mishra, R. C., Kumari, R., Iqbal, Z., Rizvi, M. M. A., & Yadav, J. P. (2020). Synthesis, characterization, comparative antidandruff efficacy and cytotoxicity studies of biosynthesized silver nanoparticles by using Glycyrrhiza glabra root. Advanced Science, Engineering and Medicine, 12(2), 156-162.
[70] Thangadurai, T. D., Manjubaashini, N., Thomas, S., & Maria, H. J. (2020). Physics and Chemistry of Nano-structures. In Nanostructured Materials (pp. 47-53). Springer, Cham.
[71] Darweesh, H. H. M. (2018). Nanomaterials: Classification and Properties-Part I. J Nanosci, 1(1), 1-11.
[72] Yardley, R. E., Kenaree, A. R., & Gillies, E. R. (2019). Triggering depolymerization: Progress and opportunities for self-immolative polymers. Macromolecules, 52(17), 6342-6360.
[73] Leiserson, C. E., Thompson, N. C., Emer, J. S., Kuszmaul, B. C., Lampson, B. W., Sanchez, D., & Schardl, T. B. (2020). There's plenty of room at the Top: What will drive computer performance after Moore's law?. Science, 368(6495).
[74] Bayda, S., Adeel, M., Tuccinardi, T., Cordani, M., & Rizzolio, F. (2020). The history of nanoscience and nanotechnology: From chemical–physical applications to nanomedicine. Molecules, 25(1), 112.
[75] Mansha, M., Khan, I., Ullah, N., & Qurashi, A. (2017). Synthesis, characterization and visible-light-driven photoelectrochemical hydrogen evolution reaction of carbazole-containing conjugated polymers. International Journal of Hydrogen Energy, 42(16), 10952-10961.
[76] Ma, W., Lopez, G., Ameduri, B., & Takahara, A. (2020). Fluoropolymer nanoparticles prepared using trifluoropropene telomer based fluorosurfactants. Langmuir, 36(7), 1754-1760.
[77] Bai, X., Wang, Y., Song, Z., Feng, Y., Chen, Y., Zhang, D., & Feng, L. (2020). The Basic roperties of Gold Nanoparticles and their Applications in Tumor Diagnosis and Treatment. International Journal of Molecular Sciences, 21(7), 2480.
[78] Chemical Engineering Journal, 390, 124392.Yuan, Y., Xiong, Y., Li, J., Yin, W., Peng, Q., Lu, H., ... & He, X. (2020). Large-scale synthesis of hollow carbon fibers with ultra-large diameter by thermally controlled pyrolysis. Journal of the American Ceramic Society
[79] Kapoor, S., Goyal, M., & Jindal, P. (2020). Effect of functionalized multi-walled carbon nanotubes on thermal and mechanical properties of acrylonitrile butadiene styrene nanocomposite. Journal of Polymer Research, 27(2), 40.
[80] Ijaz, I., Gilani, E., Nazir, A., & Bukhari, A. (2020). Detail review on chemical, physical and green synthesis, classification, characterizations and applications of nanoparticles. Green Chemistry Letters and Reviews, 13(3), 59-81.
[81] Cheng, C., Harpster, M. H., & Oakey, J. (2020). Convection-driven microfabricated hydrogels for rapid biosensing. Analyst.
[82] Kandru, A. (2020). Nanotechnology: Application in Biology and Medicine. In Model Organisms to Study Biological Activities and Toxicity of Nanoparticles (pp. 1-18). Springer, Singapore.
[83] Gulati, S. S., & Chaudhary, A. (2019). Greener Synthesis of Silver Nanoparticles using Waste of Onion (Allium cepa) and Quercetin: a comparative study.
[84] Das, C. A., Kumar, V. G., Dhas, T. S., Karthick, V., Govindaraju, K., Joselin, J. M., & Baalamurugan, J. (2020). Antibacterial activity of silver nanoparticles (biosynthesis): A short review on recent advances. Biocatalysis and Agricultural Biotechnology, 101593.
[85] Ijaz, M., Zafar, M., & Iqbal, T. (2020). Green synthesis of silver nanoparticles by using various extracts: a review. Inorganic and Nano-Metal Chemistry, 1-12.
[86] Montero, N., Alhajj, M. J., Sierra, M., Oñate-Garzon, J., Yarce, C. J., & Salamanca, C. H. (2020). Development of Polyelectrolyte Complex Nanoparticles-PECNs Loaded with Ampicillin by Means of Polyelectrolyte Complexation and Ultra-High Pressure Homogenization (UHPH). Polymers, 12(5), 1168.
[87] Zhou, L., Sun, C., Li, X., Tang, L., Guo, W., Luo, L., ... & Liang, J. (2020). Tantalum disulfide quantum dots: preparation, structure, and properties. Nanoscale research letters, 15(1), 1-8.
[88] Rowan, N. J. (2019). Pulsed light as an emerging technology to cause disruption for food and adjacent industries–Quo vadis?. Trends in Food Science & Technology, 88, 316-332.
[89] De, S., Kunal, K., & Aluru, N. R. (2016). Mixed role of surface on intrinsic losses in silicon Nanostructures. Journal of Applied Physics, 119(11), 114304.

[90] Polyakov, M. N., Schoeppner, R. L., Pethö, L., Edwards, T. E., Thomas, K., Könnyű, B., ... & Michler, J. (2020). Direct co-deposition of mono-sized nano-particles during sputtering. Scripta Materialia, 186, 387-391.

[91] Zacharias, F., George, D., Michail, D., Ioannis, P., Marianna, T., Arzou, B., ... & Emmanuel, K. N. (2020). MicroRNAs determining carcinogenesis by regulating oncogenes and tumor suppressor genes during cell cycle. Microrna, 9(2), 82-92.

[92] Fu, S., Song, J., Zhu, C., Du, D., & Lin, Y. (2020). Metal-Organic Frameworks Based Porous Carbons for Oxygen Reduction Reaction Electrocatalysts for Fuel Cell Applications. Nanocarbon Electrochemistry, 251-284.

[93] Pareek, V., Bhargava, A., Gupta, R., Jain, N., & Panwar, J. (2017). Synthesis and applications of noble metal nano-particles: a review. Advanced Science, Engineering and Medicine, 9(7), 527-544.

[94] Jadoun, Sapana, Rizwan Arif, Nirmala Kumari Jangid, and Rajesh Kumar Meena. "Green synthesis of nano-particles using plant extracts: a review." Environmental Chemistry Letters (2020): 1-20.

[95] Mercado, N., Bhatt, P., Sutariya, V., Florez, F. L. E., & Pathak, Y. V. (2019). Application of Nanoparticles in Treating Periodontitis: Preclinical and Clinical Overview. In Surface Modification of Nanoparticles for Targeted Drug Delivery (pp. 467-480). Springer, Cham.

[96] Długosz, O., Chwastowski, J., & Banach, M. (2020). Hawthorn berries extract for the green synthesis of copper and silver nanoparticles. Chemical Papers, 74(1), 239-252.

[97] Lopez, E. I. P., Saint-Laurence, P. I. M., Ramirez, C. E. A., Gomez, L. B., Flores, A. M., Jimenez, F. D. L. C., & López, I. A. (2020). Estudio de perfiles de difracción de rayos X de una aleación Ti-13Ta-3Sn obtenida por aleado mecánico. Matéria (Rio de Janeiro), 25(2).

[98] Kong, L. B. (Ed.). (2020). Functional Ceramics Through Mechanochemical Activation. IOP Publishing.

[99] Fang, Z., Wang, Y., Schlather, A. E., Liu, Z., Ajayan, P. M., García de Abajo, F. J., ... & Halas, N. J. (2014). Active tunable absorption enhancement with graphene nanodisk arrays. Nano letters, 14(1), 299-304.

[100] García-López, V., Chiang, P. T., Chen, F., Ruan, G., Martí, A. A., Kolomeisky, A. B., ... & Tour, J. M. (2015). Unimolecular submersible nanomachines. Synthesis, actuation, and monitoring. Nano letters, 15(12), 8229-8239.

[101] Jin, T., García-López, V., Kuwahara, S., Chiang, P. T., Tour, J. M., & Wang, G. (2018). fusion of Nanocars on an Air–Glass Interface. The Journal of Physical Chemistry C, 122(33), 19025-19036.

[102] Tang, L., Zhu, L., Taylor, M. A., Wang, Y., Remington, S. J., & Fang, C. (2018). Excited state structural evolution of a GFP single-site mutant tracked by tunable femtosecond-stimulated Raman spectroscopy. Molecules, 23(9), 2226.

[103] Randino, C., Moreno, M., Gelabert, R., & Lluch, J. M. (2012). Peek at the potential energy surfaces of the LSSmKate1 and LSSmKate2 proteins. The Journal of Physical Chemistry B, 116(49), 14302-14310.

[104] Sha, R., Birktoft, J. J., Nguyen, N., Chandrasekaran, A. R., Zheng, J., Zhao, X., ... & Seeman, N. C. (2013). Self-assembled DNA crystals: the impact on resolution of 5′-phosphates and the DNA source. Nano letters, 13(2), 793-797.

[105] Carroll, K. M., Giordano, A. J., Wang, D., Kodali, V. K., Scrimgeour, J., King, W. P., ... & Curtis, J. E. (2013). Fabricating nanoscale chemical gradients with thermochemical nanolithography. Langmuir, 29(27), 8675-8682.

[106] Yardley, R. E., Kenaree, A. R., & Gillies, E. R. (2019). Triggering depolymerization: Progress and opportunities for self-immolative polymers. Macromolecules, 52(17), 6342-6360.

[107] Leiserson, C. E., Thompson, N. C., Emer, J. S., Kuszmaul, B. C., Lampson, B. W., Sanchez, D., & Schardl, T. B. (2020). There's plenty of room at the Top: What will drive computer performance fter Moore's law?. Science, 368(6495).

[108] Bayda, S., Adeel, M., Tuccinardi, T., Cordani, M., & Rizzolio, F. (2020). The history of nanoscience and nanotechnology: From chemical–physical applications to nanomedicine. Molecules, 25(1), 112.

[109] Nishi, H., & Tatsuma, T. (2019). Full-Color Scattering Based on Plasmon and Mie Resonances of Gold Nanoparticles Modulated by Fabry–Pérot Interference for Coloring and Image Projection. ACS Applied Nano Materials, 2(8), 5071-5078.

[110] Lancaster, C. A., Scholl, W. E., Ticknor, M. A., & Shumaker-Parry, J. S. (2020). Uniting Top-Down and Bottom-Up Strategies Using Fabricated Nanostructures as Hosts for Synthesis of Nanomites. The Journal of Physical Chemistry C, 124(12), 6822-6829.
[111] Ashok, A., Kumar, A., & Tarlochan, F. (2020). Colloidal metal oxide nanocrystals in catalysis. In Colloidal Metal Oxide Nanoparticles (pp. 247-288). Elsevier.
[112] Ashok, A., Kumar, A., & Tarlochan, F. (2020). Colloidal metal oxide nanocrystals in catalysis. In Colloidal Metal Oxide Nanoparticles (pp. 247-288). Elsevier.
[113] Darweesh, H. H. M. (2018). Nanomaterials: Classification and Properties-Part I. J Nanosci, 1(1), 1-11.
[114] Soroka, I. L., Bjervås, J., Ceder, J., Wallnerström, G., Connan, M., Tarakina, N. V., ... & Kiros, Y. (2020). Particle size effect of Ag-nanocatalysts deposited on carbon as prepared by γ-radiation induced synthesis. Radiation Physics and Chemistry, 169, 108370.
[115] Gulati, S. S., & Chaudhary, A. (2019). Greener Synthesis of Silver Nanoparticles using Waste of Onion (Allium cepa) and Quercetin: a comparative study.
[116] Das, C. A., Kumar, V. G., Dhas, T. S., Karthick, V., Govindaraju, K., Joselin, J. M., & Baalamurugan, J. (2020). Antibacterial activity of silver nanoparticles (biosynthesis): A short review on recent advances. Biocatalysis and Agricultural Biotechnology, 101593.
[117] Ijaz, M., Zafar, M., & Iqbal, T. (2020). Green synthesis of silver nanoparticles by using various extracts: a review. Inorganic and Nano-Metal Chemistry, 1-12.
[118] Shankar SS, Absar A, Murali S, (2003). Geranium leaf assisted biosynthesis of silver nanoparticles. Biotechnol Prog 19:1627–1631.
[119] Beveridge TJ and Murray RGE (1980). Site of metal deposition in the cell wall of Bacillus subtilis. J Bacteriol 141:876–887.
[120] Thangadurai, T. D., Manjubaashini, N., Thomas, S., & Maria, H. J. (2020). Physics and Chemistry of Nano-structures. In Nanostructured Materials (pp. 47-53). Springer, Cham.
[121] Dengo, N., Faresin, A., Carofiglio, T., Maggini, M., Wu, L., Hofmann, J. P., ... & Gross, S. (2020). Ligand-free ZnS nano-particles: as easy and green as it gets. Chemical Communications, 56(61), 8707-8710.
[122] Pakdel, E., Wang, J., Kashi, S., Sun, L., & Wang, X. (2020). Advances in photocatalytic self-cleaning, superhydrophobic and electromagnetic interference shielding textile treatments. Advances in Colloid and Interface Science, 277, 102116.
[123] Zhang, B., Zhang, J., Hua, M., Wan, Q., Su, Z., Tan, X., ... & Cheng, X. (2020). Highly Electrocatalytic Ethylene Production from CO2 on Nanodefective Cu Nanosheets. Journal of the American Chemical Society, 142(31), 13606-13613.
[124] Thangadurai, T. D., Manjubaashini, N., Thomas, S., & Maria, H. J. (2020). Physics and Chemistry of Nano-structures. In Nanostructured Materials (pp. 47-53). Springer, Cham.
[125] Al-Hakkani, M. F. (2020). Biogenic copper nano-particles and their applications: A review. SN Applied Sciences, 2(3), 1-20.
[126] Kim YT, Han JH, Hong BH, Kwon YU (2010) Electrocardiogram synthesis of CdSe quantum-dot arrays on a graphene basal plane using mesoporous silica thin-film templates. Adv Mater 22:515–518.
[127] Al-Hakkani, M. F. (2020). Biogenic copper nano-particles and their applications: A review. SN Applied Sciences, 2(3), 1-20.
[128] Bisht, M., Rajwar, D., & Raju, M. (2020). Nanotechnology for Agricultural and Environmental Sustainability at Higher Altitudes. In Microbiological Advancements for Higher Altitude Agro-Ecosystems & Sustainability (pp. 465-491). Springer, Singapore.
[129] Alfaifi, B. Y., Bayahia, H., & Tahir, A. A. (2019). Highly Efficient Nanostructured Bi2WO6 Thin Film Electrodes for Photo electrochemical and Environment Remediation. Nano-materials, 9(5), 755..
[130] Lee JY, Hong BH, Kim WY, Min SK, Kim Y, Jouravlev MV, Bose R, Kim KS, Hwang I-C, Kaufman LJ (2009) Near-field focusing and magnification through self-assembled nano-scale spherical lenses. Nature 460:498.
[131] Govindaraju K, Tamilselvan S, Kiruthiga V, Singaravelu G. Biogenic silver nanoparticles by Solanum torvum and their promising antimicrobial activity. Journal of Biopesticides 2010; 3(1): 394-399.

CURRICULUM VITAE

Alla Ahmad Muhamad AMIN

[redacted]

[redacted]

EDUCATION

Master Degree	**:** "Synthesis Of Silver, Copper And Bimetallic Nanoparticles Using Quercetin And Gallic Acid: Optical And Anti- Microbialproperties "FIRAT University, Graduate School of Natural and Applied Science, Department of Chemistry, Year 2021 Supervisor : Prof. Dr. Habibe ÖZMEN
Bachelor	**:** Koya University, Science Faculty, Department of Chemistry, Year 2012
High School	**:** Ranya, Sulemanı City, Year 2008